

Advances in Civil Engineering

Towards Carbon Neutrality in Civil Engineering

Lead Guest Editor: Onn Chiu Chuen

Guest Editors: Belal ALsubari and Kim Hung Mo





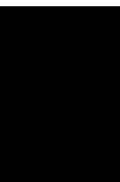
Towards Carbon Neutrality in Civil Engineering

Advances in Civil Engineering

Towards Carbon Neutrality in Civil Engineering

Lead Guest Editor: Onn Chiu Chuen

Guest Editors: Belal ALsubari and Kim Hung Mo



Copyright © 2023 Hindawi Limited. All rights reserved.

This is a special issue published in "Advances in Civil Engineering." All articles are open access articles distributed under the Creative Commons Attribution License, which permits unrestricted use, distribution, and reproduction in any medium, provided the original work is properly cited.




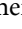
Chief Editor

Cumaraswamy Vipulanandan, USA














Associate Editors

Chiara Bedon , Italy
Constantin Chalioris , Greece
Ghassan Chehab , Lebanon
Ottavia Corbi, Italy
Mohamed ElGawady , USA
Husnain Haider , Saudi Arabia
Jian Ji , China
Jiang Jin , China
Shazim A. Memon , Kazakhstan
Hossein Moayedi , Vietnam
Sanjay Nimbalkar, Australia
Giuseppe Oliveto , Italy
Alessandro Palmeri , United Kingdom
Arnaud Perrot , France
Hugo Rodrigues , Portugal
Victor Yepes , Spain
Xianbo Zhao , Australia

Academic Editors

José A.F.O. Correia, Portugal
Glenda Abate, Italy
Khalid Abdel-Rahman , Germany
Ali Mardani Aghabaglou, Turkey
José Aguiar , Portugal
Afaq Ahmad , Pakistan
Muhammad Riaz Ahmad , Hong Kong
Hashim M.N. Al-Madani , Bahrain
Luigi Aldieri , Italy
Angelo Aloisio , Italy
Maria Cruz Alonso, Spain
Filipe Amarante dos Santos , Portugal
Serji N. Amirkhania, USA
Eleftherios K. Anastasiou , Greece
Panagiotis Ch. Anastasopoulos , USA
Mohamed Moafak Arbili , Iraq
Farhad Aslani , Australia
Siva Avudaiappan , Chile
Ozgur BASKAN , Turkey
Adewumi Babafemi, Nigeria
Morteza Bagherpour, Turkey
Qingsheng Bai , Germany
Nicola Baldo , Italy
Daniele Baraldi , Italy

Eva Barreira , Portugal
Emilio Bastidas-Arteaga , France
Rita Bento, Portugal
Rafael Bergillos , Spain
Han-bing Bian , China
Xia Bian , China
Huseyin Bilgin , Albania
Giovanni Biondi , Italy
Hugo C. Biscaia , Portugal
Rahul Biswas , India
Edén Bojórquez , Mexico
Giosuè Boscato , Italy
Melina Bosco , Italy
Jorge Branco , Portugal
Bruno Briseghella , China
Brian M. Broderick, Ireland
Emanuele Brunesi , Italy
Quoc-Bao Bui , Vietnam
Tan-Trung Bui , France
Nicola Buratti, Italy
Gaochuang Cai, France
Gladis Camarini , Brazil
Alberto Campisano , Italy
Qi Cao, China
Qixin Cao, China
Iacopo Carnacina , Italy
Alessio Cascardi, Italy
Paolo Castaldo , Italy
Nicola Cavalagli , Italy
Liborio Cavaleri , Italy
Anush Chandrappa , United Kingdom
Wen-Shao Chang , United Kingdom
Muhammad Tariq Amin Chaudhary, Kuwait
Po-Han Chen , Taiwan
Qian Chen , China
Wei Tong Chen , Taiwan
Qixiu Cheng, Hong Kong
Zhanbo Cheng, United Kingdom
Nicholas Chileshe, Australia
Prinya Chindaprasirt , Thailand
Corrado Chisari , United Kingdom
Se Jin Choi , Republic of Korea
Heap-Yih Chong , Australia
S.H. Chu , USA
Ting-Xiang Chu , China

Zhaofei Chu , China
Wonseok Chung , Republic of Korea
Donato Ciampa , Italy
Gian Paolo Cimellaro, Italy
Francesco Colangelo, Italy
Romulus Costache , Romania
Liviu-Adrian Cotfas , Romania
Antonio Maria D'Altri, Italy
Bruno Dal Lago , Italy
Amos Darko , Hong Kong
Arka Jyoti Das , India
Dario De Domenico , Italy
Gianmarco De Felice , Italy
Stefano De Miranda , Italy
Maria T. De Risi , Italy
Tayfun Dede, Turkey
Sadik O. Degertekin , Turkey
Camelia Delcea , Romania
Cristoforo Demartino, China
Giuseppe Di Filippo , Italy
Luigi Di Sarno, Italy
Fabio Di Trapani , Italy
Aboelkasim Diab , Egypt
Thi My Dung Do, Vietnam
Giulio Dondi , Italy
Jiangfeng Dong , China
Chao Dou , China
Mario D'Aniello , Italy
Jingtao Du , China
Ahmed Elghazouli, United Kingdom
Francesco Fabbrocino , Italy
Flora Faleschini , Italy
Dingqiang Fan, Hong Kong
Xueping Fan, China
Qian Fang , China
Salar Farahmand-Tabar , Iran
Ilenia Farina, Italy
Roberto Fedele, Italy
Guang-Liang Feng , China
Luigi Fenu , Italy
Tiago Ferreira , Portugal
Marco Filippo Ferrotto, Italy
Antonio Formisano , Italy
Guoyang Fu, Australia
Stefano Galassi , Italy

Junfeng Gao , China
Meng Gao , China
Giovanni Garcea , Italy
Enrique García-Macías, Spain
Emilio García-Taengua , United Kingdom
DongDong Ge , USA
Khaled Ghaedi, Malaysia
Khaled Ghaedi , Malaysia
Gian Felice Giaccu, Italy
Agathoklis Giaralis , United Kingdom
Ravindran Gobinath, India
Rodrigo Gonçalves, Portugal
Peilin Gong , China
Belén González-Fonteboa , Spain
Salvatore Grasso , Italy
Fan Gu, USA
Erhan Güneyisi , Turkey
Esra Mete Güneyisi, Turkey
Pingye Guo , China
Ankit Gupta , India
Federico Gusella , Italy
Kemal Hacıefendioğlu, Turkey
Jianyong Han , China
Song Han , China
Asad Hanif , Macau
Hadi Hasanzadehshooiili , Canada
Mostafa Fahmi Hassanein, Egypt
Amir Ahmad Hedayat , Iran
Khandaker Hossain , Canada
Zahid Hossain , USA
Chao Hou, China
Biao Hu, China
Jiang Hu , China
Xiaodong Hu, China
Lei Huang , China
Cun Hui , China
Bon-Gang Hwang, Singapore
Jijo James , India
Abbas Fadhil Jasim , Iraq
Ahad Javanmardi , China
Krishnan Prabhakan Jaya, India
Dong-Sheng Jeng , Australia
Han-Yong Jeon, Republic of Korea
Pengjiao Jia, China
Shaohua Jiang , China

MOUSTAFA KASSEM , Malaysia
Mosbeh Kaloop , Egypt
Shankar Karuppanan , Ethiopia
John Kechagias , Greece
Mohammad Khajehzadeh , Iran
Afzal Husain Khan , Saudi Arabia
Mehran Khan , Hong Kong
Manoj Khandelwal, Australia
Jin Kook Kim , Republic of Korea
Woosuk Kim , Republic of Korea
Vaclav Koci , Czech Republic
Loke Kok Foong, Vietnam
Hailing Kong , China
Leonidas Alexandros Kouris , Greece
Kyriakos Kourousis , Ireland
Moacir Kripka , Brazil
Anupam Kumar, The Netherlands
Emma La Malfa Ribolla, Czech Republic
Ali Lakirouhani , Iran
Angus C. C. Lam, China
Thanh Quang Khai Lam , Vietnam
Luciano Lamberti, Italy
Andreas Lampropoulos , United Kingdom
Raffaele Landolfo, Italy
Massimo Latour , Italy
Bang Yeon Lee , Republic of Korea
Eul-Bum Lee , Republic of Korea
Zhen Lei , Canada
Leonardo Leonetti , Italy
Chun-Qing Li , Australia
Dongsheng Li , China
Gen Li, China
Jiale Li , China
Minghui Li, China
Qingchao Li , China
Shuang Yang Li , China
Sunwei Li , Hong Kong
Yajun Li , China
Shun Liang , China
Francesco Liguori , Italy
Jae-Han Lim , Republic of Korea
Jia-Rui Lin , China
Kun Lin , China
Shibin Lin, China

Tzu-Kang Lin , Taiwan
Yu-Cheng Lin , Taiwan
Hexu Liu, USA
Jian Lin Liu , China
Xiaoli Liu , China
Xuemei Liu , Australia
Zaobao Liu , China
Zhuang-Zhuang Liu, China
Diego Lopez-Garcia , Chile
Cristiano Loss , Canada
Lyan-Ywan Lu , Taiwan
Jin Luo , USA
Yanbin Luo , China
Jianjun Ma , China
Junwei Ma , China
Tian-Shou Ma, China
Zhongguo John Ma , USA
Maria Macchiaroli, Italy
Domenico Magisano, Italy
Reza Mahinroosta, Australia
Yann Malecot , France
Prabhat Kumar Mandal , India
John Mander, USA
Iman Mansouri, Iran
André Dias Martins, Portugal
Domagoj Matesan , Croatia
Jose Matos, Portugal
Vasant Matsagar , India
Claudio Mazzotti , Italy
Ahmed Mebarki , France
Gang Mei , China
Kasim Mermerdas, Turkey
Giovanni Minafò , Italy
Masoomah Mirrashid , Iran
Abbas Mohajerani , Australia
Fadzli Mohamed Nazri , Malaysia
Fabrizio Mollaioli , Italy
Rosario Montuori , Italy
H. Naderpour , Iran
Hassan Nasir , Pakistan
Hossein Nassiraei , Iran
Satheeskumar Navaratnam , Australia
Ignacio J. Navarro , Spain
Ashish Kumar Nayak , India
Behzad Nematollahi , Australia

Chayut Ngamkhanong , Thailand
Trung Ngo, Australia
Tengfei Nian, China
Mehdi Nikoo , Canada
Youjun Ning , China
Olugbenga Timo Oladinrin , United Kingdom
Oladimeji Benedict Olalusi, South Africa
Timothy O. Olawumi , Hong Kong
Alejandro Orfila , Spain
Maurizio Orlando , Italy
Siti Aminah Osman, Malaysia
Walid Oueslati , Tunisia
SUVASH PAUL , Bangladesh
John-Paris Pantouvakis , Greece
Fabrizio Paolacci , Italy
Giuseppina Pappalardo , Italy
Fulvio Parisi , Italy
Dimitrios G. Pavlou , Norway
Daniele Pellegrini , Italy
Gatheeshgar Perampalam , United Kingdom
Daniele Perrone , Italy
Giuseppe Piccardo , Italy
Vagelis Plevris , Qatar
Andrea Pranno , Italy
Adolfo Preciado , Mexico
Chongchong Qi , China
Yu Qian, USA
Ying Qin , China
Giuseppe Quaranta , Italy
Krishanu ROY , New Zealand
Vlastimir Radonjanin, Serbia
Carlo Rainieri , Italy
Rahul V. Ralegaonkar, India
Raizal Saifulnaz Muhammad Rashid, Malaysia
Alessandro Rasulo , Italy
Chonghong Ren , China
Qing-Xin Ren, China
Dimitris Rizos , USA
Geoffrey W. Rodgers , New Zealand
Pier Paolo Rossi, Italy
Nicola Ruggieri , Italy
JUNLONG SHANG, Singapore

Nikhil Saboo, India
Anna Saetta, Italy
Juan Sagaseta , United Kingdom
Timo Saksala, Finland
Mostafa Salari, Canada
Ginevra Salerno , Italy
Evangelos J. Sapountzakis , Greece
Vassilis Sarhosis , United Kingdom
Navaratnarajah Sathiparan , Sri Lanka
Fabrizio Scozzese , Italy
Halil Sezen , USA
Payam Shafigh , Malaysia
M. Shahria Alam, Canada
Yi Shan, China
Hussein Sharaf, Iraq
Mostafa Sharifzadeh, Australia
Sanjay Kumar Shukla, Australia
Amir Si Larbi , France
Okan Sirin , Qatar
Piotr Smarzewski , Poland
Francesca Sollecito , Italy
Rui Song , China
Tian-Yi Song, Australia
Flavio Stochino , Italy
Mayank Sukhija , USA
Piti Sukontasukkul , Thailand
Jianping Sun, Singapore
Xiao Sun , China
T. Tafsirojjaman , Australia
Fujiao Tang , China
Patrick W.C. Tang , Australia
Zhi Cheng Tang , China
Weerachart Tangchirapat , Thailand
Xiixin Tao, China
Piergiorgio Tataranni , Italy
Elisabete Teixeira , Portugal
Jorge Iván Tobón , Colombia
Jing-Zhong Tong, China
Francesco Trentadue , Italy
Antonello Troncone, Italy
Majbah Uddin , USA
Tariq Umar , United Kingdom
Muahmmad Usman, United Kingdom
Muhammad Usman , Pakistan
Mucteba Uysal , Turkey

Ilaria Venanzi , Italy
Castorina S. Vieira , Portugal
Valeria Vignali , Italy
Claudia Vitone , Italy
Liwei WEN , China
Chunfeng Wan , China
Hua-Ping Wan, China
Roman Wan-Wendner , Austria
Chaohui Wang , China
Hao Wang , USA
Shiming Wang , China
Wayne Yu Wang , United Kingdom
Wen-Da Wang, China
Xing Wang , China
Xiuling Wang , China
Zhenjun Wang , China
Xin-Jiang Wei , China
Tao Wen , China
Weiping Wen , China
Lei Weng , China
Chao Wu , United Kingdom
Jiangyu Wu, China
Wangjie Wu , China
Wenbing Wu , China
Zhixing Xiao, China
Gang Xu, China
Jian Xu , China
Panpan , China
Rongchao Xu , China
HE YONGLIANG, China
Michael Yam, Hong Kong
Hailu Yang , China
Xu-Xu Yang , China
Hui Yao , China
Xinyu Ye , China
Zhoujing Ye, China
Gürol Yildirim , Turkey
Dawei Yin , China
Doo-Yeol Yoo , Republic of Korea
Zhanping You , USA
Afshar A. Yousefi , Iran
Xinbao Yu , USA
Dongdong Yuan , China
Geun Y. Yun , Republic of Korea

Hyun-Do Yun , Republic of Korea
Cemal YİĞİT , Turkey
Paolo Zampieri, Italy
Giulio Zani , Italy
Mariano Angelo Zanini , Italy
Zhixiong Zeng , Hong Kong
Mustafa Zeybek, Turkey
Henglong Zhang , China
Jiupeng Zhang, China
Tingting Zhang , China
Zengping Zhang, China
Zetian Zhang , China
Zhigang Zhang , China
Zhipeng Zhao , Japan
Jun Zhao , China
Annan Zhou , Australia
Jia-wen Zhou , China
Hai-Tao Zhu , China
Peng Zhu , China
QuanJie Zhu , China
Wenjun Zhu , China
Marco Zucca, Italy
Haoran Zuo, Australia
Junqing Zuo , China
Robert Černý , Czech Republic
Süleyman İpek , Turkey

Contents

An Overview of the Utilization of Common Waste as an Alternative Fuel in the Cement Industry

Tee How Tan , Kim Hung Mo , Jiayi Lin , and Chiu Chuen Onn 

Review Article (17 pages), Article ID 7127007, Volume 2023 (2023)



Effect of Fiber Treatments on the Mechanical Properties of Sisal Fiber-Reinforced Concrete

Composites

Tsagazeab Yimer  and Abrham Gebre 



Research Article (15 pages), Article ID 2293857, Volume 2023 (2023)

Performance of Ladle Furnace Slag in Mortar under Standard and Accelerated Curing

Iffat Sultana  and G. M. Sadiqul Islam 

Research Article (14 pages), Article ID 7824084, Volume 2022 (2022)

Evaluating the Effect of China's Carbon Emission Trading Policy on Energy Efficiency of the Construction Industry Based on a Difference-in-Differences Method

Shasha Xie  and Jinjing Wang 

Research Article (12 pages), Article ID 6096435, Volume 2022 (2022)

Review Article

An Overview of the Utilization of Common Waste as an Alternative Fuel in the Cement Industry

Tee How Tan ¹, Kim Hung Mo ^{2,3}, Jiayi Lin ² and Chiu Chuen Onn ^{2,3}

¹Department of Construction Management, Faculty of Built Environment, Tunku Abdul Rahman University of Management and Technology, Kuala Lumpur 53300, Malaysia

²Department of Civil Engineering, Faculty of Engineering, Universiti Malaya, Kuala Lumpur 50603, Malaysia

³Centre for Transportation Research, Faculty of Engineering, Universiti Malaya, Kuala Lumpur 50603, Malaysia

Correspondence should be addressed to Tee How Tan; austintee28@gmail.com

Received 17 October 2022; Revised 12 June 2023; Accepted 14 September 2023; Published 11 October 2023

Academic Editor: Abdulkadir Cuneyt Aydın

Copyright © 2023 Tee How Tan et al. This is an open access article distributed under the Creative Commons Attribution License, which permits unrestricted use, distribution, and reproduction in any medium, provided the original work is properly cited.

As concrete is one of the most commonly used construction materials, there is a massive production of cement, which causes cement manufacturing to be an energy-intensive industry. A significant amount of the cost of cement production, ranging from 20% to 25%, is attributed to thermal energy. In addition, the action of mining and burning fossil fuels results in the unfavorable emission of hazardous compounds into the environment. Therefore, the switch from conventional fossil fuels to alternative fuels (AFs) in the cement manufacturing business has attracted attention due to environmental and financial concerns. In this paper, four commonly used AFs are discussed, which are waste tires, municipal solid waste, meat and bone meal, and sewage sludge. It is found that each AF has a unique calorific value and properties, attributed to its source, treatment, and technology. Furthermore, the availability of AF is important as the amount varies depending on the location. In addition, their effects on gaseous emissions from the cement plant and the quality of clinker are found to be inconsistent. Thus, there will not be a single best type of AF option to be used in the cement industry. A good AF should be able to provide sufficient thermal energy while reducing the environmental impacts and costs. A careful analysis and multicriteria decision-making approach are always vital when employing AFs in order to prevent environmental problems, cost increases, as well as clinker quality degradation.

1. Introduction

Cement is ranked as the second-most consumed material globally [1]. However, the cement industry has long been associated with high CO₂ emissions. The cement industry accounts for approximately 8% of global anthropogenic CO₂ emissions [2, 3]. It is reported that to manufacture 1 ton of cement, approximately 1 ton of CO₂ is emitted [4]. In addition to the enormous CO₂ emissions, cement production greatly depletes natural resources, including fossil fuels. Therefore, the cement manufacturing industry is under increasing pressure from environmental protection agencies to reduce its CO₂ emissions and to employ sustainable resources.

In response to the challenges, several approaches have been implemented to reduce CO₂ emissions as well as to preserve natural resources. Carbon capture, utilization, and storage (CCUS) technology in cement production has become an

attractive and active research area. Korczak et al. [5] reviewed the available technologies in decarbonization of the nonmetallic minerals industry in the European Union (EU), including the cement industry, and found that CCUS has the highest decarbonization potential, up to 60%. However, impurities such as sulfur oxide (SO_x), nitrogen oxide (NO_x), and carbon monoxide (CO) are present in significant amounts in the cement kiln flue gases [6], complicating the capture of pure CO₂. Another approach is to reduce the demand for cement by replacing cement in the concrete composition, particularly using supplementary cementitious materials, alkali-activated materials (AAM), or geopolymers. However, the relatively new nonportland binders lack building codes and data on their long-term durability, which increases the demand for the development of realistic accelerated tests and careful analysis of field performance. Nevertheless, due to the long lead times required for the completion of such tests, portland cement

will likely continue to be the primary material for several decades [4]. Thus, lowering the clinker-to-cement ratio [7] is considered the best approach due to its maturity and can be adopted immediately by almost all of the worldwide cement manufacturing plants.

A large amount of nonrenewable natural fossil fuels, such as coal, has been consumed each year to manufacture cement. To manufacture 1 ton of cement, approximately 1.5 ton of raw materials, 3,000–4,300 MJ of fuel energy, and 120–160 kW hr of electrical energy are required [8]. Nevertheless, the supply of coal is predicted to be in short supply in the near future in order to achieve the goal of halving CO₂ emissions by 2030 and reaching net zero emissions by 2050. On top of that, the cement industry is very vulnerable to fuel price fluctuations [9]. As a result of the energy-intensive characteristics of cement production processes, escalating fuel prices, and fuel shortages, the cement industry is forced to search for alternative fuel (AF) sources [9–11]. Adopting wastes as an AF in the cement industry is another viable approach to reduce CO₂ emissions and preserve natural fossil fuel, as well as cost savings. AF utilization has begun in the mid-1980s [12]. In 2014, AF accounted for 16.4% of total thermal energy demand in Japan. In 2015, AF contributed 64.6% of the total thermal energy demand in Germany's cement industry [13].

Although energy recovery is ranked fourth in the waste management hierarchy, it has seen a significant increase in interest in recent decades as a means of reusing waste or by-products rather than dumping them. This is due to the fact that prevention, reduction, and recycling are impossible to always be executed, especially when dealing with matters that are closely related to human-needed activities, such as transportation, treatment of wastewater, and more. Thus, in those scenarios, coprocessing becomes the logical first response to the issue of disposal since the solution can be implemented immediately [14]. The use of waste (both industrial and agricultural) as AF reduces the burden on landfills as well as the operational costs of the cement manufacturing industry [15]. In addition, there are several notable factors that promote the use of wastes as an AF in the cement kiln, such as the high temperatures of the cement kiln, the appropriate length of the kiln, the long amount of time the fuel is kept within the kiln, and the alkaline environment within the kiln. All of these would ensure that the use of wastes as an AF is ecologically safe [11].

The objective of this work is to give an insight into the application of wastes as AF in the cement industry, including their possible impacts on the quality of cement as well as the environment. In general, depending on local availability and energy performance, a wide range of AFs can be used in the cement industry. Nevertheless, in this work, only four solid-based AF are chosen, namely waste tires, sewage sludge (SS), refused-derived fuel (RDF), and meat and bone meal (MBM), attributed to the aim of this work is to provide an implication of AF utilization in the cement industry. These four wastes are chosen due to their widespread application as an AF in the cement industry [16]. Another important reason is due to

their abundance, as these wastes are generated by highly necessary human-related activities, such as vehicle use, treatment of wastewater, disposal of municipal solid waste (MSW), slaughtering of animals for food, and so forth. Hence, management of these wastes is more alarming and recovery of energy from these wastes is a viable approach. In this work, the potential of these wastes as an AF in the cement industry is discussed, covering the calorific value and their potential impacts on cement and the environment. A brief comparison of these fuels has been included which could be useful for experts from the AF application and cement industry.

2. Cement

Figure 1 presents the global cement production from 2010 to 2022. Since 2010, the global cement production has increased significantly. Although the rate of usage of other building materials, such as wood [20] and alternative binder materials such as AAM or geopolymers has increased, the demand for cement globally is anticipated to keep rising. This is largely due to the rapid development of a few countries, such as China. The cement production in China is estimated to be around 2,400 Mt, which is approximately 57% of the world cement production [18, 20]. On the other hand, cement production is technologically mature and widely accepted. Nevertheless, the global cement production in 2022 is estimated to reduce to 4,100 Mt as compared to the global cement production in 2021 which is estimated at 4,400 Mt. This is due to the reduction in the cement production of China in 2022, which is from 2,400 to 2,100 Mt [21], probably due to the implementation of the long period lockdown policy during the COVID-19 pandemic. As a result, it is therefore anticipated that the associated environmental pollution and depletion of natural resources from the cement industry will continue to occur in the absence of suitable intervention.

2.1. Energy Consumption. The average energy demand for producing 1 ton of cement is around 3.3 GJ of thermal energy, which equates to 120 kg of coal with a calorific value of 27.5 MJ/kg and roughly 110 kW hr/t of electrical energy [10, 22, 23]. Burning operations employ the majority of the thermal energy, whereas cement grinding utilizes the electrical energy [24, 25]. According to Oggioni et al. [26], for each ton of cement produced, energy expenditures in the form of fuel and electricity account for 40% of the total production costs. Thus, besides promoting sustainability, replacing fossil fuel with AF will help to lower the energy costs and, consequently, the production costs, giving the cement plant using this form of energy a significant advantage.

The energy efficiency of cement plants is also significantly influenced by the type of cement kiln utilized. Since the 1970s, initiatives have been made to optimize a cement kiln's energy efficiency [27], in which the cement kiln has evolved from the lengthy wet kiln to a cutting-edge dry kiln that is equipped with calciners, six-stage preheaters, and high-efficiency coolers [28]. Because of this, the total amount of energy used has gone down from 6 to around 3 GJ/t_{clinker} [29–32].

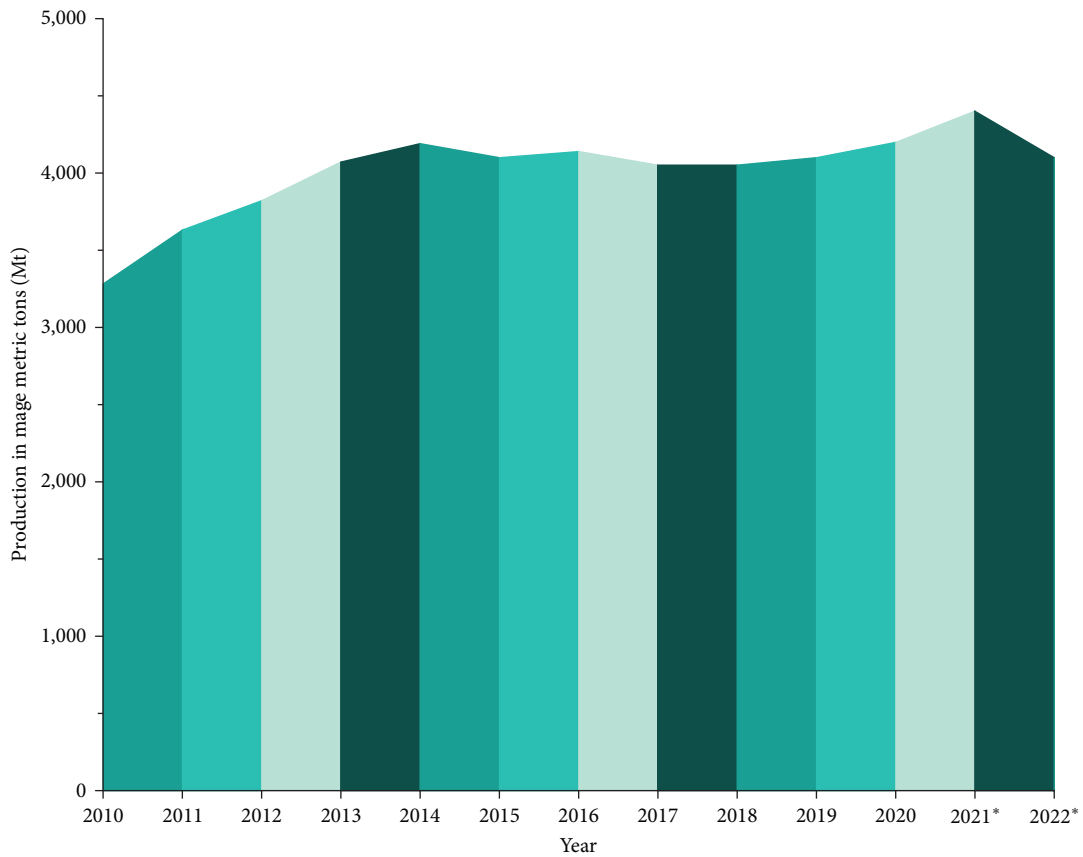


FIGURE 1: Global cement production from 2010 to 2022 [17-19]. * = estimated value.

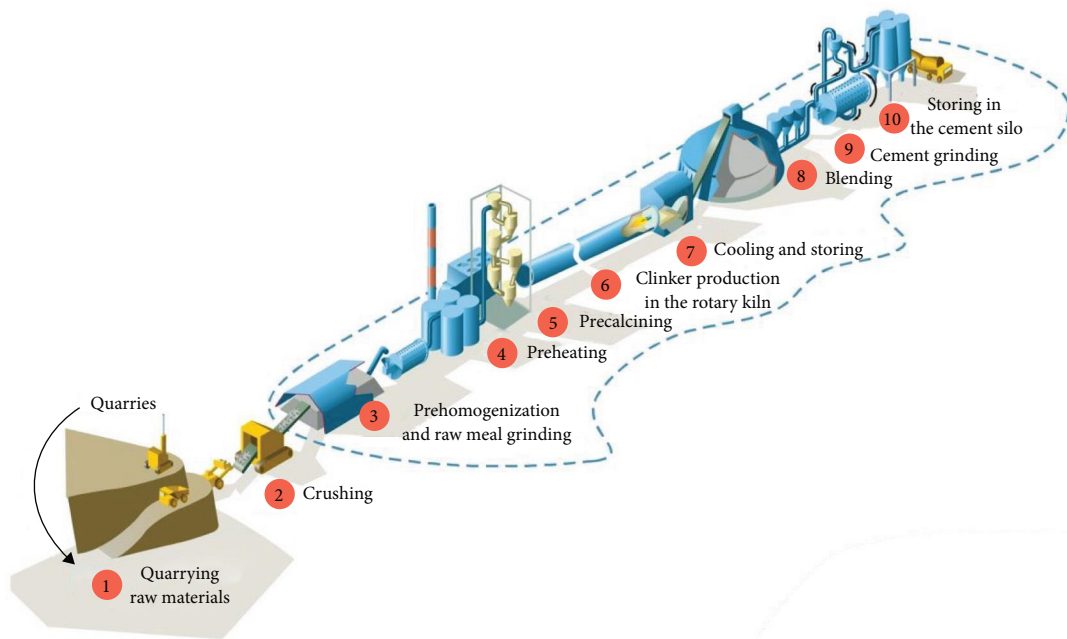


FIGURE 2: Dry kiln cement manufacturing process [33].

The cement manufacturing process in a dry kiln is shown in Figure 2. The three primary stages of the cement manufacturing process include the preparation of raw materials, clinker production, and cement manufacturing. First, raw meal, a

homogeneous mixture made by combining and milling several raw materials, is obtained. The raw meal is then preheated, precalcined, followed by calcination in a high-temperature rotary kiln, typically operating at 1,450°C, to produce clinker.

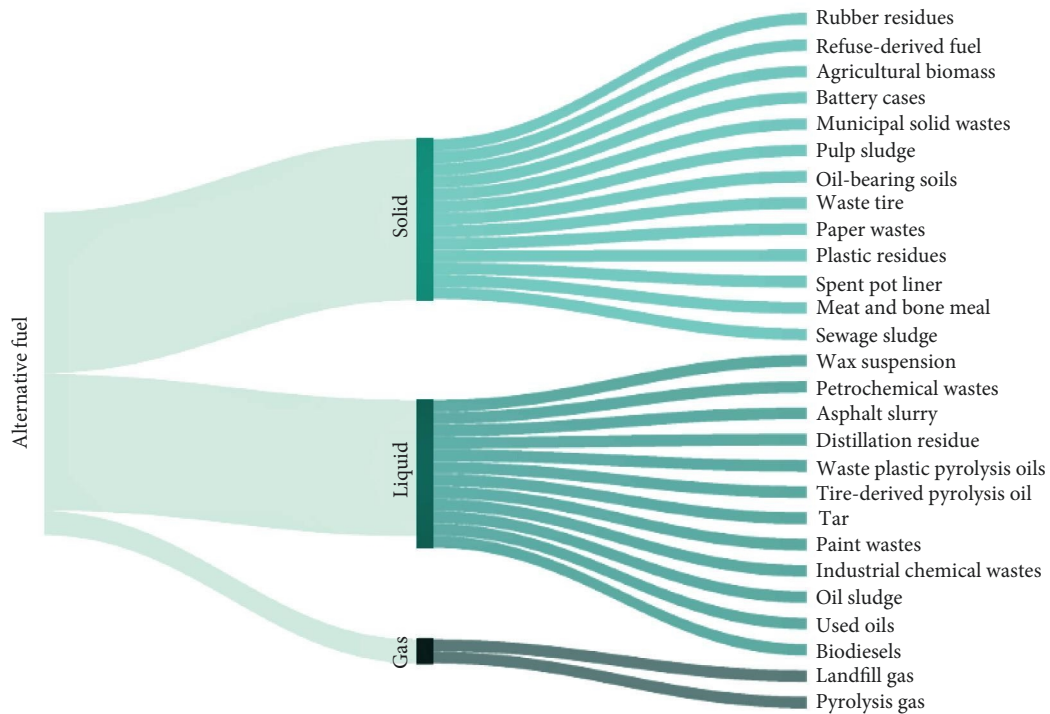


FIGURE 3: AF options for the cement industry.

Finally, the clinker is cooled, ground, and blended with gypsum to form cement. At this stage, additional cementitious ingredients, such as fly ash, may be added to produce blended cement. The grinding and blending processes can be done onsite at the kiln or at a separate grinding or blending facility.

2.2. CO₂ Emissions. The CO₂ emissions from the cement industry can be divided into three parts, which are process-related CO₂ emissions, fuel-related CO₂ emissions, and electricity-related CO₂ emissions. The process-related CO₂ emissions generally involve the decomposition of raw materials, for instance, limestone, during the clinker calcination stage. The fuel-related CO₂ emissions are directly associated with the combustion of fuel. The typical calcination temperature in the cement kiln reaches 1,450°C, which requires a large number of fuels. The electricity-related CO₂ emissions come from the consumption of electricity to run the cement plants, such as mills, fans, and other electrical equipment that are powered by electricity [34]. About 50% of the total CO₂ emissions in the cement manufacturing process are due to process-related CO₂ emissions, while fuel and electricity-related emissions account for the remaining 40% and 10% of emissions, respectively [16, 35].

3. Alternative Fuel

AF refers to materials other than conventional fuels such as fossil fuels that can be adopted to recover thermal energy, including waste materials [36]. Figure 3 presents some of the

AF that can be employed in the cement manufacturing industry, based on their physical state [37]. The AF are classified into three basic groups, which are gas, liquid, and solid [11]. Nevertheless, there are hundreds, if not thousands, of AF that can actually be used in cement plants [38] and further exploration is needed. For instance, pyrolysis oil derived from waste plastics (WPPO), which is a viable option due to waste plastics have always been a global issue [39, 40], biodiesels that can be derived from various sources, such as waste coconut, sunflower, and palm cooking oils [41] as well as pyrolysis oil derived from waste tires [42].

Every AF, even of the same type, is unique and has distinctive properties depending on the region, technology, and the route of the waste produced. BS EN ISO 21640 classifies the AF, particularly solid recovered fuels, into five classes based on their net calorific value, chlorine content, and mercury content. Thorough examination and consideration are essential during the AF selection process. A multicriteria decision-making (MCDM) method is generally employed in the selection process [43, 44]. This is because, in addition to calorific values, the effects of AF on cement, the environment, operational costs, and so forth are significant. The following traits are likely to be taken into account during AF selection [11, 24]:

- (i) Physical state of the fuel (solid, liquid, and gaseous)
- (ii) Content of circulating elements (Na, K, Cl, and S)
- (iii) Toxicity (organic compounds and heavy metals)

- (iv) Composition and content of ash
- (v) Content of volatiles
- (vi) Calorific value (>14.0 MJ/kg)
- (vii) Chlorine (Cl) content ($<0.2\%$)
- (viii) Sulfur content ($<2.5\%$)
- (ix) Polychlorinated Biphenyls (PCBs) content (<50 ppm)
- (x) Heavy metals content ($<2,500$ ppm) (out of which: mercury (Hg) <10 ppm, and total cadmium (Cd), thallium (Tl), and Hg <100 ppm)
- (xi) Physical properties (size, density, and homogeneity)
- (xii) Grinding properties
- (xiii) Moisture content
- (xiv) Proportioning technology
- (xv) The emissions
- (xvi) The cement quality and its compatibility with the environment must not decrease
- (xvii) AF must be economically viable
- (xviii) Availability of the AF.

3.1. Type of Alternative Fuel

3.1.1. Waste Tire. Waste tire is a waste that originates from the automobile industry, and it has become much more prevalent since vehicles are such a dominant mode of mobility. Around 3 billion tires are traded commercially around the globe each year, and an equivalent number are discarded when they no longer serve a purpose [45]. The United States of America, Japan, and the EU discard about 5 million tonnes of tires annually [15]. The billions of tires that are already stockpiled or buried in landfills, warehouses, and illegal sites will continue to grow over time, and they are prone to environmental threats, including becoming home to rodents and insects [38].

About 70% of the total waste tires at the end of their service life is recycled, with the majority of them converted to fuel or used for the production of various materials [45]. In the mid-1980s, waste tires became a popular AF option for the cement industry, attributed to the spike in fossil fuel prices and high calorific value [14]. According to several studies, the net calorific value of waste tires is about 27–37 MJ/kg, and they burn quickly [1, 9, 32, 46]. Tire is composed of about 88% carbon and oxygen, and its total annihilation is guaranteed at temperatures above 800°C and with gas retention at high temperatures. Complete destruction will prevent the formation of intermediate products of incomplete combustion, such as black smoke and odors [1]. Thus, the use of waste tires as AF in the cement industry has gained popularity, owing to the high temperature during calcination ($1,450^{\circ}\text{C}$), long retention time, and alkaline environment inside the kiln [1]. In addition, a tipping fee will be provided for collecting the waste tires, which will help to offset the transportation costs. Castañón et al. [9] reported that the annual fuel cost to manufacture clinker using pure petcoke was around 8,000,000 €/year, while using 40% waste tires as AF would cost only 5,938,000 €/year.



FIGURE 4: Waste tires [49].

TABLE 1: Calorific value of waste tires.

Reference	Calorific value (MJ/kg)
[37]	35.50
[51]	37.10
[52]	31.00
[53]	31.40
[54]	31.80
[1]	27.00
[55]	31.40
[56]	31.88
[9]	29.71

Utilization of waste tires as AF helps to reduce the consumption of nonrenewable fossil fuels and conserve natural resources [47]. Meanwhile, the environmental impacts due to the disposal of waste tires can be minimized. According to Fiksel et al. [48], the use of waste tire as AF in cement manufacturing plants provides more reduction in most environmental impact categories compared to other waste tires applications, after the application of artificial turf.

The waste tires can be burned as a whole or in the form of shredded and fine-grained, depending on the combustion unit, and is known as tire-derived fuel. Figure 4 shows the photos of waste tires. According to the United States Environmental Protection Agency [50], waste tires produce the same amount of energy as oil and 25% more energy than coal. Table 1 presents the calorific value of waste tires reported in the literature. On the other hand, the waste tires exhibit low moisture content and high carbon content, and the reinforced wire of the tire can be consumed as an iron source when the whole tire is burned [14, 37].

(1) Impacts of Waste Tires as AF to Cement and Environment. According to Castañón et al. [9] and Nakomcic-Smaragdakis et al. [1], the clinker quality was maintained when waste tires were used as AF. No significant variation in the clinker content, in terms of alite (C_3S) and free lime, was observed when using waste tires as AF; the C_3S content of the clinker was higher than 70%, while the free lime content was less than 2.5%. A similar observation was reported by Puertas and Blanco-Varela [57], where a comparable clinker mineralogical composition was obtained when waste shredded tires were used as AF. This is probably due to the amount of waste tire ash that incorporates into the clinker is considerably low, thus the effect is small or negligible. According to Czajczyńska et al. [58], the

TABLE 2: Chemical composition of waste tires ash [59].

Compound	Composition (%)
CaO	47.0
SiO ₂	14.1
Al ₂ O ₃	2.7
Fe ₂ O ₃	1.1
Na ₂ O	<0.01
K ₂ O	<0.01
MgO	0.7
TiO ₂	<0.01
P ₂ O ₅	<0.01
SO ₃	1.2
MnO	<0.01
ZnO	33.1

amount of waste tire ash produced after incineration is around 7%. In addition, another possible reason is due to the composition of waste tire ash, as shown in Table 2. It is observed that the main constituent of waste tire ash is reported to be CaO, SiO₂, and ZnO, while CaO and SiO₂ are the vital components for clinker formation.

Nonetheless, it has been established that the usage of waste tires as AF in the cement industry leaves no residue behind as the slag and ashes would be incorporated into the clinker during the calcination process. Table 2 depicts the waste tire ash, reported by Mónica et al. [59], which possesses a high ZnO content of up to 33.1%. This is attributed to Zn being often used in the tire-making process to enhance the vulcanization process. Thus, when waste tires are combusted in the cement kiln, the residue ash is anticipated to be incorporated into the clinker, and resulting in the increment of the ZnO level of the clinker. For instance, a high zinc (Zn) content, compared to conventional clinker, was observed in the clinker produced with shredded tires as an AF [57].

The incorporation of Zn during the clinkering process usually results in a reduced quality cement product with prolonged setting time and lower strength [36, 46] due to the diminishing or even disappearance of C₃A when the amount of Zn that is incorporated during the clinkering process has exceeded the threshold limit; typical Zn concentration in OPC is far from the threshold limit. In addition, a new product, Ca₆Zn₃Al₄O₁₅ may formed [60]. Mónica et al. [59] investigated the effect of waste tire ash (Table 2) as an additive to the clinker. The 28-day strength of the clinker produced with the addition of 30% of waste tire ash shows only a slight reduction compared to the control cement sample, which was approximately 45 and 50 MPa, respectively. Soto-Felix et al. [61] studied the effect of ZnO as an additive on the setting time and strength of cement. The results showed that adding ZnO to the cement increased the setting time and decreased the strength. Slight strength improvement was observed when a very low content of ZnO was added due to the filler effect. Therefore, due to the elevated Zn content in the clinker, the use of waste tires as AF in the cement industry is suggested to be limited to a maximum of 30% [1] to prevent the significant reduction of C₃A content

TABLE 3: Gaseous emissions with waste tires as AF.

Reference	SO ₂	NO _x	Dioxin	Furan
[63]	–	Decreased	–	–
[64]	Increased	Decreased	Decreased	Decreased
[65]	Increased	Increased	Unchanged	Unchanged
[66]	–	–	Increased	Increased
[54]	Increased	Increased	–	–
[1]	Fluctuated	Fluctuated	–	–
[62]	Increased	Unchanged	–	–
[9]	Decreased	Decreased	–	–

and formation of Ca₆Zn₃Al₄O₁₅ that results in quality degraded cement product.

On the other hand, Castañón et al. [9] compared the gaseous emissions when 100% petcoke fuel and a 6:4 fuel mix comprised of petcoke and waste tires are used. It is reported that when 40% of waste tires were employed, the NO_x and sulfur dioxide (SO₂) emissions were decreased by 17% and 28%, respectively. The reduction is highly related to the reduction of sintering temperature, lower oxygen content as well as lower sulfur content in the waste tires compared to petcoke. The sulfur content of waste tires and petcoke was around 1.3% and 6%, respectively. However, the SO₂ emissions were found to have increased in some cases, which may be due to the fact that the employed fuel is coal. Coal has a lower sulfur content compared to petcoke, which is 2.45% [62]. Another possible reason could be the incomplete combustion of waste tires [1]. Thus, the gaseous emissions are found to vary, which is believed due to the adoption of different fuels, variation in the composition of the waste tires as well as their substitution level. The SO₂, NO_x, dioxin, and furan emissions when using waste tires as an AF are tabulated in Table 3.

3.1.2. Municipal Solid Waste. Around 440 kg of MSW is produced globally per person per year [67]. MSW is typically disposed of in a sanitary landfill. However, as a result of the growing human population's impact on the amount of MSW produced and the diminishing volume of landfill space, managing MSW has turned into a significant problem. In some cases, MSW is simply dumped in open dumping areas, posing health and environmental risks such as foul odor, methane emission, soil pollution, as well as groundwater pollution caused by leachate from landfilled waste. Therefore, demand for alternative MSW treatment methods that can effectively reduce the volume of MSW while avoiding or minimizing the associated negative impacts is arising.

In the waste management hierarchy, top priority is given to waste prevention, followed by reuse, recycling, recovery, and disposal [68]. However, the first three stages may be difficult to carry out at all times; thus, energy recovery through incineration is the best solution [69]. MSW incineration possesses several benefits, such as significant volume reduction (~70%–90%), recovering energy, and eliminating pathogens [21, 67, 70]. Nevertheless, direct MSW incineration in the cement industry sometimes incurs operational issues such as incomplete combustion, increased specific

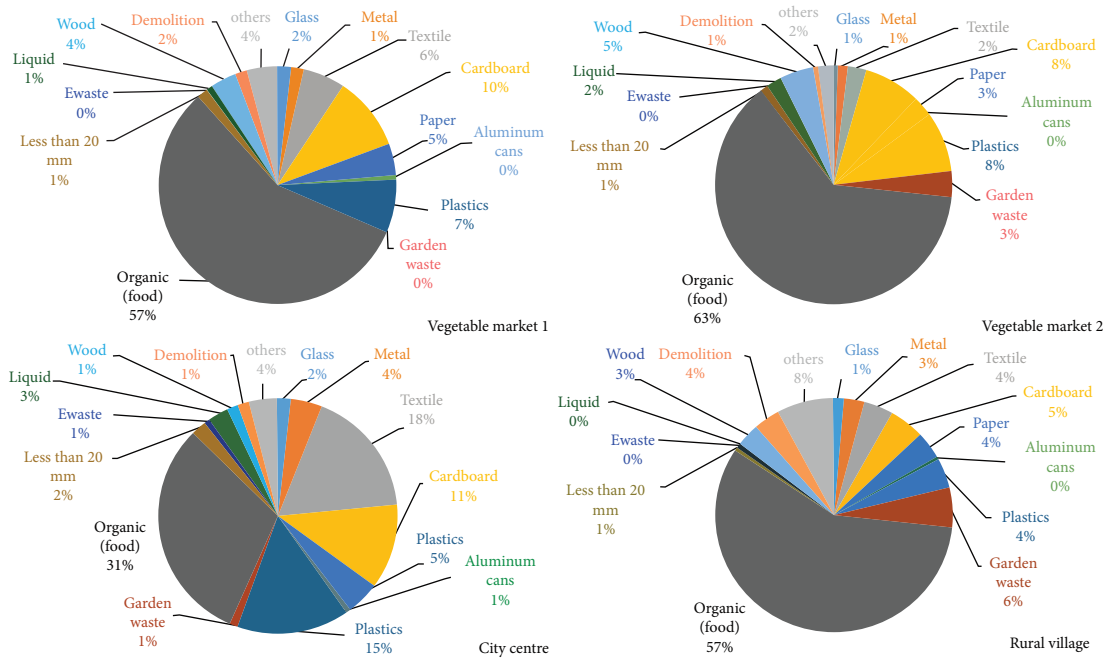


FIGURE 5: MSW composition at different sources in Irbid City, Jordan [49].

heat consumption, lower flame temperatures, and kiln coating buildup [71]. This results in the increased interest in gasification technology [67, 71]. Nevertheless, since the aim of this work is to provide an overview of the common wastes that can be used in AF in the cement industry, only the combustion technology is discussed here.

Due to cultural differences and the level of source separation, recycling, and processing, the composition of MSW varies significantly from one country to another. Figure 5 shows the MSW composition at Irbid City, Jordan [49]. Even in the same city, the MSW composition varies due to different sources. Therefore, most of the cement plants do not directly employ and burn the unsorted MSW due to its heterogeneous nature [16] that will lead to an inconsistency in combustion performance. On top of that, untreated MSW usually exhibits low calorific value, high moisture content, and contains undesired components such as noncombustible compounds that will decrease the calorific value. Generally, the calorific value of MSW is around 6.21 to 9.2 MJ/kg [72, 73].

Considering the low calorific value, higher moisture, and ash content of MSW, RDF (Figure 6) is typically employed. RDF is an AF that is obtained after the removal or rejection of noncombustible materials from the MSW, for instance, ferrous materials, grit, and glass [70]. Removing metals during the sorting process would reduce the heavy metal content in the RDF [75]. RDF made from MSW has constant thermal and energetic characteristics, a low level of pollutants as well as a high calorific value [72]. The main steps involved in producing RDF from MSW typically involve preliminary liberation, size screening, shredding, magnetic separation, and pelletizing [14]. Various RDF forms are available, including fluff, pellets, bricks, or logs [76].



FIGURE 6: RDF in pellet form [74].

Table 4 presents the composition of RDF produced from MSW as investigated by Kara [77]; the main components of RDF are PET plastic, paper, plastic bags, and textiles. Nonetheless, the composition of RDF and its calorific value can vary between places [78]. The RDF formulated by Zhao et al. [79] consists of 42% plastics, 41% paper or cardboard, 7% textiles, and 10% horticultural waste, based on Singapore's waste composition. The net calorific value of the RDF was higher than that of Kara [77], which may be attributed to the variation in RDF composition. Furthermore, when Zhao et al. [79] included chicken manure and biomass waste into the formulation of RDF, the moisture content of RDF significantly increased from 7.8% up to 23.8% while the net calorific value dropped from 23.7 to 16.1 MJ/kg. Hence, this proves that the regional variations of MSW composition,

TABLE 4: The composition of MSW and RDF [77].

Content	Input: MSW (%)	Output: RDF (%)
Textile	17.1	66.0
Paper	25.4	17.1
Organic fraction	22	0
Plastic bag	15.2	13.3
Napkin	7.0	0
Other combustible	3.7	0
PET-plastic	3.2	3.6
Wood	1.9	0
Bone	0.3	0
Tetrapac	1.2	0
Sack	0.5	0
Tin	0.6	0
Glass	0.7	0
Aluminum	0.4	0
Stone	0.8	0
Total	100	100

TABLE 5: Calorific value of RDF.

Reference	Calorific value (MJ/kg)
[80]	12.00–2100
[81]	12.69
[51]	19.90
[70]	14.64
[82]	19.40
[83]	19.67
[84]	17.79
[79]	16.10–23.70
[85]	14.90
[86]	25.02
[72]	15.21
[87]	29.11
[88]	15.97
[89]	17.90
[90]	26.82–29.26

technology level, equipment, and formulation would influence the performance of RDF. Table 5 shows the varied calorific values of the RDF, ranging from around 12.00 to 23.70 MJ/kg. The calorific value of RDF, in general, is higher than the calorific value of MSW.

(1) *Impact of MSW as AF to Cement and Environment.* Kara et al. [70] examined the potential of RDF made from MSW as an AF in cement manufacturing in Istanbul, Turkey. The RDF is composed of 66% textiles, 17.1% paper, 13.3% plastic bags, and 3.6% PET plastic. The RDF was mixed with the main fuel at a ratio in the range of 0%–20% to produce clinker, and the outcomes indicated that clinker produced with 20% RDF was satisfactory. However, when the proportion of RDF was increased, the C_3S content of the clinker was decreased (max. 5%) while belite (C_2S) content was increased (max. 3%). However, Haračić et al. [90] reported C_3S content

of clinker was increased by 2% while C_2S content decreased by 2%. This is probably due to the variation in the quality of RDF used, which is clearly indicated by the difference in calorific value of the two RDF used (Table 5). In addition, the humidity of the RDF used by Kara et al. [70] was 25%, which is higher than the RDF of Haračić et al. [90], 17.5%. Thus, it can be suggested that the variation in the clinker composition is highly due to the quality of the RDF, particularly the humidity, that influences the clinker calcination process.

On the other hand, there is a concern when using RDF as AF in the cement kiln, namely its high chlorine content that would be deleterious to the concrete [70, 77, 91]. The chlorine content of the RDF investigated by Kara et al. [70] was reported to be 0.95%. On the other hand, Özkan et al. [92] reported that the chlorine content of the RDF can be up to 1.41% while Hemidat et al. [72] stated that the chlorine content in RDF varied from 0.56% to 1.20%. The chlorine content is possibly due to the presence of plastic material in the mixture. In addition, high chlorine content could be a risk to the cement kiln as chlorine-based salts are highly volatile under the cement kiln condition, thus being the major driver of the formation of coatings and cloggings in the preheater [86]. A similar observation was observed by a waste-to-energy plant in Chengdu, China where the superheater steel tubes were corroded [91].

In 1977, the existence of dioxins were found in the emission and fly ash of a RDF incineration plant [93]. Considering the high chlorine content possessed by RDF, the effect of MSW, or particularly the RDF, adoption in cement plant toward the environment requires great attention. This is due to it is considered a source of acidic contaminants and reactive components to create dioxins [94]. In general, the adoption of MSW or RDF as AF in the cement industry delivers promising environmental benefits. Sai Kishan et al. [14] reported that the effluent gas from the mixed fuel showed a reduction in the content of SO_x , NO_x , and polycyclic aromatic hydrocarbon (PAH) content. Kara [77] also indicated that the amount of NO_x , gaseous heavy metals as well as dioxins and furans decreased with an increasing amount of RDF. This could be the high temperature in the cement kiln that encourages the formation of new minerals between the chlorine and other elements in the raw meals that avoiding dioxins formation [93]. In addition, the high temperature and long retention time of the cement kiln system aids in completely breaking down the harmful substances possessed by RDF.

3.1.3. *Sewage Sludge.* SS is a by-product of wastewater treatment, and management of SS has grown increasingly difficult over the years. This is due to the fact that besides containing high organic and mineral content, high water content, and the ability to rot, the SS contains toxic substances such as heavy metals, PAHs, PCBs, and dioxin [95], which are deemed harmful to human being and the environment. Besides that, due to the high volume of wastewater being treated, the volume of SS generated spikes up; the volume of SS generated is reported to be approximately 3% of the volume of treated wastewater [96]. Thus, the disposal of SS



FIGURE 7: Dewatered SS [96].

TABLE 6: Proximate analysis of dewatered SS [100].

Component	Raw SS (%)
Moisture	80
Ash	9.1
Volatile matter	10.1
Fixed carbon	0.8

has become a major waste management issue in response to worries about landfill space and the buildup of heavy metals or pathogenic organisms in soils [1, 97]. Furthermore, to treat and manage the SS properly that meets the environmental requirements, the cost could be as much as 50% of the operational cost of the wastewater treatment plant [95].

Considering the harmful effects, high treatment cost, and large volume of SS, the necessity to employ another treatment method is in high demand. The most commonly adopted technique of SS management is in agriculture, where the SS works as a fertilizer. Nonetheless, enforcement of legislation reducing such application, which is attributed to the presence of heavy metals and pathogenic microorganisms in SS that would become a significant problem for the soil and groundwater [96, 98]. Adoption of SS as an AF in the cement industry has been investigated and proved feasible, attributed to its calorific energy potential [99] and the high incineration temperatures in the cement kiln can sufficiently destroy the potentially dangerous compounds and substances possessed by SS, making it an appropriate method of handling SS.

Since SS is made up of water and organic matter in the form of fine-grained solid suspensions or colloids, the raw SS typically contains a significant volume of water [14, 15, 96]. Regardless of the sludge disposal method, the SS is often mechanically dewatered (Figure 7). Table 6 depicts the proximate analysis of dewatered SS from a municipal wastewater treatment plant located in Beijing, China [100]. Although the SS is dewatered, it still contains a substantially high moisture content of around 80%. Such high moisture content usually leads to a significantly low calorific value. The calorific value of dewatered SS reported by Liu et al. [100] was around 2.43 MJ/kg. A similar outcome has been reported by Rečko

TABLE 7: Calorific value of dried SS.

Reference	Calorific value (MJ/kg)
[37]	15.80
[103]	14.80
[101]	8.30
[104]	10.70–13.00
[105]	12.60
[106]	15.60
[107]	10.73
[108]	14.40–14.60
[86]	14.94–17.72

[96], where the calorific value of municipal SS was only 0.89 MJ/kg when the moisture content is about 80.22%. Thus, dewatered SS, or raw SS, is not suitable for the AF application due to its extremely low calorific value caused by the high moisture content.

When dewatered SS is used as a fuel source in the cement industry, coal consumption will increase. This accounts for the extra energy required to evaporate the moisture in the dewatered SS [100]. Therefore, to adopt SS as an AF source, thermally drying the dewatered SS is a must [101], or the dewatered SS needs to be mixed with other fuels. This is because the calorific value of SS is highly dependent on the degree of dryness as well as the content of organic dry matter [96]. Thus, drying of SS can increase its calorific value [102]. According to Husillos Rodríguez et al. [101], the solid content of dewatered SS increased from 25% to 93% after the thermal drying process; higher solid content generally leads to higher calorific value. On the other hand, dried SS might be introduced into the cement kiln using the same feeding technology employed on pulverized coal due to its being a free-flowing powder [101], hence the additional cost and complexity on the new feeding route could be resolved. Nevertheless, even though extra energy is needed to dry the SS, the associated benefits of resolving the troublesome SS disposal issue and the manufacture of a sustainable fuel should be taken into consideration [101]. The calorific value of various dried SS is listed in Table 7.

(1) *Impact of SS as AF to Cement and Environment.* According to several investigations [100, 102, 109], the adoption of SS as AF has no detrimental effects on the clinker quality. Nonetheless, other compounds contained in the SS have the potential to migrate into the clinker as the ashes will be absorbed into the clinker during calcination. Sobik-Szołtysek and Wystalska [102] stated that the degree of clinker contamination following the use of SS as AF can rise or fall depending on the substances' concentration.

Husillos Rodríguez et al. [101] investigated the effect of thermally dried SS as an AF on portland cement clinker production. As the dried SS was mostly made of combustible organic matter (56% by mass), the remaining inorganic matter would stay as ashes and be incorporated into the clinker upon burning [101]. The high P_2O_5 content in the employed SS (Table 8) may be problematic as it is believed to influence the quality of the clinker. A similar composition is reported

TABLE 8: Chemical composition of dried SS [101].

SiO ₂	Al ₂ O ₃	CaO	MgO	MnO	P ₂ O ₅	K ₂ O	TiO ₂	LOI*
3.72	2.56	7.62	0.60	0.05	6.43	0.53	0.23	66.45

*Loss on ignition at 1,000°C.

TABLE 9: Chemical composition of cement produced with dried SS as AF [101].

Cement	Content (%)									
	SiO ₂	Al ₂ O ₃	CaO	MgO	SO ₃	Na ₂ O	K ₂ O	Cl	P ₂ O ₅	f-CaO
With SS	21.01	5.30	66.10	1.51	0.18	0.22	0.41	0.08	1.66	2.64
Without SS	20.38	4.78	65.10	1.42	0.02	0.08	0.36	0.00	0.04	0.95

by Lopes et al. [81], where the P₂O₅, sulfur, and nitrogen contents were 21.7%, 1.34%, and 4.6%, respectively.

Table 9 compares the chemical composition of the cement produced when dried SS was used as AF. The chemical composition of the manufactured cement has not changed significantly, except for the SO₃, P₂O₅, and free lime content. This proves that the ashes have been incorporated into the clinker. According to Staněk and Sulovský [110], at 0.7 wt% of P₂O₅, diminished C₃S content had been observed. C₃S formation was found to be completely suppressed at 4.5 wt% of P₂O₅, even after a 4 hr, 1,450°C clinkering process. This is possibly due to the effect of phosphorus on the α H orthorhombic polymorph of C₂S, which delays the crystallization of C₃S and affects its crystal size as well as reduces the viscosity of the melt phases [110, 111]. Therefore, when dried SS was used as an AF, a higher free lime content (Table 9) and a reduction of the C₃S/C₂S ratio from 7.7 to 3.3 have been reported by Husillos Rodríguez et al. [101]. Similar outcomes have been reported in the work of Kwon et al. [112] and Lin et al. [113]. In addition, the cement's initial and final setting times are increased when SS has been cocombusted. When SS was utilized as AF, the initial and final setting increased from 103 to 123 and 140 to 158 min, respectively [109]. Another study carried out by Lin et al. [113] indicates that clinker with a P₂O₅ content of 0.85% possessed extremely long initial and final setting times, which were 8.8 and 11.43 hr, respectively.

Incorporation of SS as an AF in the cement industry has been reported for its reduction in NO_x emissions [100, 109, 114]. Gu et al. [115] indicated that coprocessing of SS in a cement kiln at high temperatures and low oxygen content could yield significant NO_x reduction. On the other hand, SS was coincinerated at a cement plant in Cyprus, and the gaseous emissions were measured. The gaseous heavy metal concentrations amount to only 0.7960 mg/Nm³, which is only 16% of the allowable limit of 5 mg/Nm³. Zabaniotou and Theofilou [116] reported that the emission of furan and dioxin was found to be only 0.006 ng/Nm³ when SS was used, which is also lower than the allowable concentration of 0.1 ng/Nm³.

3.1.4. Meat and Bone Meal. MBM is created in rendering factories by combining, crushing, and cooking animal offal and bones. Nonetheless, after the discovery of bovine spongiform encephalopathy (BSE), MBM waste management has

TABLE 10: Proximate analysis of MBM and coal [117].

Component	MBM (%)	Coal (%)
Moisture	6.8	4.2
Ash	34.4	6.2
Volatile matter	32.7	36.6
Fixed carbon	26.1	53.0

become difficult as a result of the fact that MBM residue is forbidden to be used in animal feed or disposed of in landfills [16, 117]. Thus, a safe MBM disposal approach is required to avoid pathologically transmissible infections. Since high-temperature treatments, especially those with extended residence times and ample oxygen supplies, can eradicate the BSE bacteria, thermal treatment methods like incineration or gasification have become viable alternative. Energy recovery through the use of MBM in cement plants has been widely considered as a way to improve the waste management hierarchy [118]. Table 10 shows the proximate analysis of coal and MBM. The ash produced after the MBM combustion was about 20%–30% of its original weight, indicating that a huge volume had been eliminated [119, 120]. However, it should be noted that due to MBM's high-fat content, continual feeding into a fluidized bed reactor or combustor might cause significant agglomeration in the feeding system [121]. Similar as other AF, the calorific value of MBM, as shown in Table 11, varies due to the variation in their composition.

(1) Impact of MBM as AF to the Cement and Environment. MBM, in general, exhibits a high P₂O₅ content. According to Lopes et al. [81] and Ariyaratne et al. [123], the P₂O₅ content in MBM was 35.65% and 13.00%, respectively. The high P₂O₅ content would be deleterious to the quality of clinker as it would stabilize the C₂S and hence diminish the formation of C₃S. In addition, a prolonged cement setting time is usually observed with high P₂O₅ content. On the other hand, the high calcium content in MBM could be another potential risk as it would increase the free-lime content of clinker. According to Ariyaratne et al. [123], the free-lime content in the clinker was increased from around 1.25% to 3% when the feed rate of MBM (CaO = 13.3%) was 7 t/hr, indicating an improper burning process and poorer quality of clinker.

By contrast, the calcium content is beneficial in reducing SO₂ emissions. Rahman et al. [38] claimed that the MBM's

TABLE 11: Calorific value of MBM.

Reference	Calorific value (MJ/kg)
[37]	16.20
[81]	14.47
[122]	18.19
[123]	18.51
[107]	17.45
[62]	30.71
[86]	17.58
[124]	18.42

high calcium concentration reduced the SO_2 emissions as it could retain most of the SO_2 formed. This is due to the ability of calcium to absorb sulfur [52]. Rahman et al. [62] reported that the SO_2 emissions were reduced from 280 to around 245 mg/Nm^3 when 30% of MBM was adopted in the fuel mix. A similar outcome has been reported by Aranda Usón et al. [16], where the SO_2 emissions with 100% MBM and 100% coal were reported to be 14 and 713 mg/Nm^3 , respectively.

Nevertheless, the employment of MBM as AF could increase the NO_x emission, which is attributed to the high nitrogen content in the MBM [16]. Lopes et al. [81] and Bujak et al. [124] stated that the nitrogen content in MBM was around 8.5%. Rahman et al. [62] reported that the NO_x concentration was increased when MBM was employed in the fuel mix. With 30% of MBM, NO_x emission increased by about 9%. On the other hand, Abad et al. [125] reported that cocombustion of MBM with coal had no significant impact on the furan and dioxin emissions. To determine the effects of various MBM parameters on the coal cocombustion process, Gulyurtlu et al. [117] conducted several experiments with various MBM/coal ratios. This study revealed that increasing the MBM ratio had negligible effect on emissions, particularly those of CO and SO_2 . However, because of the high nitrogen content of MBM, its use may result in an increase in NO_x emissions.

3.2. Advantages of AF in the Cement Industry. The adoption of AF in the cement manufacturing industry has several benefits. First, AF is relatively cheaper than the commonly used fossil fuels. This is because they are usually waste products that need to be managed, either disposed of at a landfill or incinerated. Thus, extra costs, in terms of environmental or operation, are incurred by this process. With the application of AF, the cost can be reduced, including the material cost, transportation cost, and incineration cost. A tipping fee will be provided for collecting the wastes. Pitak et al. [126] reported that using 10% AF as a substitute for coal fuel results in a net savings of 754.7 USD/hr. According to Trezza and Scian [127], maximum cost reduction can be achieved if the AF can be used with minimal preparation. In addition, the use of AF can preserve nonrenewable fossil fuels, which is a great benefit to the environment while offering a safe option for the disposal of wastes, particularly those that are organic or biologically hazardous, and can alleviate the landfill shortage problem. Furthermore, Horsley et al. [15] stated

that it is considerably cheaper to adapt a cement kiln to incinerate the wastes instead of building a new, dedicated waste incinerator.

Another key advantage of employing AF in the cement industry is that the fuel combustion process in the cement kiln is a nonwaste process because the ashes can be incorporated into the clinker [16]. However, the incorporation of such ashes may have a certain influence on the quality of the cement, thus, a comprehensive understanding of the waste materials to be used as AF is a must. On the other hand, employing wastes as AF in the cement industry has been proven to reduce the common hazard and pollution caused by typical disposal methods like landfilling. For instance, utilization of MBM as AF can help to eliminate the BSE bacteria. In addition, the alkaline environment in the cement kiln is an important feature for such an application. The basic environment aids in the neutralization and capture of acid gas components that are being produced during the combustion process. Furthermore, rather than being released into the atmosphere, heavy metals that condensed on dust molecules are returned to the clinker [10].

3.3. Disadvantages of AF in Cement Industry. Although full or partial conversion of the thermal energy supply from conventional fossil fuels to AF possesses several attractive benefits, several challenges are present as AF exhibits different characteristics, even of the same type, compared to conventional fossil fuels. Some of the major challenges that have been reported when using AF in the cement industry are, but not limited to, poor heat distribution, unstable precalciner operation, blockages in the preheater cyclones, and buildups in the kiln riser ducts. In some investigations, gaseous emissions such as SO_2 , NO_x , and CO emissions were reported to have increased when AF was used [127], which is attributed to the composition of the respective AF. AF with higher sulfur and nitrogen content should be given more attention. The proportion of AF and the filter system of the cement kiln can also be the potential cause. Therefore, extensive investigations and monitoring are necessary due to the complexity of adopting AF in cement plants.

Another major concern of AF utilization in the cement industry is the incorporation of combustion residues, or ashes, into the clinker, which affects the clinker quality. The amount and type of ashes introduced by AF are largely different from those introduced by fossil fuels, introducing several unexpected components into the kiln [12]. Phosphorus, which is primarily found in MBM or SS, is a notable example. The performance of cement may be affected by the presence of phosphorus, such as decreased early strength or prolonged setting times [128]. Besides that, higher free-lime content may be observed in the clinker when AF with high phosphorus and calcium content is adopted. As a result, if the quality of a clinker is compromised, the benefits of AF utilization may be negated.

Switching to AF is sometimes detrimental to the production cost at the initial stage (conversion process), which accounts for the investment costs associated with the adjustment or replacement of the burner, implementation of the

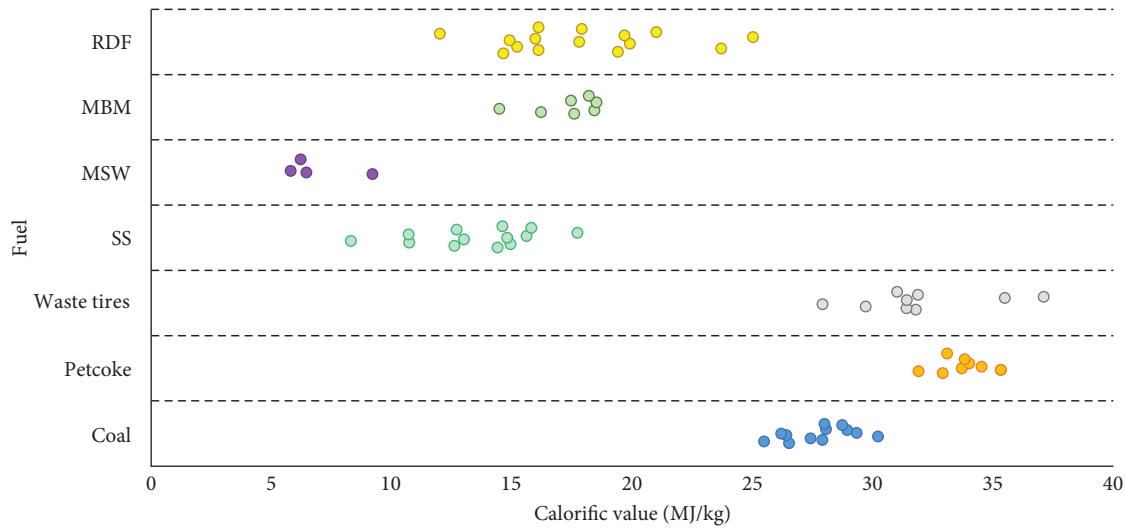


FIGURE 8: Calorific value of fuels in the cement industry [1, 9, 37, 51–56, 62, 72, 73, 77, 79–86, 88, 101, 103–108, 122–124, 129, 130].

AF delivery system, storage facilities for AF, and fuel distribution system [38]. On the other hand, the properties of AF are usually different from the traditional fuels. Therefore, in order to achieve uniform heating values, reconditioning operations (cleaning, drying, and homogenizing) must be conducted before the usage of AF, and preprocessing equipment must be installed [16].

4. Comparison of AF in Cement Industry

Figure 8 shows the calorific value of the conventional fuels (coal and petcoke) and AF that have been discussed in this work, namely waste tires, SS, MSW, RDF, and MBM. Generally, only the calorific values of the waste tires are comparable or higher than those of conventional fuels. On the other hand, the calorific value of MSW is the lowest, which may be attributed to its high organic content and moisture content. Nonetheless, the conversion of MSW into RDF significantly improves the calorific value.

According to Figure 8, it is observed that the calorific value of AF is relatively inconsistent compared to the calorific value of conventional fuels. This is attributed to the heterogeneous characteristics and properties of AF, even of the same type. Many factors can contribute to the inconsistency, including regions, the source of the wastes, composition of the wastes, technology to process the wastes, and more. Nonetheless, the standard deviation for the calorific value of the AF reported here is typically less than 3%, except for RDF. The standard deviation of the calorific value for coal, petcoke, waste tires, SS, and RDF is 1.44%, 1.03%, 2.79%, 2.54%, and 3.54%, respectively. MSW and MBM are excluded due to the limited data. The high standard deviation exhibited by RDF could be due to the source used to produce RDF, which is MSW. It is well known that the composition of MSW is different between places as it is highly dependent on various factors such as people's behavior, legislation, and more. Thus, these factors result in a RDF with unique composition and properties.

Based on this work, it can be said that waste tires may be the best option due to the following reasons:

- (i) The calorific value of waste tires is high and comparable to conventional fuels. Its caloric value is within the class 1 classification according to BS EN ISO 21640.
- (ii) The composition of tires is relatively consistent compared to MBM, MSW, RDF, and SS.
- (iii) The wires in tires can be used as an iron source in clinker production.
- (iv) The pretreatment of waste tires is simpler and less costly among others.

Although the high Zn content in waste tires could be problematic, however, the effect is negligible as long as the Zn content is below the threshold limits. Thus, a proper proportion while using waste tires in the fuel mix is required. Similar considerations shall be applied to any AF, especially those derived from waste. This is due to even of the same type, each AF is unique in nature.

On the other hand, the effect of the AF in the cement industry on the environment is found to be inconsistent, as detailed in Sections 3.1.1, 3.1.2, 3.1.3, and 3.1.4. This is due to the fact that the composition and properties of the AF may be different between regions. Furthermore, even in the same region, the technology, flue gas capturing system as well as fuel formulation between different plants may be different, which highly depends on the respective judgment and consideration. Thus, a comprehensive investigation on the feasibility of an AF to be employed needs to be comprehensively investigated before putting into application, based on the local context.

Therefore, it is inappropriate to conclude that one type of AF is superior to the others. Generally, the best AF option would be the one that aids in cost reduction, improves or maintains the current clinker quality, and does not cause additional or tremendous negative environmental impacts.

Nevertheless, it is practically impossible to have the best type of AF. The benefits of using AF in the cement industry while minimizing its negative impacts can be achieved through careful analysis and consideration. For instance, the MCDM method can be employed to facilitate the AF selection process [43, 44].

5. Conclusion

Although conventional carbon mitigation measures that are often proposed like energy efficiency improvements, use of AFs, and increasing materials substitution can only help to reduce the emissions associated with a small share of climate impacts [29], these are still regarded as a critical step in initiating and supporting the CO₂ reduction mission while emerging and innovative technologies such as CCUS may take time to be widely implemented. Moreover, the conventional mitigation measures are relatively simpler and can be put into action immediately without substantial changes to the industry itself.

There are various kinds of AFs available to be adopted in the cement industry, and four commonly used AF have been discussed, which are waste tires, MSW, SS, and MBM. Most of the investigations proved the feasibility of using AF in the cement manufacturing industry. Based on this work, the best AF option would be waste tires by considering its high calorific value and relatively easier handling process. Nevertheless, it is inappropriate to conclude that a type of AF is superior than the other as there are many factors to be considered besides the calorific value, including the availability, the local legislation, the technology, the price, the emissions, and more. Furthermore, even the same type of AF may have different combustion effects since they are not tailored for this purpose, and thus their constituents cannot be precisely controlled.

In a nutshell, the selection of AF always necessitates a thorough evaluation and careful consideration to avoid incurring additional costs, creating environmental issues, or degrading clinker quality. The MCDM approach is highly recommended to be used to analyze the suitability of an AF before putting it into the application.

Data Availability

The data supporting this work are from previously reported studies, which have been cited. The processed data are available from the corresponding author upon request.

Conflicts of Interest

The authors declare that they have no conflicts of interest.

Acknowledgments

The authors would like to acknowledge the financial support provided by Universiti Malaya under the funding IIRG002B-2020IISS entitled “Impacts of local MSW residue from co-processing on quality of low carbon cement.”

References

- [1] B. Nakomcic-Smaragdakis, Z. Cepic, N. Senk, J. Doric, and L. Radovanovic, “Use of scrap tires in cement production and their impact on nitrogen and sulfur oxides emissions,” *Energy Sources, Part A: Recovery, Utilization, and Environmental Effects*, vol. 38, no. 4, pp. 485–493, 2016.
- [2] R. M. Andrew, “Global CO₂ emissions from cement production,” *Earth System Science Data*, vol. 10, no. 1, pp. 195–217, 2018.
- [3] L. Proaño, A. T. Sarmiento, M. Figueredo, and M. Cobo, “Techno-economic evaluation of indirect carbonation for CO₂ emissions capture in cement industry: a system dynamics approach,” *Journal of Cleaner Production*, vol. 263, Article ID 121457, 2020.
- [4] P. J. M. Monteiro, S. A. Miller, and A. Horvath, “Towards sustainable concrete,” *Nature Materials*, vol. 16, pp. 698–699, 2017.
- [5] K. Korczak, M. Kochański, and T. Skoczkowski, “Mitigation options for decarbonization of the non-metallic minerals industry and their impacts on costs, energy consumption and GHG emissions in the EU—systematic literature review,” *Journal of Cleaner Production*, vol. 358, Article ID 132006, 2022.
- [6] J. G. Speight, *Handbook of Industrial Hydrocarbon Processes*, Gulf Professional Publishing, 2019.
- [7] M. Antunes, R. L. Santos, J. Pereira, P. Rocha, R. B. Horta, and R. Colaço, “Alternative clinker technologies for reducing carbon emissions in cement industry: a critical review,” *Materials*, vol. 15, no. 1, Article ID 209, 2022.
- [8] A. M. Rashad, “An exploratory study on high-volume fly ash concrete incorporating silica fume subjected to thermal loads,” *Journal of Cleaner Production*, vol. 87, pp. 735–744, 2015.
- [9] A. M. Castañón, L. Sanmiquel, M. Bascompta, A. Vega y de la Fuente, V. Contreras, and F. Gómez-Fernández, “Used tires as fuel in clinker production: economic and environmental implications,” *Sustainability*, vol. 13, no. 18, Article ID 10455, 2021.
- [10] E. Mokrzycki, A. Uliasz-Bocheńczyk, and M. Sarna, “Use of alternative fuels in the Polish cement industry,” *Applied Energy*, vol. 74, no. 1–2, pp. 101–111, 2003.
- [11] E. Mokrzycki and A. Uliasz-Bocheńczyk, “Alternative fuels for the cement industry,” *Applied Energy*, vol. 74, no. 1–2, pp. 95–100, 2003.
- [12] M. Schneider, M. Romer, M. Tschudin, and H. Bolio, “Sustainable cement production—present and future,” *Cement and Concrete Research*, vol. 41, no. 7, pp. 642–650, 2011.
- [13] G.-B. Hong, C.-F. Huang, H.-C. Lin, and T.-C. Pan, “Strategies for the utilization of alternative fuels in the cement industry,” *Carbon Management*, vol. 9, no. 1, pp. 95–103, 2018.
- [14] G. Sai Kishan, Y. Himath kumar, M. Sakthivel, R. Vijayakumar, and N. Lingeshwaran, “Life cycle assesment on tire derived fuel as alternative fuel in cement industry,” *Materials Today: Proceedings*, vol. 47, no. 15, pp. 5483–5488, 2021.
- [15] C. Horsley, M. H. Emmert, and A. Sakulich, “Influence of alternative fuels on trace element content of ordinary portland cement,” *Fuel*, vol. 184, pp. 481–489, 2016.
- [16] A. Aranda Usón, A. M. López-Sabirón, G. Ferreira, and E. L. Sastresa, “Uses of alternative fuels and raw materials in the cement industry as sustainable waste management options,” *Renewable and Sustainable Energy Reviews*, vol. 23, pp. 242–260, 2013.

- [17] IEA, *Global Cement Production, 2010–2019*, IEA, 2020.
- [18] U.S. Geological Survey, “Mineral commodity summaries 2022,” 202, 2022.
- [19] U.S. Geological Survey, “Mineral commodity summaries 2023,” 210, 2023.
- [20] G. Churkina, A. Organschi, C. P. O. Reyer et al., “Buildings as a global carbon sink,” *Nature Sustainability*, vol. 3, pp. 269–276, 2020.
- [21] K. A. Clavier, J. M. Paris, C. C. Ferraro, and T. G. Townsend, “Opportunities and challenges associated with using municipal waste incineration ash as a raw ingredient in cement production—a review,” *Resources, Conservation and Recycling*, vol. 160, Article ID 104888, 2020.
- [22] A. Jankovic, W. Valery, and E. Davis, “Cement grinding optimisation,” *Minerals Engineering*, vol. 17, no. 11–12, pp. 1075–1081, 2004.
- [23] S. Sarawan and T. Wongwuttanasatian, “A feasibility study of using carbon black as a substitute to coal in cement industry,” *Energy for Sustainable Development*, vol. 17, no. 3, pp. 257–260, 2013.
- [24] N. A. Madlool, R. Saidur, M. S. Hossain, and N. A. Rahim, “A critical review on energy use and savings in the cement industries,” *Renewable and Sustainable Energy Reviews*, vol. 15, no. 4, pp. 2042–2060, 2011.
- [25] N. A. Madlool, R. Saidur, N. A. Rahim, and M. Kamalisarvestani, “An overview of energy savings measures for cement industries,” *Renewable and Sustainable Energy Reviews*, vol. 19, pp. 18–29, 2013.
- [26] G. Oggioni, R. Riccardi, and R. Toninelli, “Eco-efficiency of the world cement industry: a data envelopment analysis,” *Energy Policy*, vol. 39, no. 5, pp. 2842–2854, 2011.
- [27] A. Cantini, L. Leoni, F. De Carlo, M. Salvio, C. Martini, and F. Martini, “Technological energy efficiency improvements in cement industries,” *Sustainability*, vol. 13, no. 7, Article ID 3810, 2021.
- [28] R. T. Kusuma, R. B. Hiremath, P. Rajesh, B. Kumar, and S. Renukappa, “Sustainable transition towards biomass-based cement industry: a review,” *Renewable and Sustainable Energy Reviews*, vol. 163, Article ID 112503, 2022.
- [29] O. Cavalett, M. D. B. Watanabe, K. Fleiger, V. Hoenig, and F. Cherubini, “LCA and negative emission potential of retrofitted cement plants under oxyfuel conditions at high biogenic fuel shares,” *Scientific Reports*, vol. 12, Article ID 8924, 2022.
- [30] N. Chatziaras, C. S. Psomopoulos, and N. J. Themelis, “Use of waste derived fuels in cement industry: a review,” *Management of Environmental Quality*, vol. 27, no. 2, pp. 178–193, 2016.
- [31] G. Habert, C. Billard, P. Rossi, C. Chen, and N. Roussel, “Cement production technology improvement compared to factor 4 objectives,” *Cement and Concrete Research*, vol. 40, no. 5, pp. 820–826, 2010.
- [32] W. Kurdowski and E. Jelito, “Rotary kilns in current cement industry,” *Cement Wapno Beton*, vol. 25, no. 2, pp. 127–136, 2020.
- [33] IEA, *Driving Energy Efficiency in Heavy Industries*, IEA, 2021.
- [34] S. Nie, J. Zhou, F. Yang et al., “Analysis of theoretical carbon dioxide emissions from cement production: methodology and application,” *Journal of Cleaner Production*, vol. 334, Article ID 130270, 2022.
- [35] WBCSD, *The Cement Sustainability Initiative: Our Agenda for Action*, WBCSD Geneva, Switzerland, 2002.
- [36] A. Naqi and J. G. Jang, “Recent progress in green cement technology utilizing low-carbon emission fuels and raw materials: a review,” *Sustainability*, vol. 11, no. 2, Article ID 537, 2019.
- [37] U. Kääntee, R. Zevenhoven, R. Backman, and M. Hupa, “Cement manufacturing using alternative fuels and the advantages of process modelling,” *Fuel Processing Technology*, vol. 85, no. 4, pp. 293–301, 2004.
- [38] A. Rahman, M. G. Rasul, M. M. K. Khan, and S. Sharma, “Recent development on the uses of alternative fuels in cement manufacturing process,” *Fuel*, vol. 145, pp. 84–99, 2015.
- [39] C. Mohanraj, T. Senthilkumar, and M. Chandrasekar, “A review on conversion techniques of liquid fuel from waste plastic materials,” *International Journal of Energy Research*, vol. 41, no. 11, pp. 1534–1552, 2017.
- [40] V. Sharma, A. K. Hossain, G. Griffiths et al., “Plastic waste to liquid fuel: a review of technologies, applications, and challenges,” *Sustainable Energy Technologies and Assessments*, vol. 53, Article ID 102651, 2022.
- [41] M. Muhammed Niyas and A. Shaija, “Performance evaluation of diesel engine using biodiesels from waste coconut, sunflower, and palm cooking oils, and their hybrids,” *Sustainable Energy Technologies and Assessments*, vol. 53, Article ID 102681, 2022.
- [42] R. G. dos Santos, C. L. Rocha, F. L. S. Felipe, F. T. Cezario, P. J. Correia, and S. Rezaei-Gomari, “Tire waste management: an overview from chemical compounding to the pyrolysis-derived fuels,” *Journal of Material Cycles and Waste Management*, vol. 22, pp. 628–641, 2020.
- [43] S. Erdogan and C. Sayin, “Selection of the most suitable alternative fuel depending on the fuel characteristics and price by the hybrid MCDM method,” *Sustainability*, vol. 10, no. 5, Article ID 1583, 2018.
- [44] B. Oztaysi, S. Cevik Onar, C. Kahraman, and M. Yavuz, “Multi-criteria alternative-fuel technology selection using interval-valued intuitionistic fuzzy sets,” *Transportation Research Part D: Transport and Environment*, vol. 53, pp. 128–148, 2017.
- [45] P. Grammelis, N. Margaritis, P. Dallas, D. Rakopoulos, and G. Mavrias, “A review on management of end of life tires (ELTs) and alternative uses of textile fibers,” *Energies*, vol. 14, no. 3, Article ID 571, 2021.
- [46] A. Luna Velasco, L. A. Lozoya Marquez, and G. Gonzalez Sanchez, “Potential of industrial wastes generated in Ciudad Juarez, Chihuahua, Mexico, as alternative fuels in a kiln,” *Revista Internacional de Contaminación Ambiental*, vol. 35, no. 3, pp. 713–722, 2019.
- [47] W. de Queiroz Lamas, J. C. F. Palau, and J. R. de Camargo, “Waste materials co-processing in cement industry: ecological efficiency of waste reuse,” *Renewable and Sustainable Energy Reviews*, vol. 19, pp. 200–207, 2013.
- [48] J. Fiksel, B. R. Bakshi, A. Baral, E. Guerra, and B. DeQuervain, “Comparative life cycle assessment of beneficial applications for scrap tires,” *Clean Technologies and Environmental Policy*, vol. 13, pp. 19–35, 2011.
- [49] S. A. Alfayez, A. R. Suleiman, and M. L. Nehdi, “Recycling tire rubber in asphalt pavements: state of the art,” *Sustainability*, vol. 12, no. 21, Article ID 9076, 2020.
- [50] United States Environmental Protection Agency, “Tire-derived fuel,” 2016.
- [51] S. Galvagno, G. Casciaro, S. Casu et al., “Steam gasification of tyre waste, poplar, and refuse-derived fuel: a comparative analysis,” *Waste Management*, vol. 29, no. 2, pp. 678–689, 2009.

- [52] M. P. M. Chinyama, "Alternative fuels in cement manufacturing," in *Alternative Fuel*, M. Manzanera, Ed., pp. 263–284, IntechOpen, 2011.
- [53] E. N. Laboy-Nieves, "Energy recovery from scrap tires: a sustainable option for small islands like Puerto Rico," *Sustainability*, vol. 6, no. 5, pp. 3105–3121, 2014.
- [54] P. Pathak, S. Gupta, and G. S. Dangayach, "Sustainable waste management: a case from Indian cement industry," *Brazilian Journal of Operations & Production Management*, vol. 12, no. 2, pp. 270–279, 2015.
- [55] B. Ślusarczyk, M. Baryń, and S. Kot, "Tire industry products as an alternative fuel," *Polish Journal of Environmental Studies*, vol. 25, no. 3, pp. 1263–1270, 2016.
- [56] D. Czajczyńska, K. M. Czajka, R. Krzyżyńska, and H. Jouhara, "Experimental analysis of waste tyres as a sustainable source of energy," *E3S Web of Conferences*, vol. 100, Article ID 00012, 2019.
- [57] F. Puertas and M. T. Blanco-Varela, "Empleo de combustibles alternativos en la fabricación de cemento. Efecto en las características y propiedades de los clínkeres y cementos," *Materiales De Construcción*, vol. 54, no. 274, pp. 51–64, 2004.
- [58] D. Czajczyńska, K. Czajka, R. Krzyżyńska, and H. Jouhara, "Waste tyre pyrolysis—impact of the process and its products on the environment," *Thermal Science and Engineering Progress*, vol. 20, Article ID 100690, 2020.
- [59] M. A. Mónica and A. N. Scian, "Scrap tire ashes in portland cement production," *Materials Research*, vol. 12, no. 4, pp. 489–494, 2009.
- [60] N. Gineys, G. Aouad, and D. Damidot, "Managing trace elements in portland cement—Part II: comparison of two methods to incorporate Zn in a cement," *Cement and Concrete Composites*, vol. 33, no. 6, pp. 629–636, 2011.
- [61] M. Soto-Felix, F. J. Baldenebro-Lopez, C. Carreño-Gallardo, and J. M. Herrera-Ramirez, "Hybrid cements with ZnO additions: hydration, compressive strength and microstructure," *Molecules*, vol. 27, no. 4, Article ID 1278, 2022.
- [62] A. Rahman, M. G. Rasul, M. M. K. Khan, and S. C. Sharma, "Assessment of energy performance and emission control using alternative fuels in cement industry through a process model," *Energies*, vol. 10, no. 12, Article ID 1996, 2017.
- [63] H. Schrama, M. Blumenthal, and E. C. Weatherhead, "A survey of tire burning technology for the cement industry," in *1995 IEEE Cement Industry Technical Conference. 37th Conference Record*, pp. 283–306, IEEE, San Juan, PR, USA, June 1995.
- [64] F. Carrasco, N. Bredin, and M. Heitz, "Gaseous contaminant emissions as affected by burning scrap tires in cement manufacturing," *Journal of Environmental Quality*, vol. 31, no. 5, pp. 1484–1490, 2002.
- [65] M. Prisciandaro, G. Mazzioti, and F. Veglió, "Effect of burning supplementary waste fuels on the pollutant emissions by cement plants: a statistical analysis of process data," *Resources, Conservation and Recycling*, vol. 39, no. 2, pp. 161–184, 2003.
- [66] J. A. Conesa, A. Gálvez, F. Mateos, I. Martín-Gullón, and R. Font, "Organic and inorganic pollutants from cement kiln stack feeding alternative fuels," *Journal of Hazardous Materials*, vol. 158, no. 2-3, pp. 585–592, 2008.
- [67] C. R. N. Ferreira, L. R. Infesta, V. A. L. Monteiro et al., "Gasification of municipal refuse-derived fuel as an alternative to waste disposal: process efficiency and thermochemical analysis," *Process Safety and Environmental Protection*, vol. 149, pp. 885–893, 2021.
- [68] F. Cucchiella, I. D'Adamo, and M. Gastaldi, "Strategic municipal solid waste management: a quantitative model for Italian regions," *Energy Conversion and Management*, vol. 77, pp. 709–720, 2014.
- [69] T. F. Astrup, D. Tonini, R. Turconi, and A. Boldrin, "Life cycle assessment of thermal waste-to-energy technologies: review and recommendations," *Waste Management*, vol. 37, pp. 104–115, 2015.
- [70] M. Kara, E. Günay, Y. Tabak, and Ş. Yıldız, "Perspectives for pilot scale study of RDF in Istanbul, Turkey," *Waste Management*, vol. 29, no. 12, pp. 2976–2982, 2009.
- [71] P. Sharma, P. N. Sheth, and B. N. Mohapatra, "Recent progress in refuse derived fuel (RDF) co-processing in cement production: direct firing in kiln/calcliner vs process integration of RDF gasification," *Waste and Biomass Valorization*, vol. 13, pp. 4347–4374, 2022.
- [72] S. Hemidat, M. Saidan, S. Al-Zu'bi, M. Irshidat, A. Nassour, and M. Nelles, "Potential utilization of RDF as an alternative fuel to be used in cement industry in Jordan," *Sustainability*, vol. 11, no. 20, Article ID 5819, 2019.
- [73] G. H. Nordi, R. Palacios-Bereche, A. G. Gallego, and S. A. Nebra, "Electricity production from municipal solid waste in Brazil," *Waste Management & Research*, vol. 35, no. 7, pp. 709–720, 2017.
- [74] A. Białowiec, M. Micuda, and J. A. Koziel, "Waste to carbon: densification of torrefied refuse-derived fuel," *Energies*, vol. 11, no. 11, Article ID 3233, 2018.
- [75] P. Wang, Y. Hu, and H. Cheng, "Municipal solid waste (MSW) incineration fly ash as an important source of heavy metal pollution in China," *Environmental Pollution*, vol. 252, pp. 461–475, 2019.
- [76] G. de Lorena Diniz Chaves, R. R. Siman, G. M. Ribeiro, and N.-B. Chang, "Synergizing environmental, social, and economic sustainability factors for refuse derived fuel use in cement industry: a case study in Espirito Santo, Brazil," *Journal of Environmental Management*, vol. 288, Article ID 112401, 2021.
- [77] M. Kara, "Environmental and economic advantages associated with the use of RDF in cement kilns," *Resources, Conservation and Recycling*, vol. 68, pp. 21–28, 2012.
- [78] R. K. Dhir, J. de Brito, C. J. Lynn, and R. V. Silva, "Municipal solid waste composition, incineration, processing and management of bottom ashes," in *Sustainable Construction Materials*, R. K. Dhir, J. de Brito, C. J. Lynn, and R. V. Silva, Eds., pp. 31–90, Woodhead Publishing
- [79] L. Zhao, A. Giannis, W.-Y. Lam et al., "Characterization of Singapore RDF resources and analysis of their heating value," *Sustainable Environment Research*, vol. 26, no. 1, pp. 51–54, 2016.
- [80] A. Gendebien, "Refuse derived fuel, current practice and perspectives," WRc Ref: CO5087-4, 2003.
- [81] H. Lopes, I. Gulyurtlu, P. Abelha et al., "Particulate and PCDD/F emissions from coal co-firing with solid biofuels in a bubbling fluidised bed reactor," *Fuel*, vol. 88, no. 12, pp. 2373–2384, 2009.
- [82] B. Reza, A. Soltani, R. Ruparathna, R. Sadiq, and K. Hewage, "Environmental and economic aspects of production and utilization of RDF as alternative fuel in cement plants: a case study of metro Vancouver waste management," *Resources, Conservation and Recycling*, vol. 81, pp. 105–114, 2013.

- [83] J. Karagiannis, C. Ftikos, and P. Nikolopoulos, "The use of wastes as alternative fuels in cement production," WOS:000697818400009, 2015.
- [84] A. Hajinezhad, E. Z. Halimehjani, and M. Tahani, "Utilization of refuse-derived fuel (RDF) from Urban waste as an alternative fuel for cement factory: a case study," *International Journal of Renewable Energy Research*, vol. 6, no. 2, pp. 702–714, 2016.
- [85] W. Paramita, D. M. Hartono, and T. E. B. Soesilo, "Sustainability of refuse derived fuel potential from municipal solid waste for cement's alternative fuel in Indonesia (a case at Jeruklegi Landfill, in Cilacap)," *IOP Conference Series: Earth and Environmental Science*, vol. 159, Article ID 012027, 2018.
- [86] G. Hannoun, A. Jaouad, L. Schebek, J. Belkziz, and N. Ouazzani, "Energetic potential and environmental assessment of solid wastes as alternative fuel for cement plants," *Applied Ecology and Environmental Research*, vol. 17, no. 6, pp. 15151–15168, 2019.
- [87] V. Kosajan, Z. Wen, F. Fei, C. D. Dinga, Z. Wang, and J. Zhan, "The feasibility analysis of cement kiln as an MSW treatment infrastructure: from a life cycle environmental impact perspective," *Journal of Cleaner Production*, vol. 267, Article ID 122113, 2020.
- [88] A. Sakri, A. Aouabed, A. Nassour, and M. Nelles, "Refuse-derived fuel potential production for co-combustion in the cement industry in Algeria," *Waste Management & Research: The Journal for a Sustainable Circular Economy*, vol. 39, no. 9, pp. 1174–1184, 2021.
- [89] M. Ungureanu, J. Jozsef, V. M. Brezoczki, P. Monka, and N. S. Ungureanu, "Research regarding the energy recovery from municipal solid waste in Maramures county using incineration," *Processes*, vol. 9, no. 3, Article ID 514, 2021.
- [90] N. Haračić, N. Merdić, I. Bušatlić, N. Bušatlić, A. Halilović, and Z. Osmanovic, "The influence of RDF (refuse derived fuels) on cement clinker reactivity," 2021.
- [91] W. Ma, T. Wenga, F. J. Frandsen, B. Yan, and G. Chen, "The fate of chlorine during MSW incineration: vaporization, transformation, deposition, corrosion and remedies," *Progress in Energy and Combustion Science*, vol. 76, Article ID 100789, 2020.
- [92] M. Özkan, K. Özkan, B. O. Bekgöz et al., "Implementation of an early warning system with hyperspectral imaging combined with deep learning model for chlorine in refuse derived fuels," *Waste Management*, vol. 142, pp. 111–119, 2022.
- [93] Y. Li, H. Wang, J. Zhang, J. Wang, and R. Zhang, "Research on dioxins suppression mechanisms during MSW co-processing in cement kilns," *Procedia Environmental Sciences*, vol. 16, pp. 633–640, 2012.
- [94] N. Watanabe, O. Yamamoto, M. Sakai, and J. Fukuyama, "Combustible and incombustible speciation of Cl and S in various components of municipal solid waste," *Waste Management*, vol. 24, no. 6, pp. 623–632, 2004.
- [95] A. Jabłońska-Trypuć, U. Wydro, L. Serra-Majem, A. Butarewicz, and E. Wolejko, "The comparison of selected types of municipal sewage sludge filtrates toxicity in different biological models: from bacterial strains to mammalian cells. Preliminary study," *Water*, vol. 11, no. 11, Article ID 2353, 2019.
- [96] K. Rečko, "Production of alternative fuels based on municipal sewage sludge and selected types of ELV waste," *Energies*, vol. 15, no. 16, Article ID 5795, 2022.
- [97] S. Naamane, Z. Rais, and M. Taleb, "The effectiveness of the incineration of sewage sludge on the evolution of physicochemical and mechanical properties of portland cement," *Construction and Building Materials*, vol. 112, pp. 783–789, 2016.
- [98] G. Przydatek and A. K. Wota, "Analysis of the comprehensive management of sewage sludge in Poland," *Journal of Material Cycles and Waste Management*, vol. 22, pp. 80–88, 2020.
- [99] Z. Yang and Z. Zhang, "Integrated utilization of sewage sludge for the cement clinker production," in *Energy Technology 2017*, L. Zhang, Ed., The Minerals, Metals & Materials Series, pp. 95–102, Springer, 2017.
- [100] H. B. Liu, J. Gu, L. Han, P. Wang, N. Zhang, and W. T. Cai, "Industrial practice of sewage sludge pump directly into cement kiln," in *Proceedings of the 3rd International Conference on Advances in Energy and Environmental Science 2015*, pp. 877–880, Atlantis Press, July 2015.
- [101] N. H. Rodríguez, S. Martínez-Ramírez, M. T. Blanco-Varela et al., "The effect of using thermally dried sewage sludge as an alternative fuel on portland cement clinker production," *Journal of Cleaner Production*, vol. 52, pp. 94–102, 2013.
- [102] J. Sobik-Szołtysek and K. Wystalska, "Coproducting of sewage sludge in cement kiln," in *Industrial and Municipal Sludge*, M. N. V. Prasad, P. J. de Campos Favas, M. Vithanage, and S. V. Mohan, Eds., pp. 361–381, Butterworth-Heinemann, 2019.
- [103] D. Vamvuka and S. Sfakiotakis, "Combustion behaviour of biomass fuels and their blends with lignite," *Thermochimica Acta*, vol. 526, no. 1–2, pp. 192–199, 2011.
- [104] S. Werle, "Potential and properties of the granular sewage sludge as a renewable energy source," *Journal of Ecological Engineering*, vol. 14, no. 1, pp. 17–21, 2013.
- [105] A. Kijo-Kleczkowska, K. Środa, and H. Otwinowski, "Study into combustion of sewage sludge as energetic fuel/badania spalania osadów ściekowych jako paliwa energetycznego," *Archives of Mining Sciences*, vol. 58, no. 4, pp. 1085–1110, 2013.
- [106] L. Jiang, J. Liang, X. Yuan et al., "Co-pelletization of sewage sludge and biomass: the density and hardness of pellet," *Bioresource Technology*, vol. 166, pp. 435–443, 2014.
- [107] M. Wzorek, "Characterization of physical and chemical properties of fuel containing animal waste," WOS:000697818400008, 2015.
- [108] A. Czechowska-Kosacka, W. Cel, J. Kujawska, and K. Wróbel, "Alternative fuel production based on sewage sludge generated in the municipal wastewater treatment," *Rocznik Ochrona Srodowiska*, vol. 17, no. 1, pp. 246–255, 2015.
- [109] P. Fang, Z.-J. Tang, J.-H. Huang, C.-P. Cen, Z.-X. Tang, and X.-B. Chen, "Using sewage sludge as a denitration agent and secondary fuel in a cement plant: a case study," *Fuel Processing Technology*, vol. 137, pp. 1–7, 2015.
- [110] T. Staněk and P. Sulovský, "The influence of phosphorous pentoxide on the phase composition and formation of portland clinker," *Materials Characterization*, vol. 60, no. 7, pp. 749–755, 2009.
- [111] M.-N. De Noirfontaine, S. Tusseau-Nenez, M. Signes-Frehel, G. Gasecki, and C. Girod-Labianca, "Effect of phosphorus impurity on tricalcium silicate T_1 : from synthesis to structural characterization," *Journal of the American Ceramic Society*, vol. 92, no. 10, pp. 2337–2344, 2009.
- [112] W.-T. Kwon, Y.-H. Kim, Y.-S. Chu, J.-K. Lee, I.-S. Kim, and S.-R. Kim, "Effect of P_2O_5 and chlorine on clinkering reaction," *Advances in Technology of Materials and Materials Processing Journal*, vol. 7, no. 1, pp. 63–66, 2005.
- [113] K.-L. Lin, D. F. Lin, and H. L. Luo, "Influence of phosphate of the waste sludge on the hydration characteristics of eco-cement," *Journal of Hazardous Materials*, vol. 168, no. 2–3, pp. 1105–1110, 2009.

- [114] D. Lv, T. Zhu, R. Liu et al., "Effects of co-processing sewage sludge in cement kiln on NO_x, NH₃ and PAHs emissions," *Chemosphere*, vol. 159, pp. 595–601, 2016.
- [115] Y. Gu, H. Cao, W. Liu et al., "Impact of co-processing sewage sludge on cement kiln NO_x emissions reduction," *Journal of Environmental Chemical Engineering*, vol. 9, no. 4, Article ID 105511, 2021.
- [116] A. Zabaniotou and C. Theofilou, "Green energy at cement kiln in Cyprus—use of sewage sludge as a conventional fuel substitute," *Renewable and Sustainable Energy Reviews*, vol. 12, no. 2, pp. 531–541, 2008.
- [117] I. Gulyurtlu, D. Boavida, P. Abelha, M. H. Lopes, and I. Cabrita, "Co-combustion of coal and meat and bone meal," *Fuel*, vol. 84, no. 17, pp. 2137–2148, 2005.
- [118] J. A. Conesa, A. Fullana, and R. Font, "Thermal decomposition of meat and bone meal," *Journal of Analytical and Applied Pyrolysis*, vol. 70, no. 2, pp. 619–630, 2003.
- [119] E. Deydier, R. Guilet, S. Sarda, and P. Sharrock, "Physical and chemical characterisation of crude meat and bone meal combustion residue: "waste or raw material?,"" *Journal of Hazardous Materials*, vol. 121, no. 1-3, pp. 141–148, 2005.
- [120] T. Staněk, P. Sulovský, and M. Boháč, "Mechanism and kinetics of binding of meat and bone meal ash into the portland cement clinker," *SN Applied Sciences*, vol. 2, Article ID 411, 2020.
- [121] E. Cascarosa, L. Gasco, G. García, G. Gea, and J. Arauzo, "Meat and bone meal and coal co-gasification: environmental advantages," *Resources, Conservation and Recycling*, vol. 59, pp. 32–37, 2012.
- [122] K. McDonnell, E. J. Cummins, C. C. Fagan, and M. Orjala, "Co-fuelling of peat with meat and bone meal in a pilot scale bubbling bed reactor," *Energies*, vol. 3, no. 7, pp. 1369–1382, 2010.
- [123] W. K. H. Ariyaratne, M. C. Melaaen, K. Eine, and L. A. Tokheim, "Meat and bone meal as a renewable energy source in cement kilns: investigation of optimum feeding rate," *Renewable Energy and Power Quality Journal*, vol. 1, no. 9, pp. 1244–1249, 2011.
- [124] J. Bujak, P. Sitarz, and M. Nakielska, "Multidimensional analysis of meat and bone meal (MBM) incineration process," *Energies*, vol. 13, no. 21, Article ID 5787, 2020.
- [125] E. Abad, K. Martínez, J. Caixach, and J. Rivera, "Polychlorinated dibenzo-*p*-dioxin/polychlorinated dibenzofuran releases into the atmosphere from the use of secondary fuels in cement kilns during clinker formation," *Environmental Science and Technology*, vol. 38, no. 18, pp. 4734–4738, 2004.
- [126] I. Pitak, D. Rinkevičius, R. Kalpokaitė-Dičkuvienė, A. Baltušnikas, and G. Denafas, "The strategy for conservation non-renewable natural resources through producing and application solid recovery fuel in the cement industry: a case study for Lithuania," *Environmental Science and Pollution Research*, vol. 29, pp. 69618–69634, 2022.
- [127] M. A. Trezza and A. N. Scian, "Burning wastes as an industrial resource: their effect on portland cement clinker," *Cement and Concrete Research*, vol. 30, no. 1, pp. 137–144, 2000.
- [128] S. Punkte and M. Schneider, "Effect of phosphate on clinker mineralogy and cement properties," *Cement International*, vol. 6, no. 5, pp. 80–93, 2008.
- [129] H. A. H. Ibrahim, "Determination of the calorific value of Syrian delayed petroleum coke," *International Journal of Petrochemical Science & Engineering*, vol. 1, no. 3, Article ID 00012, 2016.
- [130] M. Kara, E. Günay, Y. Tabak, U. Durgut, Ş. Yıldız, and V. Enç, "Development of refuse derived fuel for cement factories in Turkey," *Combustion Science and Technology*, vol. 183, no. 3, pp. 203–219, 2010.

Research Article

Effect of Fiber Treatments on the Mechanical Properties of Sisal Fiber-Reinforced Concrete Composites

Tsagazeab Yimer  and Abrham Gebre 

Department of Civil Engineering, School of Civil and Environmental Engineering, Addis Ababa University, Addis Ababa, Ethiopia

Correspondence should be addressed to Tsagazeab Yimer; tsegazeab.yimer@aait.edu.et

Received 27 August 2022; Revised 12 October 2022; Accepted 5 April 2023; Published 29 April 2023

Academic Editor: Kim Hung Mo

Copyright © 2023 Tsagazeab Yimer and Abrham Gebre. This is an open access article distributed under the Creative Commons Attribution License, which permits unrestricted use, distribution, and reproduction in any medium, provided the original work is properly cited.

The mechanical behavior of fiber-cement composites is significantly influenced by the interfacial bonding between the fiber and the cement matrix. However, natural fibers are less chemically compatible with the cement matrix. As a result, it is essential to modify the surface of natural fibers to achieve good fiber-matrix interfacial bonds. In the current study, sisal fibers intended for use as a reinforcement in concrete matrices were alkali treated with NaOH solutions (2%, 5%, and 10%) for 12 hrs, 24 hrs, and 48 hrs. Water absorption, tensile strength, and surface morphological changes in fibers were studied. The effect of fiber treatment on the concrete was also assessed by measuring its slump, compressive strength, flexural strength, and toughness. Alkali treatment was discovered to reduce the water absorption capacity of sisal fiber. On the contrary, fiber surface morphology and mechanical properties improved up to a point and then gradually declined. The addition of treated sisal fiber considerably increases concrete's flexural strength and toughness. However, an insignificant change in compressive strength was observed.

1. Introduction

The construction industry is booming around the globe. Unfortunately, this industry accounts for a significant share of climate change caused by carbon dioxide emissions worldwide. According to reference [1], the construction industry accounts for roughly 30% of global carbon dioxide emissions. Using renewable resources and green materials is one of many ways to reduce the carbon footprint of the construction sector to achieve more sustainable and eco-friendly development [2]. Among them, natural fibers obtained from renewable vegetables, such as sisal, jute, cotton, flax, and so on, seem to be a good alternative, considering their environmental friendliness [3]. As a result, using natural fibers as reinforcing materials in cement-based composites have taken a significant step toward more sustainable construction [4]. Using such fibers in concrete and cement products is thus appealing to developing countries, where natural fibers of various types are abundant.

Out of various vegetable natural fibers, sisal fiber, extracted from the Agave Sisalana plant in the form of long fiber bundles, is one of the most commonly cultivated natural fibers in tropical and subtropical regions such as Brazil, Tanzania, Kenya, and Ethiopia [5]. World sisal fiber production is estimated to be around 250,000 tons per year. According to FAO [5], Ethiopia accounts for nearly 0.3 percent of the global sisal production. Due to its low cost, low density, high strength, and widespread availability in many countries, sisal fiber ranks highly among the natural fibers available for use as a reinforcement in the construction industry [6].

Plant-based fibers are not ideal chemical bond partners for composite formation with a cement matrix. The high water absorption capacity of natural fibers causes volume expansion when fibers are added to the fresh cementitious matrix and results in contraction when the matrix dries, resulting in a partial loss of physical contact with the matrix and a formation of a very porous region [7]. For this reason,

surface treatments were generally applied to natural fibers to improve fiber-matrix interfacial adhesion in composite manufacturing [8].

The type of treatment is important as some treatments are more effective than others. Alkaline treatment is one of the most widely used chemical treatment methods for natural fibers. As mentioned by the authors of reference [9], two effects on the fiber surface resulting from the alkaline treatment are as follows: (1) a rough fiber surface resulted, which might also improve the adherence of the fiber with the matrix and (2) remove some hemicelluloses, waxes, and impurities from the fiber surface. Thus, the surface of the fibers becomes chemically more homogeneous, and the amount of cellulose exposed on the fiber surface is enhanced, generating better compatibility between the fiber and the matrix. Both the chemical concentration and the duration of the chemical treatment have an impact on the enhancement of fiber mechanical properties [10].

Jo et al. [11] studied the effect of alkali (NaOH) treatment on the mechanical properties of jute fiber-reinforced cement composite and fiber-matrix interface interaction. Their findings show that the alkali treatment of jute fibers increases tensile strength and percent elongation, which contributes to an increase in the mechanical strength of cement composites. Furthermore, the fibrillation of the fibers caused by the alkali treatment increases the effective surface area for bonding at the interface between the fiber and the matrix. Andiç-Çakir et al. [8] also reported that, after the NaOH treatment, due to the removal of some hemicelluloses, waxes, and impurities from the coir fiber surface, a rough fiber surface resulted, which might also improve the adherence of the fiber with the cement matrix. The upgrading contact between the fibers and the matrix results in the enhancement of the mechanical properties, especially the flexural strength of the composites.

As pointed out by Zhou et al. [12] the pretreatment of hemp fiber using $\text{Ca}(\text{OH})_2$ solution altered the bond strength of concrete composite considerably. They observed that the 28-day tensile and compressive strength of treated hemp fiber reinforced concrete (THFRC) were 16.9 and 10% higher, respectively, than untreated hemp fiber reinforced concrete (UHFRC) and that the fracture toughness of THFRC at 28 days was 7–13% higher than UHFRC. The authors attributed this improvement to treated hemp fiber's higher interfacial adhesion strength.

The high moisture absorption capacity and durability issue of vegetable fibers in the alkaline environment of the cement matrix is the primary concern in encouraging the widespread use of natural fibers in cementitious composites [13]. Ardanuy et al. [14] suggested that this durability problem of natural fibers in the cement matrix is associated with an increase in fiber fracture and a decrease in fiber pull-out due to a combination of weakening of the fibers by alkali attack and fiber mineralization provoked by migration of hydration products (mainly $\text{Ca}(\text{OH})_2$) to the fiber structure. The volume variation in the fibers due to their high-water absorption is another reason for to decrease in the durability of natural fiber in a cement-based composite [15].

Several approaches have been investigated to ensure the durability of natural fiber-reinforced cement-based composites. Among them, De Klerk et al. [10] investigated the effects of sisal fiber treatments such as NaOH, acetylation and combined alkali and acetylation on composite degradation. They discovered that the most effective treatment condition was a combination of alkali treatment and acetylation, followed by alkali treatment at low concentrations of sodium hydroxide, thereby improving the durability of sisal fibers in concrete. A significant decrease in strength was observed at higher sodium hydroxide concentrations. Moreover, Wei and Meyer [16] also evaluate the effects of thermal and Na_2CO_3 treatment on the degradation resistance of sisal fiber and the durability of sisal fiber-reinforced concrete. They found that both thermal and Na_2CO_3 surface treatments were shown to have the potential to improve the durability of sisal fiber in concrete.

Given the international trend toward green engineering and the development of sustainable building materials, the use of sisal fiber in cement-based composites was investigated to develop a sustainable building material. Even though there have been some recent studies [8, 11, 12] that attempt to address the effect of different natural fiber treatments on the durability and some other mechanical properties such as compressive strength and tensile strength of cement paste and mortar, the present study tries to investigate the impact of fiber treatment, exclusively NaOH treatment, in terms of the concentration of alkali solution and exposure periods of the chemical treatment, on the reinforcing sisal fiber properties and the corresponding concrete composite's compressive strength, flexural strength, and energy absorption characteristics (since the main contribution of fiber is shown in the postcracking stage of cement-based composites), thereby providing a theoretical foundation to be able to develop a sustainable and eco-friendly building unit.

2. Experimental Program

2.1. Materials. Sisal fiber obtained from the local Agave Sisalana plant was used as a reinforcing natural fiber for this research. The fibers are characterized as summarized in Table 1. Concerning aggregate, locally available river sand, and crushed gravel that satisfies the grading limits and other properties of ASTM C33 [17] were used.

To reduce hardening retardation caused by the glucose found in most natural fibers, the cement used for manufacturing the specimens was ordinary portland cement type I, manufactured by Dangote Cement PLC. OPC is identified as portland cement CEM I 42.5 R that conforms to the 42.5 R strength class of EN 197-1:2000 [18]. Commercially available sodium hydroxide, containing 99% concentration, was used as a surface modifier of the sisal fibers.

2.2. Fiber Preparation and Treatment. Before stepping into fiber treatment, the extracted sisal fiber was washed with pure water to remove any impurities from the extraction

TABLE 1: Properties of sisal fiber.

Fiber properties	Result
Fiber length	30 mm
Fiber diameter	0.15–0.18 mm
Aspect ratio	166–200
Tensile strength	517.2–602.7 MPa
Modulus of elasticity	9.2–13.1 GPa
Elongation (%)	2–2.4%
Color	Creamy white
Shape	Straight
Water absorption	93.05%

process, such as mucilage, and it was thoroughly dried in the open air. The sisal fiber bundle was then manually straightened and combed with a comb to remove any entanglement. Finally, because the isolated sisal fibers were too long to be used in the composite fabrication, they were cut to the required length of 30 mm with a pair of scissors.

The fiber treatment was made in 2, 5, and 10% (w/w; i.e., the mass percentage of solute in solution) sodium hydroxide (NaOH) solutions for 12, 24, and 48 hours, in which the fiber-to-solution weight ratio was 1:25. The alkaline treatment involved dissolving NaOH pellets according to the designated concentration. For instance, to make 1 kg of 2% NaOH concentrated solution, dissolve 20 g of NaOH pellet in 980 g of distilled water at a liquor ratio of 25:1. As reported by [10, 19], the treated sisal fibers were subsequently washed several times with distilled water containing acetic acid (1% w/w) to neutralize the excess NaOH from the sisal fiber surface (neutral pH measured for the fiber washing water), and then, the sample was thoroughly rinsed with distilled water. The pH of the rinse water was checked periodically using a pH meter. The rinsed sisal fibers were then spread out in the open air and left to dry for 2–3 days until constant weight measurements were attained. Treatment conditions are identified using the codes presented in Table 2.

2.3. Mix Design and Specimen Production. In this research, each mixture consisting of 389.5 kg/m³ cement, 743.06 kg/m³ sand, 1050.1 kg/m³ coarse aggregate, and a water-cement ratio of 0.494 was proportioned for the specified compressive strength class of C-25 (i.e., a target strength of 33.3 MPa) following ACI mix design methods [20].

The mix design for sisal fiber reinforced concrete (SFRC) was the same as that of control plain concrete, except those fibers were added. The mix designation of the concrete specimens is presented in Table 3. For clarity, an explicit nomenclature system for the samples is used in this study. For example, CM-N indicates concrete reinforced with sisal fiber treated with M% sodium hydroxide (NaOH) solution and soaked for N hours.

Six concrete cubes of size 150 mm were molded from each mix to determine the 7th- and 28th-day compressive strengths, and three prisms of size 100 mm × 100 mm × 500 mm are cast to determine flexural strength and flexural toughness, as shown in Figure 1. The concrete specimens were set in the relevant molds for 24 hours under

TABLE 2: Treatment conditions on sisal fiber.

NaOH (%)	Duration (hrs.)	Sample designation
0	0	Raw
2	12	2%–12 hr
2	24	2%–24 hr
2	48	2%–48 hr
5	12	5%–12 hr
5	24	5%–24 hr
5	48	5%–48 hr
10	12	10%–12 hr
10	24	10%–24 hr
10	48	10%–48 hr

TABLE 3: Experimental mixture design.

Mix designation	Sisal fiber (percent by cement weight)	NaOH (%)	Duration (hours)
Control	0	0	0
C0-0	1	0	0
C2-12	1	2	12
C2-24	1	2	24
C2-48	1	2	48
C5-12	1	5	12
C5-24	1	5	24
C5-48	1	5	48
C10-12	1	10	12
C10-24	1	10	24
C10-48	1	10	48

ambient conditions. After being removed from the molds, the casted cube and prism specimens were kept in a water-curing tank until testing.

2.4. Test Methods

2.4.1. Test Methods for Fiber

(1) Water Absorption. A water absorption test was performed to determine how the alkali treatment affected the fiber's water absorption capability. Six samples, each bundle of raw and treated sisal fibers weighing approximately 5 g, were initially dried in an oven at 80°C for 24 hours until they reached constant mass. The dried fiber bundle was then immersed in a beaker of distilled water, maintaining room temperature. After 24 hours, each bundle of fiber was removed from the water bath one by one, and all surface water was wiped off with a lint-free dry cloth. The amount of absorbed water in fiber (W_C %) was calculated using the following equation [21].

$$W_C = \frac{m_s - m_d}{m_d} * 100\%, \quad (1)$$

where W_C is water absorption in percent, m_s is the mass of surface dried fiber bundle, and m_d is the mass of oven dried fiber bundle.

(2) Scanning Electron Microscopy (SEM). The fiber's microstructure was investigated using SEM (JCM-6000Plus Benchtop SEM (JEOL), Japan) to characterize the sisal



FIGURE 1: Test samples. (a) Cube specimens and (b) beam specimens.

fiber surface morphological change and fiber condition as a function of the applied alkali treatment. The microscope was operated under an accelerating voltage ranging from 10 kV to 15 kV and a working distance of 19 mm for different magnifications. The samples of sisal were coated with a thin layer of silver before observation to eliminate the effects of charging during image collection. The obtained images were postprocessed using ImageJ, a Java-based image processing program. The components that are used for surface roughness analysis consideration (based on profile parameters from ISO 4287 [22]) are R_p (highest peak), R_v (lowest valley), R_t (the total height of the profile), and R_a (average roughness). A visualization of the roughness parameter values can be seen in Figure 2 [23].

(3) *Mechanical Properties.* The effect of chemical treatment on the mechanical properties of sisal fibers in terms of tensile strength, tensile modulus, and % elongation was determined using a 1 kN capacity texture analyzer (LLOYDЖ, TA plus Ametek, UK 2007). The tensile strength of the treated and untreated sisal fibers was measured following the standard test method for a single fiber tensile test ASTM D 3822-07 [24]. A gauge length of 100 mm was employed with a fixed loading rate of 15 N/min. The mechanical properties of a total of 5 single strand samples of sisal fiber from each alkali treatment condition were measured in this investigation, and the average results were recorded.

The tensile strength of the treated and untreated sisal fibers was measured based on equations (2) as per ASTM D 3822-07 [24].

$$\sigma_u = \frac{P}{5A}, \quad (2)$$

where P is the failure load in N and A is the average cross-sectional area of a single fiber determined by scanning the electron microscopy (SEM) in mm^2 .

2.4.2. Test Methods for Sisal Fiber-Reinforced Concrete (SFRC)

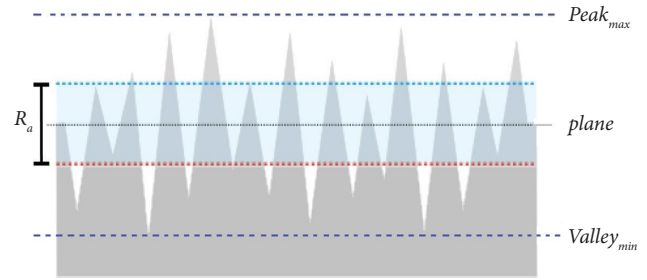


FIGURE 2: Surface roughness profile.

(1) *Workability.* A slump test was conducted following ASTM C143 [25] to evaluate the workability (which indicates its fresh properties) of concrete and to infer variation in the workability with the addition of raw and treated sisal fibers in concrete. For a water cement ration of 0.494, the target mix was assumed to have a slump of 25 to 75 mm.

(2) *Compressive Strength.* The compression behavior of each casted cube was evaluated following the British Standard Specification [26] using a compression testing machine equipped with a capacity of 3000 kN and a loading rate of 0.28 MPa/s (in compliance with a standard loading rate of 0.2–0.4 MPa/s). The experimental setup is shown in Figure 3. The compression stress is calculated using the following equation.

$$\sigma_c = \frac{P}{A}, \quad (3)$$

where σ_c is the compression stress, in MPa, P is the maximum applied force indicated by the testing machine, in N, and A is the cross-sectional area of specimen, in mm^2 .

(3) *Flexural Performance Parameters.* This test method evaluates the effect of fiber treatment conditions on the flexural performance of sisal fiber reinforced concrete (SFRC) using parameters derived from the load-deflection curve obtained by testing a simply supported beam under a third-point loading testing setup, as shown in Figure 4. The



FIGURE 3: Compressive strength testing setup.

beams were tested using a universal testing machine with an external data acquisition system connected to two transducer sensors (to measure the midspan deflection of the prism without a support settlement).

The flexural modulus, toughness index, residual strength factor, flexural toughness, and equivalent flexural strength ratio from the recorded load-deflection curve, as defined in Figure 5, were determined using ASTM C1018 [27] and ASTM C1609 [28] standards, as follows:

- (i) The flexural strength is calculated using the first maximum load (the load value at the first point on the load-deflection curve where the slope is zero) and can be obtained using the following equation.

$$f = \frac{P_1 L}{bd^2}, \quad (4)$$

where b and d are the average width and depth of specimen at the section of failure, respectively.

- (ii) According to reference [27], the flexural toughness of fiber reinforced concrete (FRC) is characterized by energy dimensionless toughness indices (I_5 , I_{10} , and I_{20}). These indices are determined by dividing the area underneath the load-deflection curve upto a limiting deflection of 3, 5.5, and 10.5 times the first-crack deflection (δ), by the first-crack toughness (area OAL in Figure 5), respectively, as shown in Figure 5. In this study, only I_5 and I_{10} were investigated.
- (iii) The residual strength factor ($R_{5,10}$) is intended to represent the average postcracking load that the specimen may carry over a specific deflection interval, and it is derived from the toughness indices as follows:

$$R_{5,10} = 20(I_{10} - I_5). \quad (5)$$

- (iv) ASTM C1609 specifies a single toughness value (T_{150}^D). Toughness is defined as the absolute area beneath the load-deflection curve upto the deflection of certain values ($\delta = L/150$) for a given load-deflection curve, as shown in the area OABCDEF of Figure 5.
- (v) In addition to the energy-based toughness measure T_{150}^D , the ASTM C1609 standard recommends the use of an equivalent flexural strength ratio ($R_{T,150}^D$), which is a parameter that relates the first peak flexural strength (modulus of rupture) to the toughness of the composite [29]. The equivalent flexural strength ratio is computed using the following equation.

$$(R_{T,150}^D) = \frac{150 * T_{150}^D}{f_1 * b * d^2} * 100\%. \quad (6)$$

3. Results and Discussion

3.1. Fiber Properties

3.1.1. Water Absorption. Table 4 shows that in its natural state, sisal fiber can absorb water approximately 93.05% of its weight. Meanwhile, all the applied treatments to sisal fiber resulted in a decrease in the water absorption capacity of the fiber, of which 10%–48 hr treatment had the lowest percentage. The absorption of alkali-treated sisal fiber was between 53.3% and 86%, depending on the concentration and time of the treatment. The alkali concentration and treatment time were inversely proportional to the water absorption of the treated fiber, which agrees with the previous report [30]. The phenomenon behind this

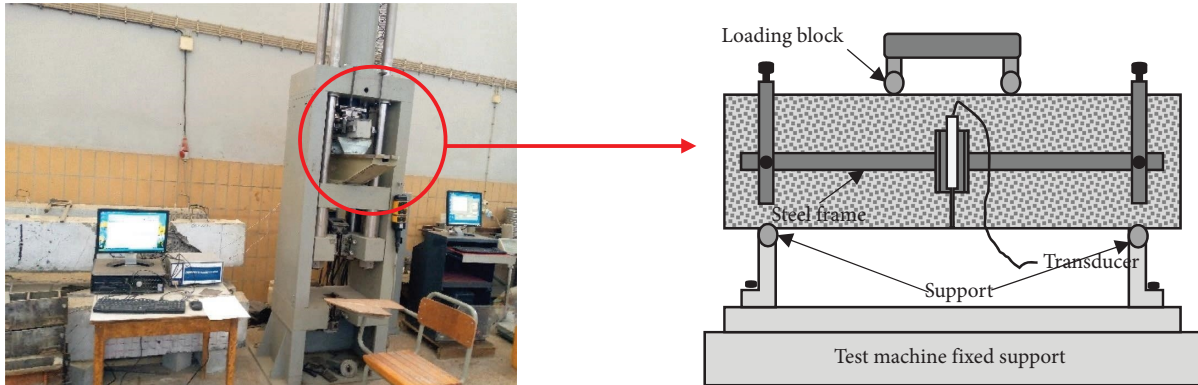


FIGURE 4: Flexural strength testing setup.

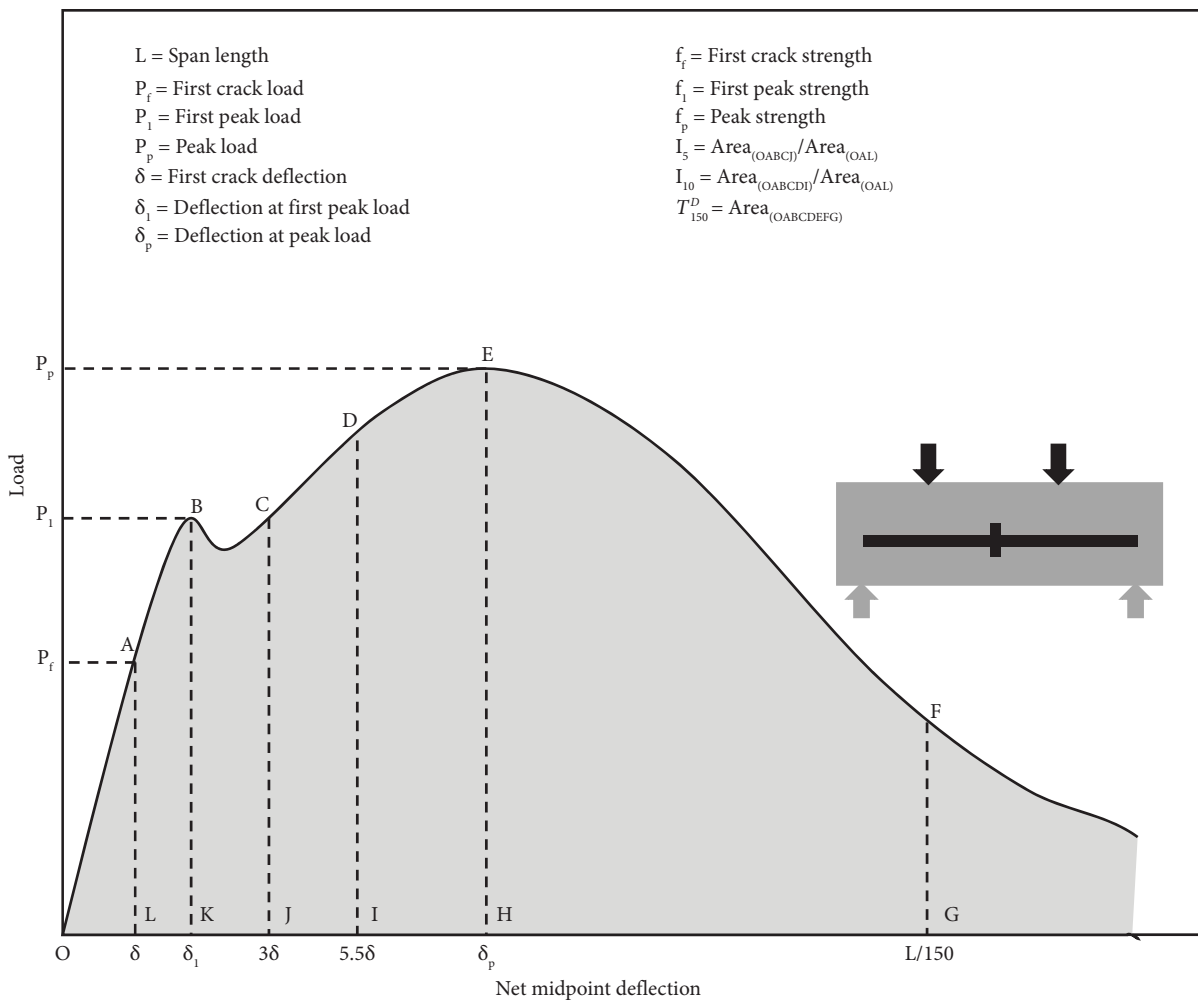


FIGURE 5: Schematic of load vs. deflection curve and definition of toughness parameters according to ASTM C1018 and ASTM C1609.

reduction in the water absorption capacity for the alkali-treated sisal fibers can be explained as follows: according to Ferreira et al. [31], this reduction is correlated with the change in the surface morphology of the fibers due to the removal of hydrophilic chemical compounds, such as hemicelluloses and lignin, by surface alkali treatment,

which consequently reduces the capacity of water absorption of the fibers. Furthermore, the changes in the flexible bonds between cellulose and hemicellulose by stiffer cellulose-cellulose bonds make the fibers more hydrophobic, which promotes a reduction in the fiber water intake capacity [32].

TABLE 4: Water absorption of sisal fibers.

Fiber treatment conditions	Water absorption (%)
Raw	93.05
2%–12 hr	86
2%–24 hr	79.4
2%–48 hr	73.6
5%–12 hr	76.8
5%–24 hr	71.4
5%–48 hr	67.5
10%–12 hr	69.7
10%–24 hr	60.2
10%–48 hr	53.3

3.1.2. Scanning Electron Microscopy. Using the SurfChar1q, an ImageJ plugin, the surface morphological characteristics of sisal fiber were analyzed in terms of different roughness parameters (R_a , R_v , R_p , and R_t). As shown in Table 5, the R_a (average roughness) values show an increment with fiber alkali treatment. In addition, average roughness shows improvement with increases in alkali concentration and fiber exposure time in the solution. Similar to R_a , the value of R_v (the lowest point) increases with increasing concentration and exposure. This observation had good agreement with recent research work reported by Zin et al. [33], which found that as alkali concentration further increased, damage on the fiber surface became more severe due to the corrosive effect of the alkaline solution, which led to excessive delignification that caused fiber deterioration. Observing R_p (the highest peak point) and R_t (the absolute distance between the highest and the lowest peak), improvement shows upto 5%–24 hr, and beyond this treatment condition, a gradual decrease in those properties was observed. Sample SEM images of raw and treated sisal fibers are shown in Figure 6.

3.1.3. Mechanical Properties of Fibers. The results of tensile strength, modulus, and % elongation of untreated and alkali-treated sisal fibers for different treatment conditions are presented in Table 6, which shows a gradual increase in mechanical properties with an increase in the concentration of NaOH upto 2% and then deterioration in properties. Compared to untreated sisal fibers, the highest improvements in tensile strength, modulus, and % elongation recorded were about 9, 58, and 109%, respectively, corresponding to 2%–48 hr. A similar pattern is also observed by Akram Khan et al. [34], where there is an increase in the tensile strength of fiber upto 2%, and beyond that, it shows a reducing trend. As the NaOH concentration went higher than 2%, the tensile properties of sisal fiber started to show a decreasing pattern. These could have been attributed to the substantial delignification and degradation of crystalline cellulose chains of the sisal fibers in high NaOH concentrations and longer-duration alkali treatments, resulting in weak or damaged sisal fibers [35]. Similar effects were seen on modulus and elongation following treatment. Unlike the results for the tensile strength, young's modulus, and % elongation, these decrease slightly with an increase in the concentration of NaOH and soaking time.

3.2. SFRC Properties

3.2.1. Workability. The measured slump of the fresh concrete mixes is presented in Table 7. The addition of sisal fibers to the concrete matrix resulted in a general decrease in workability. This is due to the absorption of a significant portion of the water required for cement hydration by the hydrophilic natural fibers from the concrete mixture [36]. This trend is consistent with the information found in the literature [37], and it is explained by the fact that the excess absorption of mixing water by the reinforcing sisal fiber makes it difficult for the concrete to be workable. Although the treated SFRC mix has lower workability than the unreinforced concrete mix, the improvement is observed compared to the raw SFRC mix. Of all the reinforced concrete mixes, the increased slump of 45 mm is achieved for mix C10–48. The percentage increase of C10–48 is about 80% compared to the raw SFRC (C0-0). Furthermore, it was noticed that the workability of the concrete increased when increasing the alkali concentration and fiber immersion periods. This improvement in the workability of concrete may be ascribed to the less hydrophilic nature of the treated sisal fibers that change the mixture's workability due to less absorption of mixing water. Therefore, the higher the NaOH concentration and soaking time, the harder it is for the fiber to absorb the mixing water, and thereby, the higher the slump of the mix. Nonetheless, the measured slump values for all the concrete mixtures considered in this study were within the design slump limit (25–75 mm).

3.2.2. Compressive Strength. On the 7th day, the compressive strength of the raw SFRC specimen is increased by 17.73% compared to that of the reference conventional control specimen (its 7-day compressive strength is 24.31 MPa). An alkali-treated SFRC composite displays an average increment of about 4.33%. However, compared to the untreated SFRC composite, the alkali-treated SFRC composites show an 11.38% average decrease. With increased curing time, the compressive strength of treated sisal fiber-reinforced concrete composites starts to decline with an increase in the concentration and duration of treatment, as shown in Figures 7 and 8. This increment in concentration and treatment duration could create voids and pores in the fiber structure that generates more interface zones between the sisal and the concrete constituent's interfaces [38]. Consequently, the number of permeable and microcrack regions in the concrete composites increased, which brought about insufficient compaction, and as a result, the compressive strength deteriorated, which agrees with some previous findings [39].

In the present work, it is found that the optimum treatment condition of fiber that is treated with a 5% concentrated alkali solution for 24 hours increased the compressive strength of the concrete composite by approximately 0.46% and 13.12% after 28 days compared to the raw sisal fiber reinforced concrete and conventional unreinforced concrete (its 28-day compressive strength is 37.37 MPa), respectively. This is possibly owing to the manifestation of good fiber-cement compatibility [11].

TABLE 5: Roughness parameters of sisal fiber at different treatment conditions.

Fiber treatment conditions	R_a (μm)	R_v (μm)	R_p (μm)	R_t (μm)
Raw	19.4	-78.6	42.6	121.3
2%-12 hr	25.6	-83.9	45.8	129.7
2%-24 hr	25.7	-93.3	51.2	144.5
2%-48 hr	26.5	-94.0	55.4	149.4
5%-12 hr	26.9	-96.7	57.0	153.7
5%-24 hr	27.0	-103.6	60.3	163.9
5%-48 hr	27.6	-103.9	57.6	161.5
10%-12 hr	27.6	-107.9	51.1	158.9
10%-24 hr	29.9	-110.4	38.7	149.0
10%-48 hr	32.4	-112.4	35.7	148.1

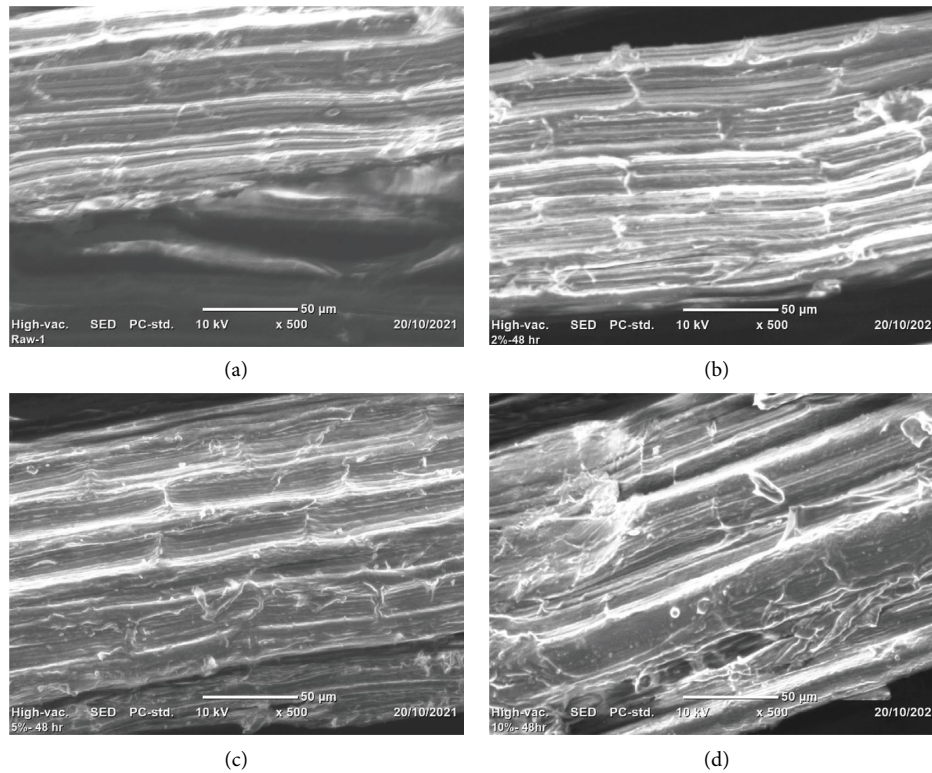


FIGURE 6: Sample morphology of sisal fiber: (a) raw, (b) 2%-48 hr, (c) 5%-48 hr, and (d) 10%-48 hr.

TABLE 6: Effect of treatment conditions on mechanical properties of sisal fiber.

Fiber treatment condition	Tensile strength (MPa)	Young's modulus (GPa)	Elongation at break (%)
Raw	556.2	10.4	2.2
2%-12 hr	560.7	12.7	2.7
2%-24 hr	587.6	14.4	4.3
2%-48 hr	607.7	16.7	4.6
5%-12 hr	591.2	15.6	4.1
5%-24 hr	580.7	13.1	3
5%-48 hr	561.8	12.4	2.7
10%-12 hr	512.4	10.6	2.4
10%-24 hr	494.2	9.7	2.1
10%-48 hr	324.1	9	2

TABLE 7: Slump of SFRC and plain concrete.

Mix designation	Slump (mm)	% reduction in slump
Control	65	0
C0-0	25	61.55
C2-12	30	53.85
C2-24	30	53.85
C2-48	35	46.15
C5-12	35	46.15
C5-24	35	46.15
C5-48	40	38.45
C10-12	40	38.45
C10-24	40	38.45
C10-48	45	30.75

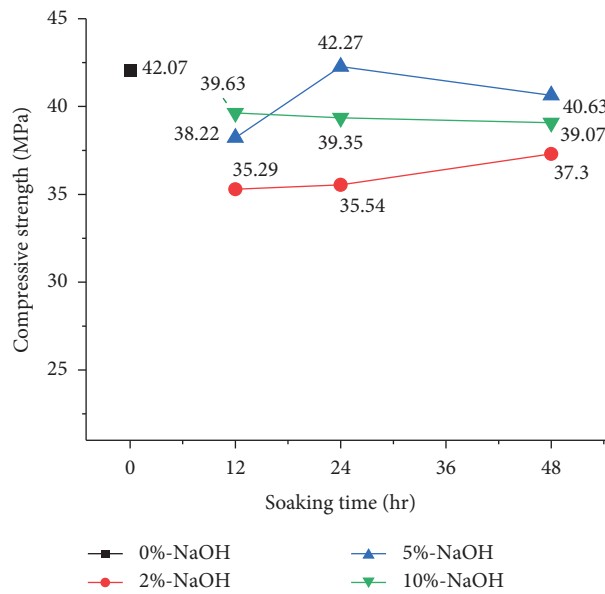


FIGURE 7: 7 days compressive strength.

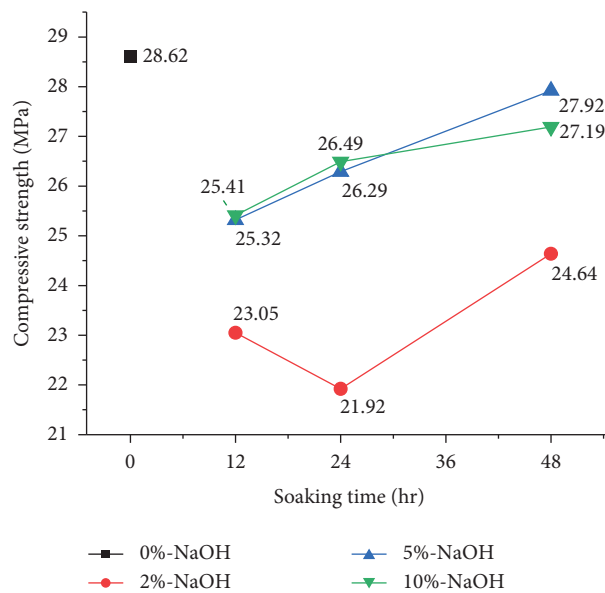


FIGURE 8: 28 days compressive strength.

TABLE 8: ANOVA test for the compressive strength of SFRC.

	Source of variation	SS	df	MS	F	P value	F crit	Remarks*
7 days	Alkali concentration	134.29	3	44.76	47.08	0	3.01	Significant
	Soaking time	15.52	2	7.76	8.16	0.002	3.4	Significant
	Interaction	10.87	6	1.81	1.91	0.121	2.51	Insignificant
	Within	22.82	24	0.95				
	Total	183.5	35					
28 days	Alkali concentration	174.03	3	58.01	51.64	0	3.01	Significant
	Soaking time	7.77	2	3.89	3.46	0.048	3.4	Significant
	Interaction	24.76	6	4.13	3.67	0.01	2.51	Significant
	Within	26.96	24	1.12				
	Total	233.52	35					

Significant at 5% probability ($p < 0.05$). df, degrees of freedom; F, F-test for ANOVA two-way; MS, mean square; SS, sum of squares; P value, calculated probability.

TABLE 9: Flexural strength test results.

Mix designation	Mean flexural strength (MPa)	Relative strength gain compared to raw SFRC (%)
Control	3.931	
C0-0	3.950	
C2-12	4.079	3.285
C2-24	4.160	5.336
C2-48	4.440	12.403
C5-12	4.549	15.180
C5-24	4.337	9.795
C5-48	4.259	7.843
C10-12	4.336	9.775
C10-24	4.037	2.219
C10-48	3.908	-1.064

TABLE 10: ANOVA test for the flexural tensile strength of SFRC.

Source of variation	SS	df	MS	F	P value	F crit	Remarks*
Alkali concentration	0.9198	3	0.3066	9.65464	0.00023	3.00879	Significant
Soaking time	0.07955	2	0.03977	1.25244	0.30383	3.40283	Insignificant
Interaction	0.55891	6	0.09315	2.9333	0.02725	2.50819	Significant
Within	0.76216	24	0.03176				
Total	2.32043	35					

Table 8 shows the ANOVA results for the compressive strength of SFRC. The analysis is conducted at a significance level of $\alpha = 0.05$. The concentration of NaOH is the most significant parameter in this table because the calculated value of the F-ratio is higher than F critical for a given confidence interval and the P value is considerably lower than $\alpha = 0.05$ for both 7th- and 28th-day compressive strength. The interaction between alkali concentration and soaking time is statistically insignificant in the case of 7-day curing age.

3.2.3. Flexural Strength. Table 9 depicts the effect of various fiber treatment conditions on the flexural strength of a concrete composite. When untreated sisal fibers are replaced with NaOH-treated sisal fibers, a significant impact on flexural properties is observed. The flexural strength behavior of the

specimen reinforced with treated sisal fiber increases with increasing alkali concentration and soaking time upto 5%–12 hr and afterward decreases with increasing concentration and duration. The optimum sisal fiber treatment concentration of NaOH suggested is 5%, with flexural strength increased from 4.259 to 4.549 MPa for different treatment periods. Among various treatment durations corresponding to 5% alkali concentration, reinforcing sisal fiber that was treated for 12 hours (C5–12) yields an approximate 15.7% and 15.18% improvement in flexural strength as compared to the conventional and raw sisal fiber reinforced concrete specimen, respectively. Next to C5–12, C2–48 shows better performance and is almost 12.9% and 12.4% greater than unreinforced concrete and raw SFRC, respectively.

Except for the concrete reinforced with sisal fiber treated with 10% NaOH solution for 48 hours, the modules of rupture of other treated SFRC were higher than those of

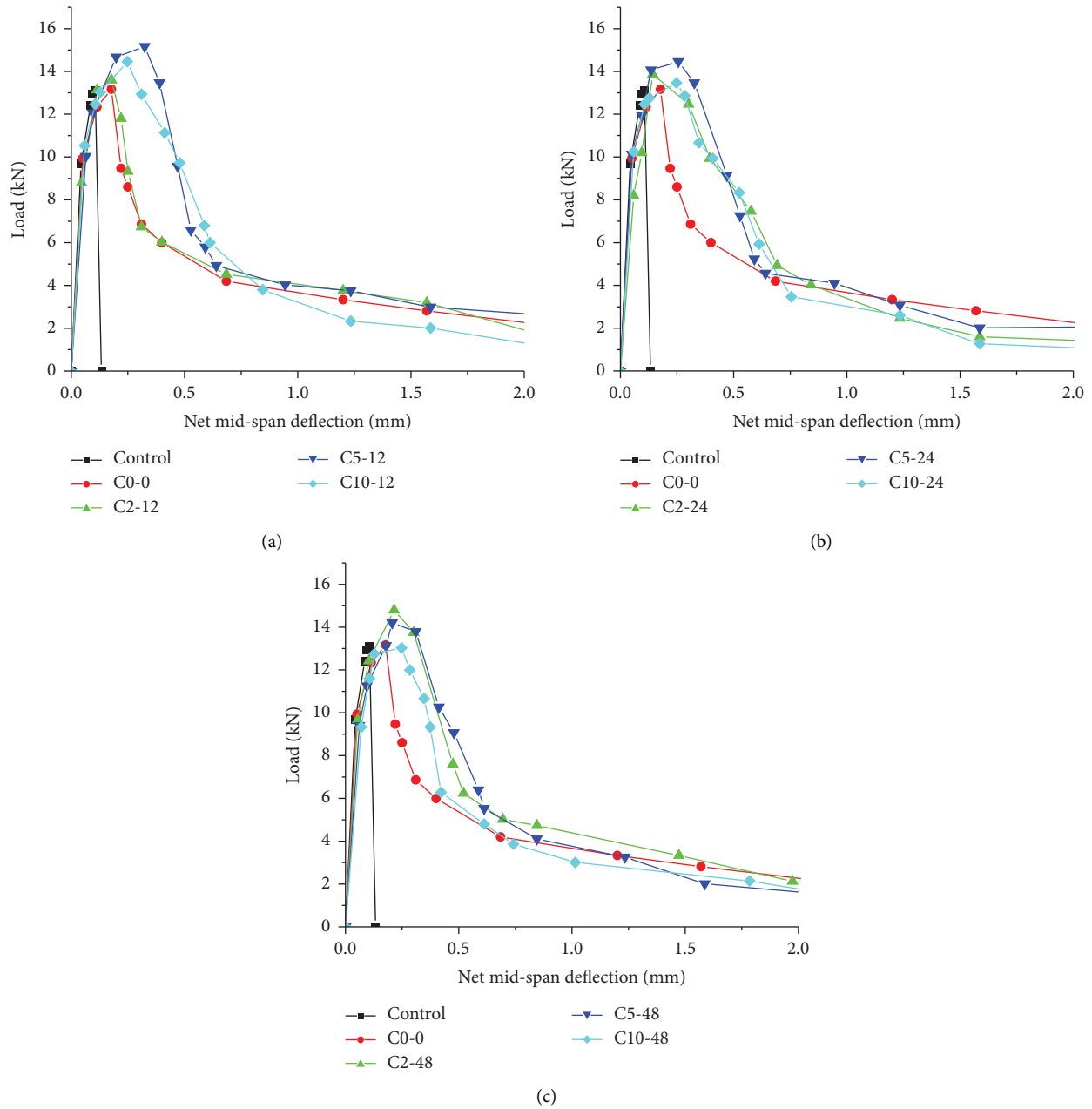
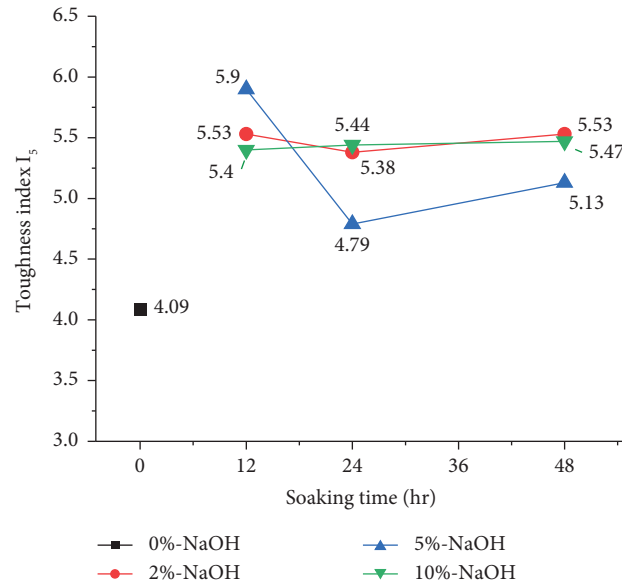


FIGURE 9: Load vs. mid-span deflection curves for different soaking time; (a) 12 hr, (b) 24 hr, and (c) 48 hr.

control specimens of plain concrete, ranging from 2.7 to 15.7%. Furthermore, except for C10-48, alkali-treated SFRC outperforms raw sisal-reinforced concrete. The reason for the observed increase in flexural strength is the enhanced fiber surface roughness and removal of fiber surface impurities resulting from the chemical treatment process [40]. Concerning fibers that are treated in a highly concentrated alkali medium for a longer duration, the effect of the treatment on the flexural strength of the concrete composite is detrimental. Indeed, it permits substantial delignification and degradation of crystalline cellulose chains of the fiber, resulting in weaker or damaged fiber [35].

Table 10 shows the ANOVA results at a 95% confidence interval, and it is found that the duration of sisal fiber treatment has no significant effect on the flexural strength performance of the concrete composite with a P value of <0.05 , indicating that the null hypothesis is true. In contrast, the concentration of NaOH has a statistically significant effect on the flexural tensile strength of SFRC. There was also a significant effect from the interactions between fiber soaking time and NaOH concentration.

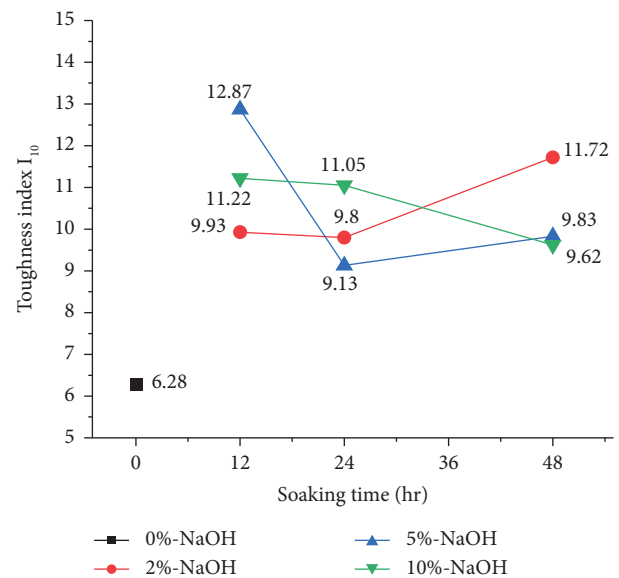
3.2.4. Postcracking Behaviors. In this study, the postcrack behaviors of concrete composites are characterized by the load-deflection curve of the flexural test following ASTM

FIGURE 10: Toughness index I_5 .

C1018 and ASTM C1609 standards. Figure 9 shows a typical load-deflection curve for control, raw SFRC, and alkali-treated SFRC beam specimens. Three samples from each batch of concrete were tested to get the average value of the postcrack behaviors. For each category, one average curve was presented from three load-deflection curves of each sample code.

(1) *ASTM C1018 Toughness Parameters.* In this study, two flexural toughness indexes, I_5 and I_{10} , are calculated from the averaged load vs. deflection curve, as shown in Figure 9. It can be observed in Figures 10 and 11 that a notable effect in toughness indexes is recorded when untreated sisal fibers are replaced by NaOH-treated sisal fibers. The increase in toughness indexes implies that the crack-arresting behavior of the composite increases with the treatment of reinforcing fiber. The reasons for these experimental results are mainly due to the removal of the fiber surface impurity and the increased surface roughness, thus increasing the fiber-matrix compatibility and fiber-matrix interfacial bonding, resulting in better performance in the relative postpeak behavior. Compared to control conventional concrete ($I_5 = I_{10} = 1$), the toughness index of fiber-reinforced concrete has increased significantly regardless of treatment condition. These could be due to the inhibition of crack propagation by the fibers after the appearance of the first crack in raw and treated fiber-reinforced concrete composites [11].

The maximum value of I_5 and I_{10} is given by reinforcing fiber treated for 12 hours in a 5% alkali-concentrated solution (C5-12), which is 44% and 105% greater than that of raw SFRC. As observed from the flexural strength result, C2-48 also shows better performance in toughness indexes next to C5-12, and it is almost 35.2% and 86.6% greater than that of raw SFRC specimens for I_5 and I_{10} , respectively.

FIGURE 11: Toughness index I_{10} .

The second observation that can be made based on the Figure 11 is that the effect of fiber alkali treatment is more pronounced in I_{10} than in I_5 for all mixtures. These were because the contribution of fibers to postcrack toughness came into play and accurately reflected at higher deflection (5.5δ) [27].

Residual strength factors characterize the remaining strength after the first crack in fiber-reinforced concrete and are derived from the toughness index. The designated residual strength chosen for this study was $R_{5,10}$, which represents the average strength retained between 3δ and 5.5δ . As shown in Figure 12, the ASTM residual strength factor

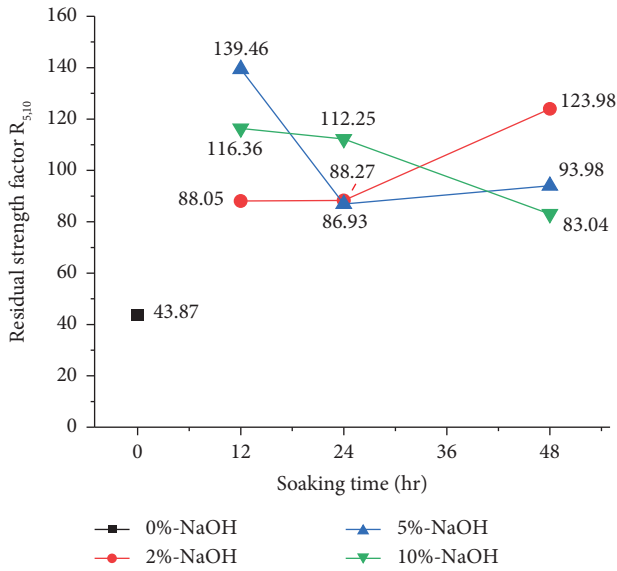


FIGURE 12: Residual strength factor ($R_{S,10}$).

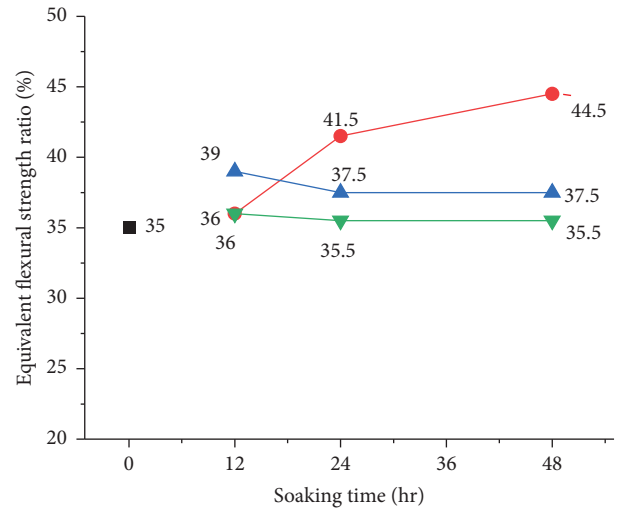


FIGURE 14: Equivalent flexural strength ratio.

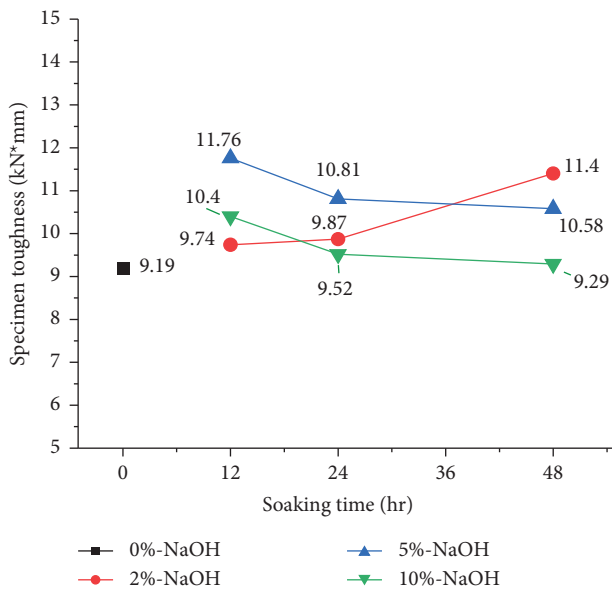


FIGURE 13: Specimen toughness of SFRC.

($R_{S,10}$) seemed to be improved by the fiber alkali treatment compared to that of raw sisal fiber-reinforced concrete. Similarly to flexural strength and toughness indexes, the highest residual strength factors were obtained with a 5%–12 hr fiber treatment.

(2) *ASTM C1609 Toughness Parameters.* The two performance parameters (specimen toughness and equivalent flexural strength ratio) from the ASTM C1609 standard have been summarized using Figures 13 and 14. As seen in Figure 13, changing the surface morphology of the reinforcing fiber by alkali treatment affects the toughening performance of the SFRC mixture composites. The results indicate that treated SFRC has a greater overall energy

absorption capacity than untreated SFRC. The increase in toughness values is between 1.1% and 28% of the raw sisal fiber-reinforced concrete specimen. The ability to sustain loads after cracking is very much dependent on the tensile strength of individual fibers and the bond between the fiber and matrix [41]. Therefore, the enhanced mechanical properties of alkali-treated sisal fiber due to the removal of surface impurity correlated with a change of the morphological and chemical structures in microfibrils of the fiber lead to get a superior result in terms of flexural toughness compared to the raw SFRC counterpart.

Another noticeable observation in the toughness development among the mixtures is that the rates of toughness development with different treatment conditions are quite different. For all treated reinforcing sisal fibers, the toughness showed a gradual increment with increasing alkali concentration and fiber soaking time upto 5% and 24 hours, respectively. With further increases in concentration and duration, the specimen flexural toughness values gradually reduced. The possible explanations for this result are that as the alkali concentration and soaking time increased, a highly rough fiber surface resulted, which led to a strong interface bond between the matrix and reinforcing fiber. Accordingly, no debonding and slippage take place, and the result is a strong but brittle material [42]. Furthermore, as alkali concentration further increased, damage on the fiber surface became more severe and consequently reduced the tensile strength of the reinforcing sisal fiber. These, in turn, promote a reduction in the fiber-bridging effect.

The equivalent flexural strength ratio ($R_{T,150}^D$) is another ASTM C1609 toughness performance parameter used in this study to characterize the flexural toughness of sisal fiber-reinforced concrete and is expressed as a percentage. As shown in Figure 14, for various treatment conditions on the reinforcing sisal fiber, the equivalent flexural strength ratio increases with increasing alkali concentration and fiber

soaking time up to 2% and 48 hours, respectively, and gradually decreases with further increases in treatment concentration and duration. The increase in $R_{T,150}^D$ values is between 1.4% and 27% of the raw sisal fiber-reinforced concrete specimen.

4. Conclusions

The following conclusions are drawn from experimental work performed in relation to the study's objectives:

- (i) All applied treatments resulted in a reduction of the water absorption capacity and an increase in the surface roughness of the sisal fiber. Significant improvements in the mechanical properties (tensile strength, modulus, and % elongation) of sisal fibers were obtained by treating them for 48 hours in a 2% NaOH solution. When sisal fiber was treated with more than 2% NaOH solutions, mechanical property values dropped consistently, owing to excessive delignification of sisal fiber.
- (ii) Regardless of the treatment conditions used, the inclusion of sisal fiber in the concrete matrix reduced the workability of the SFRC. Except for the concrete reinforced with 10%–48 hr treated sisal fiber, the flexural strength of the concrete composites reinforced with alkali-treated sisal fibers improved. However, compared to their untreated SFRC counterparts, treating sisal fiber did not improve the compressive strength of the composites at any age.
- (iii) The toughness of fiber-incorporated concrete has revealed a considerable enhancement. This effect becomes more significant for alkali-treated sisal fibers. However, at higher concentrations and treatment durations, the increase becomes minimal and even experiences a reduction.

Based on the abovementioned remarks, it becomes evident that treating sisal fiber is an excellent method for enhancing the flexural and postcrack performance of SFRC, thus bringing new trends in composite materials.

Data Availability

The data used to support the findings of this study are available upon request from the corresponding author.

Conflicts of Interest

The authors declare that they have no conflicts of interest.

References

- [1] H.-O. Pörtner, *Climate change 2022: impacts, adaptation, and vulnerability. Contribution of working group II to the sixth assessment report of the intergovernmental panel on climate change*, International Plant Protection Convention, Rome, Italy, 2022.
- [2] R. Prakash, S. N. Raman, C. Subramanian, and N. Divyah, "Eco-friendly fiber-reinforced concretes," in *Handbook of Sustainable Concrete and Industrial Waste Management*, pp. 109–145, Elsevier, Amsterdam, Netherlands, 2022.
- [3] R. Prakash, R. Thenmozhi, S. N. Raman, C. Subramanian, and N. Divyah, "Mechanical characterisation of sustainable fibre-reinforced lightweight concrete incorporating waste coconut shell as coarse aggregate and sisal fibre," *International Journal of Environmental Science and Technology*, vol. 18, no. 6, pp. 1579–1590, 2021.
- [4] D. Lilargem Rocha, L. U. D. Tambara Júnior, M. T. Marvila, E. C. Pereira, D. Souza, and A. R. G. de Azevedo, "A review of the use of natural fibers in cement composites: concepts, applications and Brazilian history," *Polymers*, vol. 14, no. 10, p. 2043, 2022.
- [5] Fao, *Market and Policy Analysis of Raw Materials, Horticulture and Tropical (RAMHOT) Products Team Trade and Markets Division*, Food and Agriculture Organization of the United Nations, Rome, Italy, 2018.
- [6] J. Ahmad, A. Majdi, A. F. Deifalla, N. Ben Kahla, and M. A. El-Shorbagy, "Concrete reinforced with sisal fibers (SSF): overview of mechanical and physical properties," *Crystals*, vol. 12, no. 7, p. 952, 2022.
- [7] X. Zhou, S. H. Ghaffar, W. Dong, O. Oladiran, and M. Fan, "Fracture and impact properties of short discrete jute fibre-reinforced cementitious composites," *Materials & Design*, vol. 49, pp. 35–47, 2013.
- [8] Ö. Andiç-Çakir, M. Sarikanat, H. B. Tüfekçi, C. Demirci, and Ü. H. Erdoğan, "Physical and mechanical properties of randomly oriented coir fiber-cementitious composites," *Composites Part B: Engineering*, vol. 61, pp. 49–54, 2014.
- [9] X. Li, L. G. Tabil, and S. Panigrahi, "Chemical treatments of natural fiber for use in natural fiber-reinforced composites: a review," *Journal of Polymers and the Environment*, vol. 15, no. 1, pp. 25–33, 2007.
- [10] M. D. De Klerk, M. Kayondo, G. M. Moelich, W. I. de Villiers, R. Combrinck, and W. P. Boshoff, "Durability of chemically modified sisal fibre in cement-based composites," *Construction and Building Materials*, vol. 241, Article ID 117835, 2020.
- [11] B. W. Jo, S. Chakraborty, and H. Kim, "Efficacy of alkali-treated jute as fibre reinforcement in enhancing the mechanical properties of cement mortar," *Materials and Structures*, vol. 49, no. 3, pp. 1093–1104, 2016.
- [12] X. Zhou, H. Saini, and G. Kastiukas, "Engineering properties of treated natural hemp fiber-reinforced concrete," *Frontiers in Built Environment*, vol. 3, no. 33, 2017.
- [13] J. Wei and C. Meyer, "Degradation mechanisms of natural fiber in the matrix of cement composites," *Cement and Concrete Research*, vol. 73, pp. 1–16, 2015.
- [14] M. Ardanuy, J. Claramunt, and R. D. Toledo Filho, "Cellulosic fiber reinforced cement-based composites: a review of recent research," *Construction and Building Materials*, vol. 79, pp. 115–128, 2015.
- [15] F. Pacheco-Torgal and S. Jalali, "Cementitious building materials reinforced with vegetable fibres: a review," *Construction and Building Materials*, vol. 25, no. 2, pp. 575–581, 2011.
- [16] J. Wei and C. Meyer, "Improving degradation resistance of sisal fiber in concrete through fiber surface treatment," *Applied Surface Science*, vol. 289, pp. 511–523, 2014.
- [17] Astm, *Standard Specification for Concrete Aggregates I*, American Society of Testing and Materials, West Conshohocken, PE, USA, 1999.
- [18] Committee for Standardization, *Cement - Part 1: Composition, Specifications and Conformity Criteria for Common Cements*, European Committee for Standardization, Brussels, Belgium, 2000.

- [19] S. M. Mbeche and T. Omara, "Effects of alkali treatment on the mechanical and thermal properties of sisal/cattail polyester commingled composites," *PeerJ Materials Science*, vol. 2, p. e5, 2020.
- [20] Aci, *Standard Practice for Selecting Proportions for Normal, Heavyweight, and Mass Concrete*, American Concrete Institute, Farmington Hills, MI, USA, 2002.
- [21] O. Fadele, I. N. Oguocha, A. G. Odeshi, M. Soleimani, and L. G. Tabil, "Effect of chemical treatments on properties of raffia palm (*Raphia farinifera*) fibers," *Cellulose*, vol. 26, no. 18, pp. 9463–9482, 2019.
- [22] ISO, *Geometrical Product Specifications (GPS)—surface Texture: Profile Method—Rules and Procedures for the Assessment of Surface Texture*, ISO, London, UK, 1996.
- [23] L. Tonietto, L. Gonzaga, M. R. Veronez, C. D. S. Kazmierczak, D. C. M. Arnold, and C. A. D. Costa, "New method for evaluating surface roughness parameters acquired by laser scanning," *Scientific Reports*, vol. 9, no. 1, Article ID 15038, 2019.
- [24] Astm, *Standard Test Methods for Tensile Properties of Single Textile Fibers*, American Society of Testing and Materials, West Conshohocken, PE, USA, 2007.
- [25] Astm, *Standard Test Method for Slump of Hydraulic-Cement Concrete*, American Society of Testing and Materials, West Conshohocken, PE, USA, 2015.
- [26] BS, *Testing concrete. Method for Determination of Compressive Strength of concrete Cubes*, British Standards Institute, London, UK, 1983.
- [27] Astm, *Standard Test Method for Flexural Toughness and First-Crack Strength of Fiber-Reinforced Concrete (Using Beam with Third-Point Loading)*, American Society of Testing and Materials, West Conshohocken, PE, USA, 1997.
- [28] Astm, *Standard Test Methods for Flexural Performance of Fiber-Reinforced Concrete (Using Beam with Third-Point Loading)*, American Society of Testing and Materials, West Conshohocken, PE, USA, 2010.
- [29] M. Dopko, *Fiber Reinforced concrete: Tailoring Composite Properties with Discrete Fibers*, Iowa State University, Ames, LA, USA, 2018.
- [30] P. Ramadevi, D. Sampathkumar, C. V. Srinivasa, and B. Bennehalli, "Effect of alkali treatment on water absorption of single cellulosic abaca fiber," *Bioresources*, vol. 7, no. 3, pp. 3515–3524, 2012.
- [31] S. R. Ferreira, F. D. A. Silva, P. R. Lima, and R. D. Toledo Filho, "Effect of fiber treatments on the sisal fiber properties and fiber-matrix bond in cement-based systems," *Construction and Building Materials*, vol. 101, pp. 730–740, 2015.
- [32] M. Mohammed, R. Rahman, A. M. Mohammed et al., "Surface treatment to improve water repellence and compatibility of natural fiber with polymer matrix: recent advancement," *Polymer Testing*, vol. 115, Article ID 107707, 2022.
- [33] M. H. Zin, K. Abdan, N. Mazlan, E. S. Zainudin, and K. E. Liew, "The effects of alkali treatment on the mechanical and chemical properties of pineapple leaf fibres (PALF) and adhesion to epoxy resin," *IOP Conference Series: Materials Science and Engineering*, vol. 368, no. 1, Article ID 012035, 2018.
- [34] M. Akram Khan, S. Guru, P. Padmakaran, D. Mishra, M. Mudgal, and S. Dhakad, "Characterisation studies and impact of chemical treatment on mechanical properties of sisal fiber," *Composite Interfaces*, vol. 18, no. 6, pp. 527–541, 2011.
- [35] L. Y. Mwaikambo and M. P. Ansell, "Mechanical properties of alkali treated plant fibres and their potential as reinforcement materials II. Sisal fibres," *Journal of Materials Science*, vol. 41, no. 8, pp. 2497–2508, 2006.
- [36] S. Chakraborty, S. P. Kundu, A. Roy, B. Adhikari, and S. B. Majumder, "Effect of jute as fiber reinforcement controlling the hydration characteristics of cement matrix," *Industrial & Engineering Chemistry Research*, vol. 52, no. 3, pp. 1252–1260, 2013.
- [37] A. A. Okeola, S. O. Abuodha, and J. Mwero, "Experimental investigation of the physical and mechanical properties of sisal fiber-reinforced concrete," *Fibers*, vol. 6, no. 3, p. 53, 2018.
- [38] I. Soto Izquierdo, O. Soto Izquierdo, M. A. Ramalho, and A. Taliercio, "Sisal fiber reinforced hollow concrete blocks for structural applications: testing and modeling," *Construction and Building Materials*, vol. 151, pp. 98–112, 2017.
- [39] Z. Li, X. Wang, and L. Wang, "Properties of hemp fibre reinforced concrete composites," *Composites Part A: Applied Science and Manufacturing*, vol. 37, no. 3, pp. 497–505, 2006.
- [40] D. Sedan, C. Pagnoux, A. Smith, and T. Chotard, "Mechanical properties of hemp fibre reinforced cement: influence of the fibre/matrix interaction," *Journal of the European Ceramic Society*, vol. 28, no. 1, pp. 183–192, 2008.
- [41] H. A. Razak and T. Ferdiansyah, "Toughness characteristics of Arenga pinnata fibre concrete," *Journal of Natural Fibers*, vol. 2, no. 2, pp. 89–103, 2005.
- [42] M. D. Campbell and R. S. P. Coutts, "Wood fibre-reinforced cement composites," *Journal of Materials Science*, vol. 15, no. 8, pp. 1962–1970, 1980.

Research Article

Performance of Ladle Furnace Slag in Mortar under Standard and Accelerated Curing

Iffat Sultana  and G. M. Sadiqul Islam 

Department of Civil Engineering, Chittagong University of Engineering & Technology, CUET, Chattogram 4349, Bangladesh

Correspondence should be addressed to G. M. Sadiqul Islam; gmsislam@cuet.ac.bd

Received 20 June 2022; Revised 24 August 2022; Accepted 9 September 2022; Published 17 October 2022

Academic Editor: Onn Chiu Chuen

Copyright © 2022 Iffat Sultana and G. M. Sadiqul Islam. This is an open access article distributed under the Creative Commons Attribution License, which permits unrestricted use, distribution, and reproduction in any medium, provided the original work is properly cited.

This research preliminarily investigated the suitability of a locally available ladle furnace slag (LFS) as a partial replacement of cement in mortar. The raw material was first characterized to obtain its chemical and physical properties through particle size distribution, X-ray fluorescence (XRF), X-ray diffraction (XRD), and scanning electron microscopy (SEM). Later, the raw LFS was classified into two categories: (i) raw LFS and (ii) sieved (passing through #200 sieve) LFS and incorporated in mortars as a partial replacement of cement. Mortar prisms with 5, 10, 15, 20, 25, and 50% LFS (raw and sieved) were prepared and cured under normal temperature (NTC) for 7, 28, and 56 days. Additional mortar prisms (with raw and sieved LFS) were prepared by curing them under high-temperature accelerated curing (HTAC) for 7 days. The characterization tests suggest that CaO, SiO₂, MgO, and Al₂O₃ are the main compounds of raw LFS used in this study. The mineralogical phases present in the raw slag are calcio-olivine, akermanite, α -quartz, merwinite, magnetite (Fe₃O₄), and calcium-aluminium oxide. Both raw and sieved LFS-blended mortars yield good consistency up to 25% cement replacement in mortars. The compressive strength of NTC mortar suggests that 5% and 10% replacement of cement with raw and sieved LFS yields higher strength than the control mortar. Seven days strengths of raw and sieved LFS blended mortars obtained for HTAC are closely comparable to that of 28 days under NTC. This study recommends that LFS could be a sustainable supplementary material to use as a partial replacement of cement in mortar, preferably up to a level of 15% for standard works.

1. Introduction

Concrete, the second most utilized material on Earth (after water), creates environmental issues, arising mainly from its constituent materials. For example, excessive use of natural sand and aggregates creates environmental instability; use of drinking water abundantly is an issue since it causes gradual lowering of the groundwater table. The production and use of cement, a critical component of concrete, is proven to impact the environment negatively. Studies report that 8% of the global greenhouse gas (GHG) emission is due to the production of cement [1].

Globally, cement production has been reduced or kept checked in the last decade due to the negative impact on the environment [2]. In contrast, Bangladesh has seen an increase in cement production by 10–12% in the past decade

[3]. An increase in cement production means an increase in cement use, consequently increasing the negative impacts on environment. It is essential to reduce the use of cement as much as possible to curb the environmental pollution. This could be achieved by diverging towards sustainable concrete production incorporating supplementary cementitious materials (SCM) and/or supplementary filler materials (SFM) and/or recycled water and reducing the dependency on drinking water [4].

Various studies report effective alternative use of different types of solid wastes, e.g., waste clay brick, ceramic waste powder, and glass powder [5, 6]. Pozzolanic and cementitious properties are available in industrial by-products, e.g., ground granulated blast furnace slag (GGBS), silica fume, steel slag, cement kiln dust [7–11]; ashes, e.g., fly ash [12], rice husk ash (RHA) [13], sugarcane bagasse ash

[14], coconut ash [15], wood fibre ash and corn fibre ash [16]; and ceramic wastes [17]. These materials can be used either directly (as-received raw materials) or after being chemically treated (with an activator or reagent to improve their properties as SCM).

In Bangladesh, several studies considered SCM [18–20] for mortars and concrete. Mainly, fly ash and RHA have been the point of interest to the researchers. Steel slags, available in plenty, primarily due to the growing industries (~400 steel mills), have also been considered for a smaller number of studies [21]. Approximately, 1.1–1.3 million metric tonnes of steel slag are produced per annum in Bangladesh [21]. These include ladle furnace slag (LFS)—a secondary by-product of the steel making process. LFS in general is generated in the second stage of the steel manufacturing process resulting in a lesser production compared with the primary slags, e.g., basic oxygen furnace slag (BOFS) and electric arc furnace slag (EAFS). Nevertheless, considering a LFS generation of 0.3–0.7% of the steel production, the annual production (30 million tonnes) of LFS worldwide is quite significant [22]. Previously, the steel industry in Bangladesh used to dump this LFS into open lands just as waste. In recent times, several alternative (other than SCM) uses of this by-product have been identified by the researchers: (i) brick production with other steel slags; (ii) filtering bed material; (iii) in the rotatory furnace of Portland clinker; and (iv) agricultural fertilizer. However, the application is still limited [23, 24].

The applicability of LFS as SCM has been investigated in mortars, concrete pavement work [24], and self-compacting concrete [25]; mortar for rigid and flexible concrete [26]; soil improvement [27]; stabilizing embankment soil [28]; filler material in asphalt mix [29]; and strengthening clay soil [11].

On the properties of LFS as SCM, a database is available globally [8, 24, 28, 30–33]. Previous studies report that LFS contains calcium oxide (CaO), silicon dioxide (SiO₂), aluminium oxide (Al₂O₃), and magnesium oxide (MgO) on many occasions. Kriskova et al. [34] report that the concentration of these materials is 92.3% and Shi and Hu [35] report that it is 92.2% in total. The overall presence of primary constituents varies from 88% to 94% [36–38]. The ladle finally refines steel by removing these oxides as waste form inside the ladle slag.

The morphology of LFS particles, in general, is found to have rough surfaces with local crystalline growth, dusty materials, and greyish white powder-like appearance [24, 26, 39, 29] (Figure 1). Shi [31] reports that LFS alone may not induce reasonable cementitious properties in a mortar, but LFS-GGBS blended cement paste with an activator (e.g., sodium silicate, Na₂SiO₃) can produce good quality mortar [24]. Manso et al. [32] report that if LFS is used as a substitution of binder and fine aggregates, it may produce mortars of standard quality. Shi and Hu [35] blended LFS with silica flour and fly ash, and then cured under autoclave (~175°C) to induce good cementitious properties.

A recently published review article [40] on LFS has incorporated substantial amount of study reports. This and other studies indicate that LFS has the potential to be a

partial cement supplement, but its physical and mineral properties vary broadly and are dependent on the geography and industrial processes [40]. Therefore, local LFS products need proper investigation before being considered for application in construction, especially when the manufacturing process is unique, for example, in the steel mills of Bangladesh, no BOFS is produced and LFS is generated only in the ladle refining furnace (LRF). As such, this study focused on the assessment of LFS as a partial replacement of cement.

This study reports the results of mechanical properties of raw and sieved (through #200 sieve) LFS blended mortars following the characterization of the raw LFS powder. The characterization results include chemical, physical, mineralogical, and morphological properties of raw LFS, identified through sophisticated testing facilities and compared with standard cement samples, i.e., CEM-I. The mechanical properties of raw and sieved LFS blended mortars are investigated under normal temperature curing (NTC) and compared with the control samples. Additionally, mechanical properties of LFS blended mortars under high-temperature accelerated curing (HTAC) are investigated to quantify the effect of temperature on strength gain/loss.

2. Materials

2.1. Regular Mortar Materials. Cement (CEM-I) was used as the reference material. As per EN-197, its strength class is 42.5N. The key properties of CEM-I: normal consistency = 25%, soundness by Le Chatelier's test = 4.5 mm, specific gravity = 3.12, clinker = 95–100%, and gypsum = 0–5%. For preparing mortars, EN standard sand was used. This (reference) sand is a natural siliceous material composed of rounded particles and has a silica content of at least 98%. The moisture content was less than 2%, represented by the mass of the dry sample as a percentage. Tap water was used for preparing mortar prisms.

2.2. Supplementary Material Used to Replace Cement. Ladle furnace slag (LFS) was used as the prospective supplementary cementitious material (SCM). The material was collected from a renowned local Steel Re-Rolling Mill of Bangladesh. An impression of just produced LFS from the furnace is shown in Figure 2. Two types of LFS samples were used. The as-received LFS powder is termed as 'raw LFS' and the one sieved through a #200 sieve is termed as 'sieved LFS' (see Figure 3). The use of a finer LFS sample allowed to investigate the effect of fineness since the fineness of steel slag can play a role in improving the fresh and hardened properties of mortar [41, 42].

3. Experimental Program

3.1. Characterization Tests of LFS and CEM-I. X-ray fluorescence (XRF) spectroscopy was used to characterize and identify the elements in CEM-I and raw LFS powders. The method uses a primary incident X-ray on a sample that allows the sample to emit secondary rays called-fluorescent. The fluorescent rays are unique for a specific element in a material, thus allowing characterization and identification of

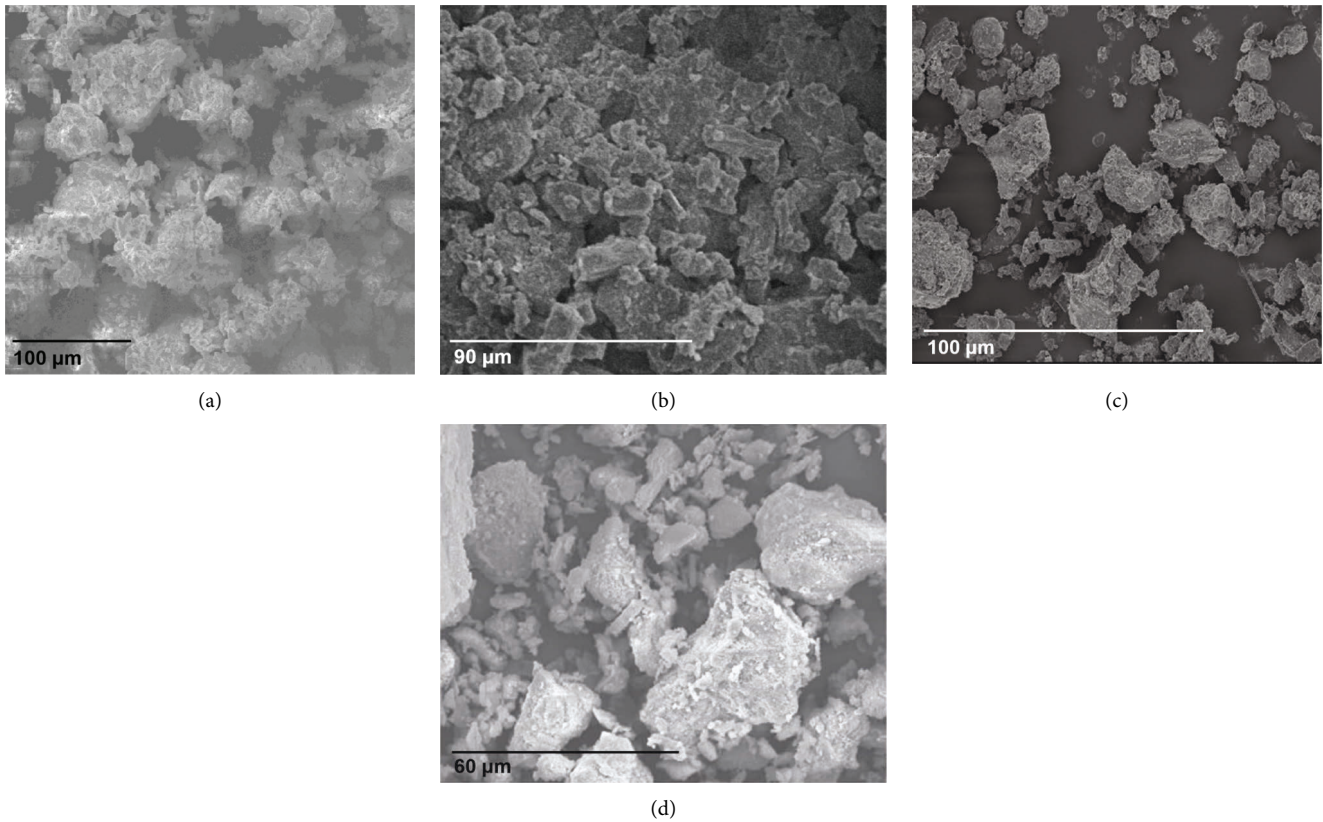


FIGURE 1: SEM images of LFS: (a) [24]; (b) [26]; (c) [39]; (d) [29].



FIGURE 2: LFS as produced in Mirsarai plant of BSRM.

elements in a sample. Details of XRF method can be found in Irshidat and Al-Nuaimi [43], and Rodriguez et al. [44].

The crystalline phases or compounds of CEM-I and raw LFS were identified using X-ray diffraction (XRD) technique. X-ray diffractometer with monochromatic $\text{CuK}\alpha$ source and curved graphite, and single-crystal chromator (40 kV, 30 mA) was used. Samples were firmly compacted on the reverse side of the specimen holder, against a glass slide. Each sample was analysed (for potential diffraction paths of the lattice) over a 2θ range of 3° – 60° at a scan rate of 1° per minute with an increment of

0.1° . More details can be read from Meier et al. [45] and De Villiers and Lu [46]. Figure 4 illustrates XRD method (adapted from [46]).

The morphology and topography (size and shape and surface texture) of the particles of CEM-I and raw LFS were assessed from the microscopic images using scanning electron microscopy (SEM) technique with an accelerating voltage of 15 kV. SEM can visualize the surface of a particle with high to ultra-high-resolution images of a particle in a sample with its crystallography composition [47].



FIGURE 3: Powdered ladle furnace slag (LFS) used in this study (a) raw LFS powder; (b) sieved (#200) LFS powder.

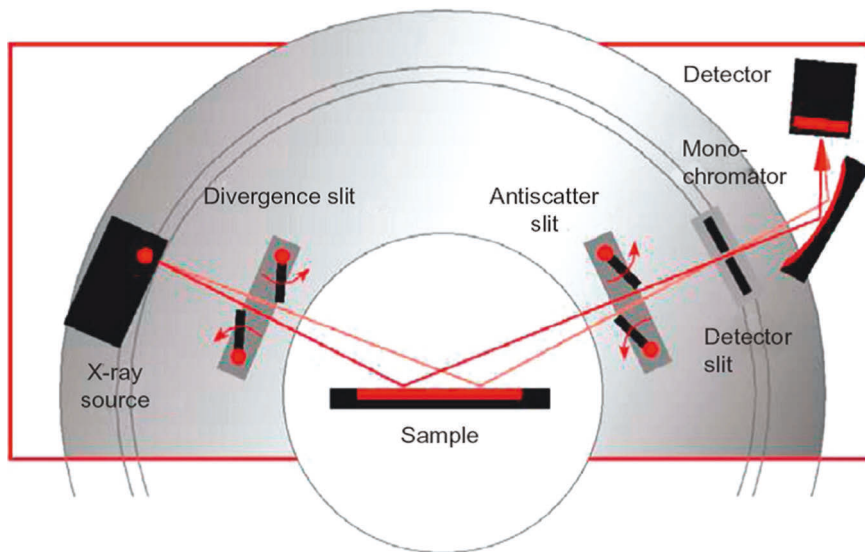


FIGURE 4: The Bragg-Brentano geometry used in modern diffractometers [46].

3.2. Mortar Constituents and Compositions. A total of 15 control mortar prisms was prepared with cement, sand, and water. A total of 132 (includes 3 replicates) LFS blended mortar prisms were prepared with cement, LFS (66 with raw and 66 with sieved), sand, and water. The mixing ratio was 1 : 3 : 0.5 (binder: sand: water) according to EN 196-1. Cement in the mortar was partially replaced by 5, 10, 15, 20, 25, and 50% LFS (both for raw and sieved, separately) by weight. An additional 36 mortar prisms (with raw and sieved LFS) were prepared for HTAC tests. The detailed mix compositions and sample names of mortars are given in Table 1.

3.3. Flow of Mortar. Required amount of materials for mortar was mixed in a mechanical mixer machine as per EN 196-1. The mixer machine was comprised of a stainless-steel bowl (capacity ~5 litres) and blades. The bowl was placed in such way that it was firmly attached to the mixer frame during mixing. The blade rotated about its axis, powered by an electric motor in planetary motion around the axis of the bowl. The speeds of the blade were controlled automatically.

The flow of hydraulic cement mortar was determined using the flow table in compliance with ASTM C1437. The

test specimen was moulded on a 250 mm diameter table ASTM C230. A conical frustum shape mould with a bottom diameter of 100 mm and a top diameter of 70 mm was used. Once filled with mortar paste, the mould was removed, leaving the mortar on the table, and the table was cyclically lowered and raised 25 times (within 15 seconds). After that, the flow, i.e., the increase in the average diameter of the fresh specimen was measured. Flow value was calculated after dividing the increased diameter by the original diameter and reported as a percentage. Flow value for each type of sample was tested for three times in order to obtain mean value.

3.4. Compressive Strength of Mortar. Mortars for strength tests were prepared as mentioned above. The sample with plastic consistency from the mixer machine was poured inside a 3-gang steel mould of 40 × 40 × 160 mm internal dimensions. The mortars were compacted using a regular jolting method inside the mould. The specimens were kept in the mould for about 24 h in a humid environment and then demoulded. As mentioned earlier, 108 mortar prisms with 5–50% cement replacement were prepared using raw and sieved LFS for different curing periods (7, 28, and 56 days).

TABLE 1: Mix composition of mortars for a single mix in a mixer machine as adopted in this study.

Sl	Sample name	Cement (gm)	LFS (gm)	Sand (gm)	Water (gm)
1	ML0 = control (no LFS)	450	—		
2	ML5R = 5% raw LFS	427.5	22.5		
3	ML10R = 10% raw LFS	405	45		
4	ML15R = 15% raw LFS	382.5	67.5		
5	ML20R = 20% raw LFS	360	90		
6	ML25R = 25% raw LFS	337.5	112.5		
7	ML50R = 50% raw LFS	225	225	1350	225
8	ML5S = 5% sieved LFS	427.5	22.5		
9	ML10S = 10% sieved LFS	405	45		
10	ML15S = 15% sieved LFS	382.5	67.5		
11	ML20S = 20% sieved LFS	360	90		
12	ML25S = 25% sieved LFS	337.5	112.5		
13	ML50S = 50% sieved LFS	225	225		

The mortar prisms were then cured under normal water until the compressive strength was tested.

Few samples (30 in total; including control) were prepared for longer age curing (90 and 180 days) with selected blends, viz. 0, 25, and 50% LFS (only three different percentages were considered due to restricted time and budget). Curing time significantly affects mortar properties as the hydration of cement depends on the availability of sufficient water. Proper curing also helps fill the micropores in the hydrated cement paste, thereby increasing the density of mortar. The microstructural improvement contributes to the strength development of the cement paste matrix [48].

The compressive strengths of all cured mortar specimens were measured using a jig inside the standard (EN 196-1) compression testing machine. The jig could hold the mortar prism in such a way that the square area (40×40 mm) was set under the loading plate. The resultant of the forces passed through the centre of the specimen.

3.5. Mortar with High-Temperature Accelerated Curing (HTAC). To investigate the effect of high-temperature curing, i.e., accelerated curing, additional mortar samples were prepared following the guidelines set in BS 3892 (1982). A total of 18 prisms with raw LFS and 18 with sieved LFS were cast which included 3 replicates of each type, i.e., 5, 10, 15, 20, 25, and 50% of LFS. Prepared samples were demolded after 24 hours and then kept in a water bath for standard temperature curing ($20 \pm 1^\circ\text{C}$) for 4 days. After that, the samples were transferred to another water bath for high-temperature curing at $50 \pm 1^\circ\text{C}$ for 46 hours (Figure 5) and then shifted to a standard temperature regime. After 2 hours of standard curing ($20 \pm 1^\circ\text{C}$), essentially producing samples of 7 days curing, the mortar specimens were taken for compressive strength testing.

4. Test Results and Discussion

4.1. Particle Size Distribution (PSD). Particle size distributions of CEM-I and raw LFS are shown in Figure 6. Approximately, 90% of the CEM-I particles are smaller than $107 \mu\text{m}$ in size, and 10% are smaller than $4.28 \mu\text{m}$. The mean and median particle sizes of CEM-I are $22.8 \mu\text{m}$ and $29.2 \mu\text{m}$,

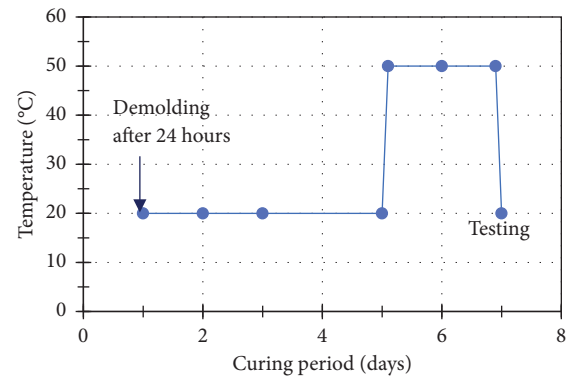


FIGURE 5: Temperature variation with time for HTAC samples.

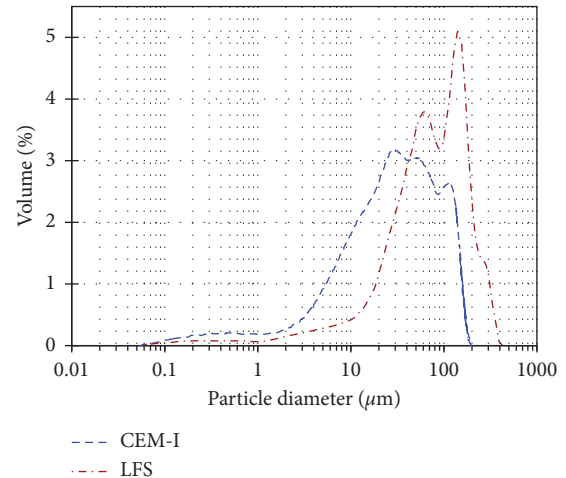


FIGURE 6: Particle size distribution of CEM-I and raw LFS.

respectively. For raw LFS, 90% of the particles are smaller than $188 \mu\text{m}$, and 10% are smaller than $16.0 \mu\text{m}$. The mean and median particle sizes of raw LFS are $59.2 \mu\text{m}$ and $73.7 \mu\text{m}$, respectively. The SEM test results also indicate that raw LFS comprises coarser-sized particles than CEM-I [49]. Therefore, the material was sieved using a $75 \mu\text{m}$ sieve to get the finer part as the size of the particles plays a vital role in

the reactions in cementitious media and influences hardened mortar properties [41, 50]. PSD for sieved was not determined in this study.

In general, raw LFS used in this study has larger sized particles compared with the previous studies. For example, Türker et al. [51] reported that 92% of the raw LFS particles were smaller than $30\ \mu\text{m}$, and Salman et al. [52] reported that 80% of the raw LFS particles were smaller than $59\ \mu\text{m}$. Salman et al. [52] also found that d_{50} of raw LFS is $35.7\ \mu\text{m}$. Researchers studied the suitability of LFS processed to finer particle size, e.g., $d_{50} = 10\text{--}28\ \mu\text{m}$ [33, 39]. This study also considered sieving of raw materials to bring them to a size finer than $75\ \mu\text{m}$ and compared the performance of both raw and sieved LFS as SCM.

4.2. Chemical Composition of Test Materials. The chemical compositions of CEM-I and LFS are given in Table 2. The main compounds found are CaO, SiO₂, MgO, and Al₂O₃, representing more than 92% of the total mass. A study found CaO, SiO₂, MgO, and FeO (low percentage) as the main chemical compositions and comprised about 88–92% of the total mass of LFS [53]. Other studies (e.g., [8, 54]) suggest that CaO, SiO₂, MgO, and Al₂O₃ are present in LFS (see Table 2), which is common for any carbon and steel production slags [40]. These oxides were mentioned as inevitable constituents of silicates and aluminates of calcium and magnesium found in LFS [26].

4.3. Mineralogical Composition of Test Materials. The crystalline compositions of CEM-I and raw LFS are shown in Figures 7(a) and 7(b), respectively. Table 3 illustrates the denotation and chemical formula of the phases present in both CEM-I and LFS. Dominant hump of diffraction was noticed in between $2\theta = 29^\circ$ and 35° in the case of CEM-I. The mineralogical phases detected in CEM-I are Alite (C3S), larnite, i.e., calcium silicate (Ca₂SiO₄) in polymorph states, e.g., β -Ca₂SiO₄, Aluminate (C3A), Brownmillerite (C4AF) and Periclase (MgO). Higher amount of CaO content has the contribution in developing C-S-H gel. Besides, the reaction between CaO and CO₂ is the cause of forming calcite [49].

The mineralogical compounds detected in LFS could be attributed to calcio-olivine (Ca₂SiO₄), akermanite (Ca₂Mg(Si₂O₇)), α -quartz (SiO₂), merwinite (Ca₃MgSi₂O₈), magnetite (Fe₃O₄), and calcium-aluminium oxide (CaAl₂O₄). Important changes in the peak were observed in the range of $2\theta = 27^\circ$ and 33° . The results of the XRD analysis of the investigated LFS are also comparable with the results reported in a previous study [49]. Calcium and silicates under various allotropic forms were the major compounds available in LFS. Calcium-aluminium oxide present in LFS helps to form CaCO₃ and C-S-H gel. Besides, unreacted slag fills the pores and voids which has an effect in densifying the matrix, thus the strength increased [55].

4.4. Morphological Properties Obtained by SEM. Figures 8(a) and 8(b) give SEM micrographs of CEM-I and LFS, respectively. CEM-I is mainly composed of clinker

(95%). SEM image shows relatively smooth and angular surfaces of the grinded clinker. LFS is found with a dusty product on its surface. The surface morphology of LFS particles indicates rough-edged surfaces. A significant number of surface cracks are also noticed. The cracks occur mainly on the periphery of the grains and are parallel to the edges of the grains. Radenović et al. [54]; Natali Murri et al. [39], and Skaf et al. [29] also found similar topography and shape of LFS particles in their studies. The particle size distribution analysis described earlier is also well matched with this SEM data.

4.5. Flow Value of Mortar. Mortar pastes prepared with cement and various levels of both raw and sieved LFS were tested for workability. The workability of raw and sieved LFS blended mortars are compared with that of the control mortar in Figure 9. The flow value of the control cement mortar was found to be 105%. In general, the flow value of LFS blended mortar decreases with the increase in SCM as cement replacement. The flow variation was 14–23% in the case of raw LFS replacement. When the cement is replaced with 5–25% sieved LFS, it varies from 2 to 19%. Reasonably good consistency mortar was produced for up to 20% LFS replacement. According to Balakrishnan et al. [56] and McCarthy et al. [57], flow values of masonry mortar with 10–50% cement replacement with fly ash did not exceed 30% relative to the control mortar. Santamaria et al. [58] reported that SCM of polyhedral crystals creates an inwards capillary action to fill the hollow spaces when water comes into contact. According to the PSD curve (Figure 5), the mean size of raw LFS is higher than cement. As a result, with higher cement replacement, the free space between particles increases, affecting their external capillarity. This may lead to the increase-decrease-increase pattern of flow values. As shown in the figure, mortar with sieved LFS shows better workability compared with the raw LFS as it acts as a filler. Compared with cement, sieved LFS possesses a high specific area and the voids between cements are filled with sieved LFS, increasing the particle contact. Even though both particles absorb water, due to external capillarity, higher water absorption is noticed. Therefore, it is concluded that a higher presence of fines (50% replacement) demanded increased water. An earlier study by Zykova et al. [59] concluded that the composition with complex filler fractions has the highest water absorption.

4.6. Compressive Strength of Mortar

4.6.1. Influence of LFS Size. Figures 10(a) (for raw LFS) and 10(b) (for sieved LFS) present the compressive strength of mortar as a function of LFS replacement levels (7, 28, and 56 days curing under standard temperature, i.e., $20\pm 1^\circ\text{C}$). In general, sieved LFS provides better strength performance than raw LFS. The trend follows earlier study with fly ash [60] which reports that smaller particles have higher reactivity in cementitious media. Similar better performance with finer LFS was reported by Shi and Hu [35]. On the other hand, when the total cementing material content was

TABLE 2: Chemical composition of CEM-I and raw LFS used in this study.

Oxides	CEM-I (this study)	Raw LFS (this study)	Raw LFS [54]	Raw LFS [8]
CaO (%)	60.4	47.4	48.4	30~60
SiO ₂ (%)	29.4	29.4	15	2~35
Al ₂ O ₃ (%)	2.6	2.6	14.3	4.1~35.9
Fe ₂ O ₃ (%)	2.8	0.7	1.5	—
FeO (%)	—	—	—	0~15
MgO (%)	2	2.3	15.3	1~12.6
Na ₂ O (%)	1.5	1.6	0.4	0.06~0.07
K ₂ O (%)	0.7	0.1	0.4	0.01~0.02
TiO ₂ (%)	0.6	0.9	0.2	0.2~0.9
MnO (%)	0.04	1.6	-	0~5

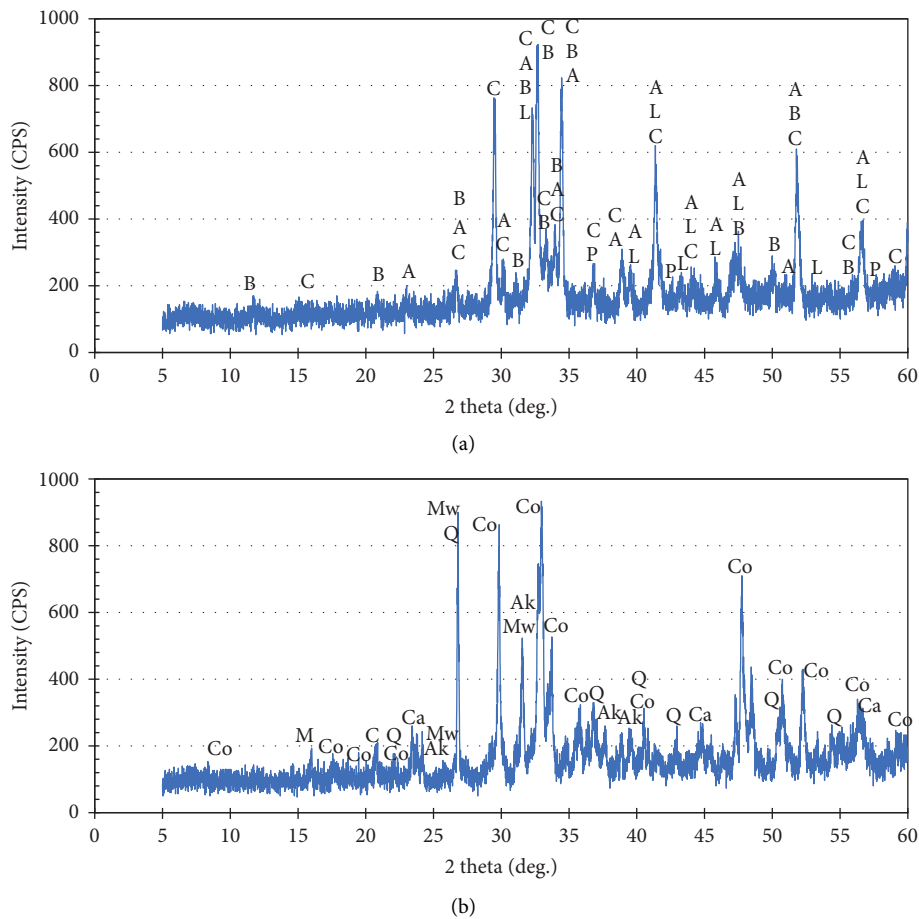


FIGURE 7: XRD patterns of (a) CEM-I and (b) LFS.

reduced with coarser SCM particles, it lowers the volume of hydration products [61].

The performance of sieved LFS is significantly better at an early age (7 days). This may be due to the nucleation effects in mortars [5]. At later ages, the unreacted LFS helps to fill the voids and form a denser mixture. Pozzolanic reaction products are more effective in filling pores. This filler effect can improve the transition zone and cement matrix property [62]. The water-cement ratio increases with SCM dosage. As a result, water-filled capillary space also increases, increasing the degree of hydration [61].

4.6.2. Influence of LFS Replacement. As shown in Figures 10(a) and 10(b), 7-days compressive strength of the control mortar is 35.6 MPa. For 5% raw LFS, the strength increased by 12% compared with the control, while 21.5% increase in strength for sieved LFS is achieved. The strength is comparable to the control (within $\pm 10\%$) up to 10% replacement by raw LFS and 15% by sieved LFS. The secondary reaction between cement hydration by-products and the aluminosilicate compounds present in the LFS creates further bonding and improves the strength. Beyond these replacement levels, the strength decreases linearly, and a

TABLE 3: Mineralogical phases present in CEM-I and LFS with a chemical formula.

Symbol	Compound	Chemical formula
C	Alite/tricalcium silicate	$3\text{CaO}\cdot\text{SiO}_2$ (C_3S)
A	Tri calcium aluminate	$\text{Ca}_3\text{Al}_2\text{O}_6$ (C_3A)
B	Brownmillerite/tetracalcium aluminoferrite	$4\text{CaO}\cdot\text{Al}_n\text{Fe}_{2-n}\text{O}_3$ (C_4AF)
L	Larnite/dicalcium silicate	$\beta\text{-Ca}_2\text{SiO}_4$
P	Periclase	MgO
Co	Calcio-olivine	$\gamma\text{-Ca}_2\text{SiO}_4$
M	Magnetite	Fe_3O_4
Mw	Merwinite	$\text{Ca}_3\text{Mg}[\text{SiO}_4]_2$
Q	α -Quartz	SiO_2
Ca	Calcium-aluminium oxide	CaAl_2O_4
Ak	Akermanite	$\text{Ca}_2\text{Mg}[\text{Si}_2\text{O}_7]$

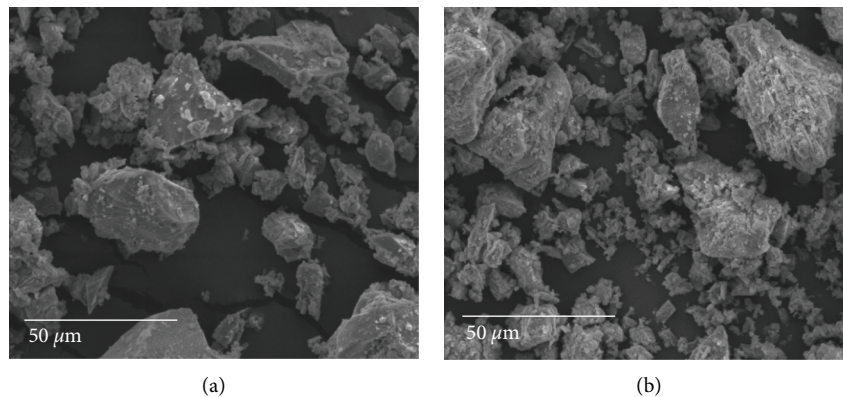


FIGURE 8: Morphology of (a) CEM-I and (b) LFS obtained from SEM.

dramatic fall is observed for 50% LFS replacement. Wang [63] reports that reactivity of SCM reduces with the increase in replacement dosage.

As can be seen from Figure 10(a) (results of raw LFS), for 28 days curing, 5% raw LFS in mortar gives 5% higher compressive strength than that of the control mortar (43.7 MPa). Strength with 10% raw LFS replacement is similar to control mortar. For other replacement amount (i.e., 15%, 20%, 25%, and 50%), the strength reduces by 10.2%, 17.4%, 21.2%, and 57.4%, respectively. For the case of 56 days curing, 5% and 10% replacement with raw LFS gives 8.6% and 3.4% higher strength than the control mortar (48.2 MPa). The strength gain with SCM can be attributed to the fact that the reaction between silica (SiO_2) or alumina (Al_2O_3) and $\text{Ca}(\text{OH})_2$ leads to form C-S-H gel. The dilution effect of SCM on compressive strength is found to be dominant after a specific dosage. Beyond this, for 15%, 20%, 25%, and 50% replacement, the strength reduces by 1.8%, 8.3%, 11.5%, and 56.5%, respectively.

As can be seen from Figure 10(b) (sieved LFS), for 28 days curing, compressive strength increases by 8.6% for 5% sieved LFS replacement and then decreases as the sieved LFS in mortars increases. Strengths are 5.9%, 10.2%, 12.7%, 62.8% lower (compared with control) for the case of 15%, 20%, 25%, and 50% cement replacement with sieved LFS. Although, 10% replacement gives identical compressive strength as of the control mortar. For the case of 56 days curing, compressive strengths of 5% and 10% sieved LFS

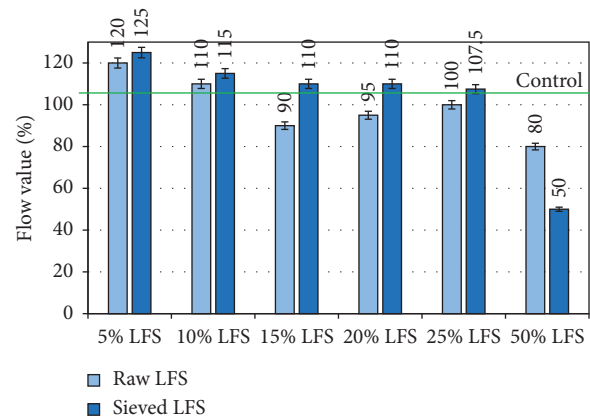


FIGURE 9: Flow value obtained for different LFS (raw and sieved) contents in mortar.

replacement in mortars are found to be higher (15.2% and 6.4%, respectively). Beyond that, the strength gradually reduces by 0.5%, 4.7%, 7.8%, and 44.7% for sieved LFS replacement of 15%, 20%, 25%, and 50%, respectively. Overall, sieved LFS shows better compressive strength than the raw material. With the increase of fineness, the hydration rate of C3S gets accelerated, resulting in strength increase [66].

An earlier study by Santamaria et al. [58] reports that 8%, 16%, 26%, and 46% strength loss can occur if of 10%, 20%, 30%, and 40% of cement in mortar is replaced by LFS.

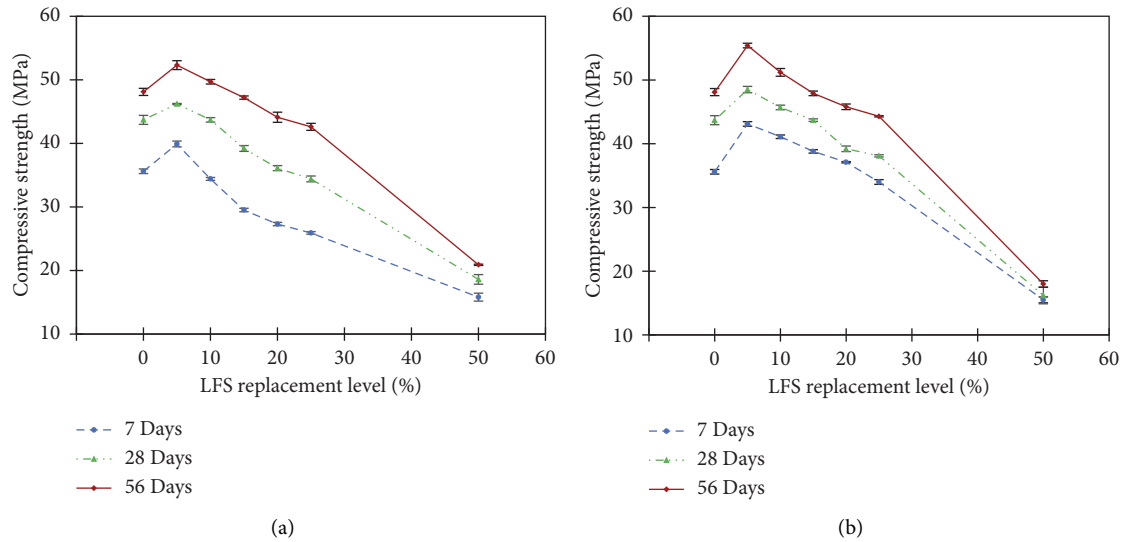


FIGURE 10: Relationship between compressive strength and LFS level in mortar: (a) mortar with raw LFS; (b) mortar with sieved LFS.

Another study reports that compressive strength reduces for mortars partially replaced (more than 20%) with LFS [42]. Previous studies recommend a different amount of LFS replacement, for example, [24]. Manso et al. [32] suggest up to 43% LFS to use in concrete, whereas Chang et al. [65] recommend up to 20% cement replacement with LFS to use in concrete. This study broadly suggests that up to 15% cement replacement with LFS would produce mortar of acceptable strength for regular construction.

4.6.3. Effect of Curing Time on Mortar Strength. The strengths of a few selected mortar samples with prolonged curing are shown in Figure 11, which presents relationships between compressive strength and curing time (7, 28, 56, 90, and 180 days) for raw LFS (Figure 11(a)) and for sieved LFS (Figure 11(b)). The strength of control mortar is compared with 25% and 50% LFS blended mortars of both types (raw and sieved).

The reason for above phenomenon may be attributed to hydration of cement. The cement hydration reaction starts immediately after adding water to cement. Even after replacing the cement with SCM, a reaction process initiates by which the mixture gets stiffened and attains its strength. The heat helps in faster hydration reaction and forms C-S-H gel rapidly. The pozzolanic effect also gets intensified at higher temperatures. However, in some cases, the ‘crossover effect’ at high temperature may cause reduction of strength [66]. Türkel and Alabas [67] report 65–70°C as the optimum temperature for accelerated curing. If the curing temperature crosses this limit for a more extended period, a drastic later age strength reduction may occur. This study, therefore, considered a limited period of high-temperature curing regime as per BS 3892 [68].

Results obtained for LFS blended 7 days HTAC mortars are compared with LFS blended 28 days NTC mortars in

Figure 13. Figure 13(a) presents compressive strength as a function of raw LFS level and Figure 13(b) presents same for the sieved samples. It is evident from Figures 13(a) and 13(b) that by increasing the curing temperature, mortars can gain their strength much quicker than it would gain under standard or normal temperature curing. For both raw and sieved LFS blended mortars, strengths of 7 days’ HTAC mortars at 5%, 10%, 15%, 20%, 25%, and 50% replacements are close (within 10%) to that of 28 days’ NTC mortars. Mortars under accelerated curing were reported by Esen and Kurt [69] where cement was replaced partially by nanosilica, and by Islam [60] where cement was partially replaced by fly ash. They observed that compressive strength was increased by 5–11% when the curing temperature was accelerated. Erdem et al. [70] discuss that an accelerated curing system is incorporated in the prefabrication industry to reduce the cycle time of strength gain eventually allowing for cost-saving.

For 25% LFS replacement, an increase in compressive strength can be noticed at 90 days curing, which is true for both raw (Figure 11(a)) and sieved LFS blends (Figure 11(b)). However, 50% LFS (both raw and sieved) replacement gives no promising results even for an extended curing period, probably due to greater loss of reactivity with increased SCM [63]. For both percentages, strength improvement between 90 and 180 days is insignificant, again, true for both raw and sieved LFS blends (Figures 11(a) and 11(b)). For sieved LFS at 90 days curing, strength of 25% LFS blended mortar is within the 10% of control mortar (Figure 11(b)): compressive strength value of 45 MPa at this age (90 days) would be promising for any structural use, especially for foundation work where continuous hydration by groundwater is possible. From Figures 11(a) and 11(b), the similar strength of raw and sieved LFS at 90 days indicates that all materials can eventually react with time regardless of size.

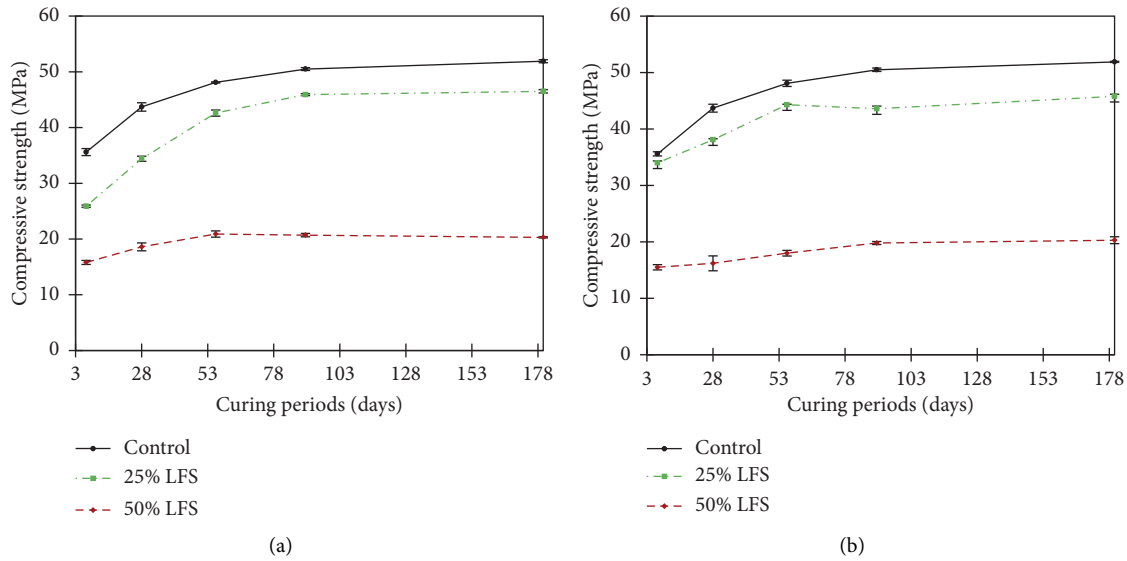


FIGURE 11: Relationship between compressive strength of mortar and curing period: (a) mortars with raw LFS; (b) mortars with sieved LFS.

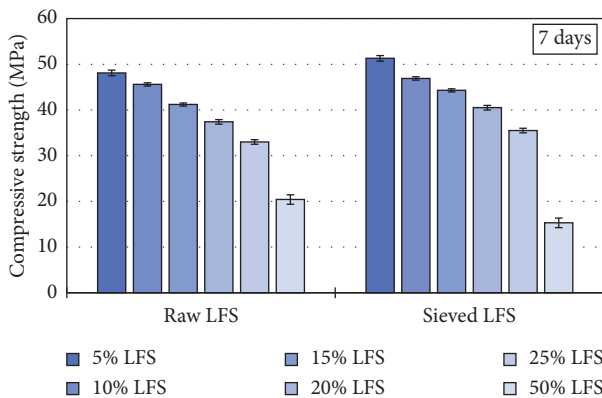


FIGURE 12: Compressive strength (nominal 7 days) of LFS-blended HTAC mortars (7 days include 46 hours high-temperature curing at $50\pm 1^\circ\text{C}$).

4.7. Mortar Strength for High-Temperature Accelerated Curing (HTAC). The effect of high-temperature accelerated curing (HTAC) on mortar strength is discussed here based on Figure 12. Limited period high-temperature (46 hours at $50\pm 1^\circ\text{C}$) curing (overall about 7 days curing) shows a significant influence on the compressive strength of LFS blended mortars (raw and sieved) of various replacement percentages (5, 10, 15, 20, 25, and 50%). Results for LFS blended HTAC (both raw and sieved) mortars indicate that 5–20% cement replacement with LFS gives higher strength (above 37 MPa). These values are close to 28 days’ strength (36.1 MPa) of mortars in normal temperature curing (NTC). As can also be seen from Figure 12, under HTAC, sieved LFS blended mortar performs better (which was true for sieved LFS mortars under NTC; Figure 10(b)).

4.8. Practical Implications. Apart from producing eco-friendly mortar (which is a default benefit), use of LFS as a partial replacement to cement may reduce the construction cost. Figure 14 (considering 5% more or less) gives an approximate estimation of the cost savings—standard market prices of the constituent ingredients are considered. In Bangladesh, the cost of 1 tonne LFS is \$30 (USD), according to a steel mill’s contract with a known company (personal communication). That means 50 kgs of LFS would cost approximately \$1.5. An additional \$0.5 can be considered (from experience) for other costs, such as transportation, handling, and storage. Then the total cost would be \$2. On the other hand, 50 kgs (1 bag) of Portland cement in Bangladesh costs approximately \$6 (3 times higher than the cost of LFS). Therefore, partial replacement of about 15% (as can be derived from this study) of cement by LFS may substantially reduce the cost, and an eventual reduction of cement use by 15%. For the case where strength is reduced by 10–20% when cement is replaced by LFS for up to 25% replacement, the compromised strength of the blended cement could still be used for non-structural work, and production of cement can be reduced by 25% as well. With a 15% blending of LFS in cement, the overall cost-saving will probably be 11% (Figure 14). This saving will increase up to 18.5% for 25% cement replacement with LFS.

In addition, the environmental benefit of using LFS as SCM can also be quantified, indirectly though. Recent and previous reports mention that appx. 90% of CO_2 can be emitted during cement production [71, 72], i.e., 900 kg of CO_2 is being released when 1 tonne cement is produced. A simple calculation results as shown in Figure 15 suggests that 20% of LFS use will cause 72% of CO_2 generation which would otherwise cause a 90% CO_2 generation if only cement

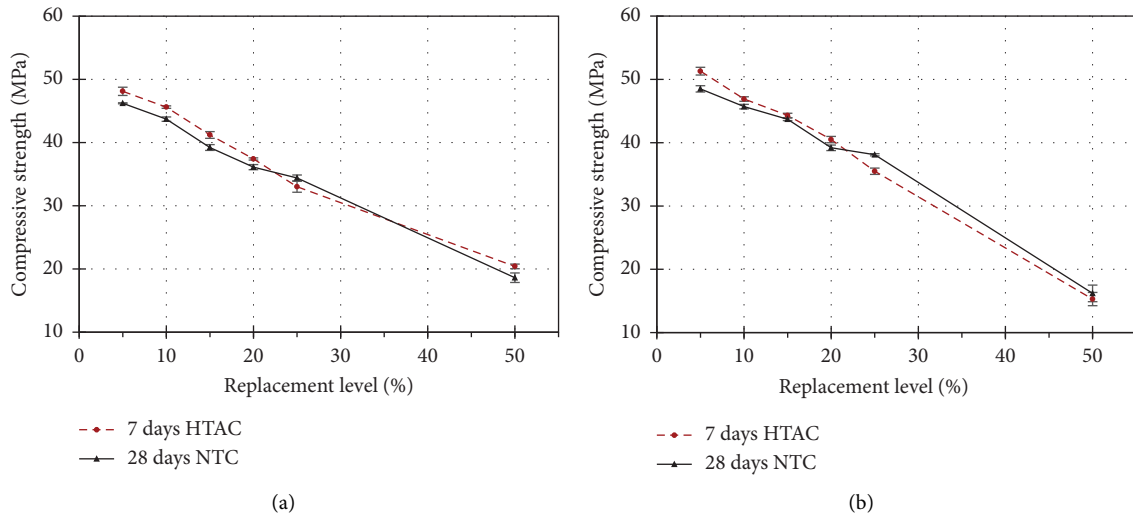


FIGURE 13: Strength comparison between 7 days HTAC mortars and 28 days NTC mortars. (a) Raw LFS-blended mortars; (b) Sieved LFS-blended mortars.

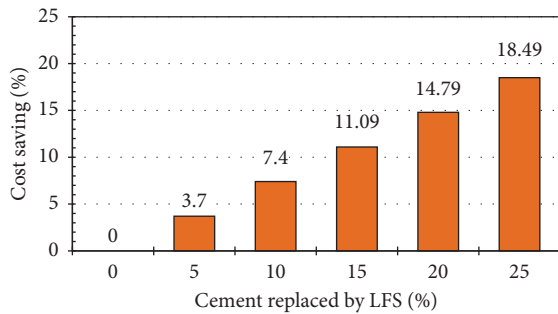


FIGURE 14: Probable economic benefit of partial cement replacement by LFS.

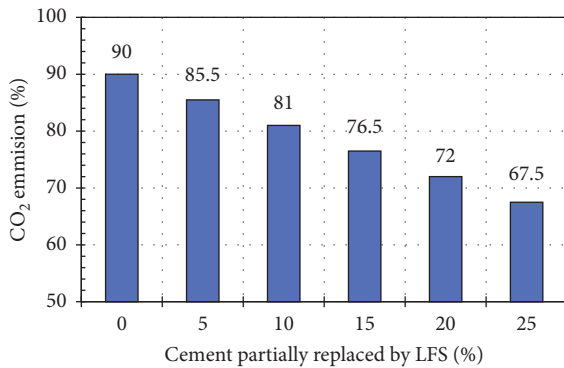


FIGURE 15: Probable reduction in CO₂ generation due to LFS use.

was used (any emission attributed to LFS production is ignored here). This is in line with the published report of Campos et al. [73] that states a yearly reduction of 100 thousand tonnes of CO₂ when cement in concrete is reduced by 5 kg per cubic metre.

Further evidences of environmental benefit of using LFS in mortar (or concrete in a broader sense) can be inferred from the study of Perez-garcia et al. [74]. They

conducted a leachate test on Portland cement and LFS (30% substitution) for selected chemical elements and reported that leaching potential was less in LFS mixed concrete compared with control concrete. They have further reported that presence of chromium (Cr) was significant in control concrete. For the case of LFS, the level of Cr was within the Code of Federal Regulation limit (5 mg/L). It was concluded that LFS replaced with cement may dilute the cement matrix paste and absorb this element, hence, no additional environmental hazard would take place. Other leachates were found like the conventional concrete. Their report hints that it is wise to manage LFS slag by encapsulating it into cementitious media rather than depositing it as a landfill. Direct deposition in landfill may leach the harmful chemical compounds/heavy metals to the environment [75].

5. Conclusion

In this study, a locally available LFS was first characterized for its chemical and physical properties. Then, the LFS was incorporated in mortar as a partial replacement of cement. Two forms of the LFS were used: raw (as-received) and sieved (#200 sieve). The compressive strengths of mortars, prepared with various LFS percentages (0, 5%, 10%, 15%, 20%, 25%, 50%) of raw and sieved LFS and cured under normal temperature (NTC) for 7, 28, and 56 days, were obtained and reported. Selected samples were cured for 90 and 180 days. Additionally, raw and sieved LFS blended mortars under high-temperature accelerated curing (HTAC) were tested (at 7 days) and reported in this study. The key conclusions arisen from this study on raw and sieved LFS blended mortars, are as follows:

- (1) Chemical composition of LFS gives similar oxides to that of CEM-I. The amount of CaO, SiO₂, MgO, and Al₂O₃ in raw LFS collectively cover more than 92% of the total mass.

- (2) The mineralogical phases present in the raw LFS are calcio-olivine, akermanite, α -quartz (SiO_2), merwinite, magnetite, and calcium-aluminium oxide.
- (3) Morphology of LFS is a whitish dusty surface. The grains are found with sharp edges. The surface contains significant cracks with roughness.
- (4) The performance of LFS in mortar is improved using smaller size by sieving. In general, 5–15% cement replacement with LFS (raw and sieved) provides better or comparable performance than/to control mortars. Reasonable compressive strength is found with 15% LFS replacement.
- (5) Compressive strength of the raw and sieved LFS blended mortars generally increases with curing period up to 90 days. Further curing beyond that offers very marginal strength.
- (6) Seven days compressive strengths of raw and sieved LFS blended HTAC mortars were found to be well comparable to the strengths of 28 days NTC mortars.

This study endorses that LFS considered in this study can be an excellent SCM, preferably up to 15% cement substitution. However, further investigation is indispensable to explore the mechanical and durability properties of hardened concrete prepared with similar LFS as SCM. This is being considered by the authors and will be reported in a forthcoming paper.

Data Availability

Some or all data, models, or codes that support the findings of this study are available from the corresponding author upon reasonable request.

Conflicts of Interest

The authors declare that they have no conflicts of interest.

Authors' Contributions

Iffat Sultana was responsible for conceptualization; methodology; experimental work; analysis; and original draft preparation. G. M. Sadiqul Islam was involved in conceptualization; methodology; material arrangement; editing; and supervision.

Acknowledgments

The laboratory support from the Department of Civil Engineering, Chittagong University of Engineering and Technology (CUET), Department of Petroleum and Mining Engineering, CUET, and Industrial Chemistry Lab, School of Civil Engineering and Built Environment, Liverpool John Moores University, UK, are greatly acknowledged. Besides, the authors would like to thank the authority of Bangladesh Steel Re-rolling Mills, Mirsarai plant for supplying LFS.

References

- [1] J. Lehne and F. Preston, *Making Concrete Change; Innovation in Low-carbon Cement and Concrete*, Chatham House Rep, London, UK, pp. 1–122, 2018.
- [2] IEA, *Cement*, IEA, Paris, 2020.
- [3] BCMA, *Overview of Cement Industry*, Dhaka, Bangladesh, 2021.
- [4] I. Sultana and G. M. S. Islam, *Applicability of Treated Industrial Wastewater in concrete Construction*, pp. 12–13, Southern University Bangladesh, Chittagong, 2018.
- [5] G. S. Islam, M. H. Rahman, and N. Kazi, "Waste glass powder as partial replacement of cement for sustainable concrete practice," *International Journal of Sustainable Built Environment*, vol. 6, no. 1, pp. 37–44, 2017.
- [6] A. Naceri and M. C. Hamina, "Use of waste brick as a partial replacement of cement in mortar," *Waste Management*, vol. 29, no. 8, pp. 2378–2384, 2009.
- [7] H. Toutanji and T. El-Korchi, "The influence of silica fume on the compressive," *Cement and Concrete Research*, vol. 25, pp. 1591–1602, 1995.
- [8] I. Z. Yildirim and M. Prezzi, "Chemical, mineralogical, and morphological properties of steel slag," *Advances in Civil Engineering*, vol. 2011, pp. 1–13, 2011.
- [9] A. A. Phul, M. J. Memon, S. N. R. Shah, and A. R. Sandhu, "GGBS and fly ash effects on compressive strength by partial replacement of cement concrete," *Civil Engineering J*, vol. 5, no. 4, pp. 913–921, 2019.
- [10] R. Roy and V. Sairam, "Effect of Silica Fume and Foundry waste sand on strength characteristics of Geogrid and Ferro cement panel," *Materials Today Proceedings*, vol. 7, pp. 362–372, 2019.
- [11] B. Xu and Y. Yi, "Soft clay stabilization using ladle slag-ground granulated blastfurnace slag blend," *Applied Clay Science*, vol. 178, Article ID 105136, 2019.
- [12] P. Saloni, Y. Y. Lim, Y. Y. Lim, T. M. Pham, and P. Negi, "Performance enhancement of rubberised-alkali-activated-concrete utilising ultra-fine slag and fly ash," *Cleaner Materials*, vol. 4, Article ID 100080, 2022.
- [13] G. M. S. Islam and A. Akter, "Rice husk ash as a sustainable construction material for Bangladesh," in *1st International Conference on Advances in Civil Engineering (ICACE 2012)* Department of Civil Engineering, Chittagong University of Engineering & Technology (CUET), Chittagong, Bangladesh, 2012.
- [14] K. H. Mo, U. J. Alengaram, M. Z. Jumaat, S. P. Yap, and S. C. Lee, "Green concrete partially comprised of farming waste residues: a review," *Journal of Cleaner Production*, vol. 117, pp. 122–138, 2016.
- [15] K. Perumal, A. Kumar, N. Lingeshwaran, and S. Susmitha, "Experimental studies on flexural behaviour of self compact concrete beam," *Materials Today: Proceedings. Elsevier*, vol. 33, no. 1, pp. 129–135, 2020.
- [16] J. Payá, J. Monzó, M. V. Borrachero, L. Soriano, J. L. Akasaki, and M. M. Tashima, "New inorganic binders containing ashes from agricultural wastes," *Sustainable and Nonconventional Construction Materials Using Inorganic Bonded Fiber Composites. Elsevier, Chapter 5*, pp. 127–164, 2017.
- [17] G. Martínez-Barrera, C. E. Barrera-Díaz, E. Cuevas-Yañez et al., "Waste cellulose from tetra pak packages as reinforcement of cement concrete," *Advances in Materials Science and Engineering, Special Issue, Green Composite Materials*, vol. 2015, 6 pages, 2015.

- [18] D. Barua, "Effectiveness of use of rice husk ash as partial replacement of cement in concrete," in *Proceedings of the 4th International Conference on Civil Engineering for Sustainable Development*, KUET, Khulna, Bangladesh, 2018.
- [19] M. A. Hasan, "A Study on the Use of rice Husk Ash (RHA) as Partial Replacement of Cement in concrete," *Engineering Heritage Journal*, vol. 3, no. 1, pp. 01–04, 2020.
- [20] G. M. S. Islam, M. M. Islam, A. Akter, and M. S. Islam, "Green construction materials – Bangladesh perspective," in *Proceedings of the International Conference on Mechanical Engineering and Renewable Energy (ICMERE2011)*, Department of Mechanical Engineering, CUET, Bangladesh., Chittagong, 2011.
- [21] S. I. Ahmad, "Mechanical and Durability Properties of Induction-Furnace-Slag-Incorporated Recycled 2018," *Journal of Building Engineering*, vol. 61, Article ID 105301, 2018.
- [22] M. Mahoutian and Y. Shao, "Low temperature synthesis of cement from ladle slag and fly ash," *Journal of Sustainable Cement-Based Materials*, vol. 5, no. 4, pp. 247–258, 2016.
- [23] Y. Jiang, T. C. Ling, C. Shi, and S. Y. Pan, "Characteristics of steel slags and their use in cement and concrete—a review," *Resources, Conservation and Recycling*, vol. 136, pp. 187–197, 2018.
- [24] J. M. Manso, M. Losañez, J. A. Polanco, and J. J. Gonzalez, "Ladle furnace slag in construction," *Journal of Materials in Civil Engineering*, vol. 17, no. 5, pp. 513–518, 2005.
- [25] G. S. Islam, S. Akter, and T. B. Reza, "Sustainable high-performance, self-compacting concrete using ladle slag," *Cleaner Engineering and Technology*, vol. 7, Article ID 100439, 2022.
- [26] J. Setién, D. Hernández, and J. J. González, "Characterization of ladle furnace basic slag for use as a construction material," *Construction and Building Materials*, vol. 23, no. 5, pp. 1788–1794, 2009.
- [27] J. M. Manso, V. Ortega-López, J. A. Polanco, and J. Setién, "The use of ladle furnace slag in soil stabilization," *Construction and Building Materials*, vol. 40, pp. 126–134, 2013.
- [28] J. M. Montenegro, D. Ph, J. Cañizal, D. Ph, J. Setién, and D. Ph, "Ladle Furnace Slag in the Construction of Embankments: Expansive Behavior Ladle Furnace Slag in the Construction of Embankments," *Expansive Behavior, Journal of Materials in Civil Engineering*, vol. 25, no. 8, 2013.
- [29] M. Skaf, V. Ortega-López, J. A. Fuente-Alonso, A. Santamaría, and J. M. Manso, "Ladle furnace slag in asphalt mixes," *Construction and Building Materials*, vol. 122, pp. 488–495, 2016.
- [30] C. Shi and J. Qian, "High performance cementing materials from industrial slags — a review," *Resources, Conservation and Recycling*, vol. 29, no. 3, pp. 195–207, 2000.
- [31] C. Shi, "Characteristics and cementitious properties of ladle slag fines from steel production," *Cement and Concrete Research*, vol. 32, no. 3, pp. 459–462, 2002.
- [32] J. M. Manso, Á. Rodríguez, Á. Aragón, and J. J. Gonzalez, "The durability of masonry mortars made with ladle furnace slag," *Construction and Building Materials*, vol. 25, no. 8, pp. 3508–3519, 2011.
- [33] E. Adesanya, H. Sreenivasan, A. M. Kantola et al., "Ladle slag cement – characterization of hydration and conversion," *Construction and Building Materials*, vol. 193, pp. 128–134, 2018.
- [34] L. Kriskova, Y. Pontikes, Ö. Cizer et al., "Effect of mechanical activation on the hydraulic properties of stainless steel slags," *Cement and Concrete Research*, vol. 42, no. 6, pp. 778–788, 2012.
- [35] C. Shi and S. Hu, "Cementitious properties of ladle slag fines under autoclave curing conditions," *Cement and Concrete Research*, vol. 33, no. 11, pp. 1851–1856, 2003.
- [36] Y.-N. Sheen, D.-H. Le, and T.-H. Sun, "Innovative usages of stainless steel slags in developing self-compacting concrete," *Construction and Building Materials*, vol. 101, pp. 268–276, 2015.
- [37] M. Salman, Ö. Cizer, Y. Pontikes et al., "Cementitious binders from activated stainless steel refining slag and the effect of alkali solutions," *Journal of Hazardous Materials*, vol. 286, pp. 211–219, 2015.
- [38] S. Choi, J.-M. Kim, D. Han, and J.-H. Kim, "Hydration properties of ladle furnace slag powder rapidly cooled by air," *Construction and Building Materials*, vol. 113, pp. 682–690, 2016.
- [39] A. Natali Murri, W. D. A. Rickard, M. C. Bignozzi, and A. Van Riessen, "High temperature behaviour of ambient cured alkali-activated materials based on ladle slag," *Cement and Concrete Research*, vol. 43, pp. 51–61, 2013.
- [40] O. Najm, H. El-Hassan, and A. El-Dieb, "Ladle slag characteristics and use in mortar and concrete: a comprehensive review," *Journal of Cleaner Production*, vol. 288, Article ID 125584, 2021.
- [41] A. Bougara, C. Lynsdale, and K. Ezziane, "Activation of Algerian slag in mortars," *Construction and Building Materials*, vol. 23, no. 1, pp. 542–547, 2009.
- [42] I. Papayianni and E. Anastasiou, "Effect of granulometry on cementitious properties of ladle furnace slag," *Cement and Concrete Composites*, vol. 34, no. 3, pp. 400–407, 2012.
- [43] M. R. Irshidat and N. Al-Nuaimi, "Industrial waste utilization of carbon dust in sustainable cementitious composites production," *Materials*, vol. 13, no. 15, p. 3295, 2020.
- [44] A. Rodriguez, I. Santamaria-Vicario, V. Calderón, C. Junco, and J. García-Cuadrado, "Study of the expansion of cement mortars manufactured with Ladle Furnace Slag (LFS)," *Materiales de Construcción*, vol. 69, no. 334, p. 183, 2019.
- [45] R. Meier, J. Anderson, and S. Verryn, "Industrial X-ray diffraction analysis of building materials," *Reviews in Mineralogy and Geochemistry*, vol. 74, no. 1, pp. 147–165, 2012.
- [46] J. P. R. De Villiers and L. Lu, "XRD analysis and evaluation of iron ores and sinters," *Iron Ore Mineral. Process. Environ. Sustain.* vol. 85, p. 100, 2015.
- [47] Z. He, C. Qian, Y. Zhang, F. Zhao, and Y. Hu, "Nano-indentation characteristics of cement with different mineral admixtures," *Science China Technological Sciences*, vol. 56, no. 5, pp. 1119–1123, 2013.
- [48] M. A. Uddin, M. Jameel, H. R. Sobuz, N. M. S. Hasan, M. S. Islam, and K. M. Amanat, "The effect of curing time on compressive strength of composite cement concrete," *Applied Mechanics and Materials*, vol. 204–208, pp. 4105–4109, 2012.
- [49] N. Yong-Sing, L. Yun-Ming, H. Cheng-Yong et al., "Evaluation of flexural properties and characterisation of 10-mm thin geopolymer based on fly ash and ladle furnace slag," *Journal of Materials Research and Technology*, vol. 15, pp. 163–176, 2021.
- [50] M. J. McCarthy, G. M. S. Islam, L. J. Csetenyi, and M. R. Jones, "Refining the foam index test for use with air-entrained fly ash concrete," *Magazine of Concrete Research*, vol. 64, no. 11, pp. 967–978, 2012.
- [51] H. T. Türker, M. Balçikanlı, I. H. Durmuş, E. Özbay, and M. Erdemir, "Microstructural alteration of alkali activated slag mortars depend on exposed high temperature level," *Construction and Building Materials*, vol. 104, pp. 169–180, 2016.

- [52] M. Salman, Ö. Cizer, Y. Pontikes, L. Vandewalle, B. Blanpain, and K. Van Balen, "Effect of curing temperatures on the alkali activation of crystalline continuous casting stainless steel slag," *Construction and Building Materials*, vol. 71, pp. 308–316, 2014.
- [53] C. Shi, "Steel slag—its production, processing, characteristics, and cementitious properties," *Journal of Materials in Civil Engineering*, vol. 16, no. 3, pp. 230–236, 2004.
- [54] A. Radenović, J. Malina, and T. Sofilić, "Characterization of ladle furnace slag from carbon steel production as a potential adsorbent," *Advances in Materials Science and Engineering*, vol. 20136 pages, 2013.
- [55] G. Kürklü, "The effect of high temperature on the design of blast furnace slag and coarse fly ash-based geopolymers mortar," *Composites Part B: Engineering*, vol. 92, pp. 9–18, 2016.
- [56] B. Balakrishnan, A. S. M. A. Awal, A. H. B. Abdullah, and M. Z. Hossain, "Flow properties and strength behaviour of masonry mortar incorporating high volume fly ash," *International Journal of GEOMATE*, vol. 12, no. 31, pp. 121–126, 2017.
- [57] M. J. McCarthy, G. M. S. Islam, L. J. Csetenyi, and M. R. Jones, *Evaluating test methods for rapidly assessing fly ash reactivity for use in concrete*, World of Coal Ash Conference, Lexington, Kentucky, USA, 2013.
- [58] A. Santamaria, V. Ortega-Lopez, M. Skaf et al., "Ladle furnace slag as cement replacement in mortar mixes," *Sustain. Constr. Mater. Technol.* vol. 1, 2019.
- [59] A. K. Zykova, P. V. Pantyukhov, N. N. Kolesnikova, A. A. Popov, and A. A. Olkhov, "Influence of particle size on water absorption capacity and mechanical properties of polyethylene-wood flour composites," *AIP Conference Proceedings*, vol. 1683, 2015.
- [60] G. M. S. Islam, *Evaluating Reactivity and Sorptivity of Fly Ash for Use in concrete Construction*, University of Dundee, Dundee, Scotland, 2012.
- [61] N. Neithalath, "Quantifying the effects of hydration enhancement and dilution in cement pastes containing coarse glass powder," *Journal of Advanced Concrete Technology*, vol. 6, no. 3, pp. 397–408, 2008.
- [62] M. Singh, A. Srivastava, and D. Bhunia, "An investigation on effect of partial replacement of cement by waste marble slurry," *Construction and Building Materials*, vol. 134, pp. 471–488, 2017.
- [63] X. Y. Wang, "Effect of fly ash on properties evolution of cement based materials," *Construction and Building Materials*, vol. 69, pp. 32–40, 2014.
- [64] V. L. Bonavetti, V. F. Rahhal, and E. F. Irassar, "Studies on the carboaluminate formation in limestone filler-blended cements," *Cement and Concrete Research*, vol. 31, no. 6, pp. 853–859, 2001.
- [65] S. Y. Chang, S. C. Chen, C. Tu, and Y. W. Tseng, "Ladle furnace slag as a sustainable binder for masonry mortars," *Key Engineering Materials*, vol. 801, pp. 385–390, 2019.
- [66] J. Payá, J. Monzó, E. Peris-Mora, M. V. Borrachero, R. Tercero, and C. Pinillos, "Early-strength development of portland cement mortars containing air classified fly ashes," *Cement and Concrete Research*, vol. 25, no. 2, pp. 449–456, 1995.
- [67] S. Türkel and V. Alabas, "The effect of excessive steam curing on Portland composite cement concrete," *Cement and Concrete Research*, vol. 35, no. 2, pp. 405–411, 2005.
- [68] A. F. Abdalqader, F. Jin, and A. Al-Tabbaa, "Development of greener alkali-activated cement: utilisation of sodium carbonate for activating slag and fly ash mixtures," *Journal of Cleaner Production*, vol. 113, pp. 66–75, 2016.
- [69] Y. Esen and A. Kurt, "Effect of high temperature in concrete for different mineral additives and rates," *KSCE Journal of Civil Engineering*, vol. 22, no. 4, pp. 1288–1294, 2018.
- [70] T. K. Erdem, L. Turanlı, and T. Y. Erdogan, "Setting time: an important criterion to determine the length of the delay period before steam curing of concrete," *Cement and Concrete Research*, vol. 33, no. 5, pp. 741–745, 2003.
- [71] S. C. Bostanci, "Use of waste marble dust and recycled glass for sustainable concrete production," *Journal of Cleaner Production*, vol. 251, Article ID 119785, 2020.
- [72] M. Nisbet and M. G. Van Geem, "Environmental life cycle inventory of Portland cement and concrete," *World Cem*, vol. 28, 1997.
- [73] H. F. Campos, N. S. Klein, and J. Marques Filho, "Proposed mix design method for sustainable high-strength concrete using particle packing optimization," *Journal of Cleaner Production*, vol. 265, Article ID 121907, 2020.
- [74] F. Perez-garcia, A. Gonzalez-herrera, M. Jos, and M. D. Rubio-cintas, "Concrete: Mechanical, Physical and Environmental Properties," *Cement and Concrete Research*, vol. 27, no. 12, pp. 1817–1823, 2019.
- [75] S. S. Varanasi, V. M. R. More, M. B. V. Rao, S. R. Alli, A. K. Tangudu, and D. Santanu, "Recycling ladle furnace slag as flux in steelmaking: a review," *J. Sustain. Metall.* vol. 5, no. 4, pp. 449–462, 2019.

Research Article

Evaluating the Effect of China's Carbon Emission Trading Policy on Energy Efficiency of the Construction Industry Based on a Difference-in-Differences Method

Shasha Xie  and Jinjing Wang 

School of Civil Engineering and Architecture, Wuhan Institute of Technology, Wuhan 43000, China

Correspondence should be addressed to Jinjing Wang; wjin1994@163.com

Received 10 July 2022; Revised 15 August 2022; Accepted 16 August 2022; Published 30 August 2022

Academic Editor: Onn Chiu Chuen

Copyright © 2022 Shasha Xie and Jinjing Wang. This is an open access article distributed under the Creative Commons Attribution License, which permits unrestricted use, distribution, and reproduction in any medium, provided the original work is properly cited.

China's construction industry makes important contributions to energy consumption and pollution emissions. It is significant to improve energy efficiency in the construction industry. Since 2011, the introduction of China's carbon emission trading policy has had a great impact on energy conservation and emission reduction. The implementation of the carbon emission trading policy provides us with an opportunity to find solutions to improve the energy efficiency of the construction industry (EECI) in China. In this article, the implementation of carbon emission trading is regarded as a quasi-natural experiment, and the impact of the carbon emission trading policy on the energy efficiency of the construction industry is evaluated by analyzing the panel data related to the energy of the construction industry in 30 provincial regions from 2008 to 2016 through a difference-in-differences method. The main conclusions are as follows. First, the carbon emission trading policy can improve EECI. Second, the carbon emission trading policy can achieve the policy effect of improving EECI by optimizing the allocation of construction machinery resources and enhancing regional technical innovation. At the same time, strengthening government environmental regulation can strengthen the policy effect as well. Finally, some policy implications based on the study are proposed.

1. Introduction

Since the twentieth century, the coordination between economic development and environmental protection has gradually attracted the attention of most of the world. To realize sustainable development, some consensus on environmental protection has been reached among many countries [1]. Climate change is one of the most important issues, and some international clauses have been signed. For example, the Paris Agreement reached in 2015 is a measure for mankind to jointly deal with climate change after the United Nations Framework Convention on Climate Change in 1992 and the Kyoto Protocol in 1997, which committed to reducing greenhouse gas emissions. Representatives of China signed the Paris Agreement in 2016, which was followed by the approval of the National People's Congress Standing Committee [2]. In 2020, the President Xi of the People's Republic of China announced at the 75th UN

General Assembly that China is striving to peak its carbon dioxide emissions by 2030 and to achieve the carbon-neutral target by 2060.

As a matter of fact, the Chinese government has implemented several policies trying to achieve energy conservation and emission reduction in the past two decades, and the carbon emissions trading policy is one of them. Carbon emission trading policy is considered as a market-oriented environmental regulation [3], which has been effectively carried out in Europe and other regions; and has recently proved to be an effective energy conservation and emission reduction policy implemented in China by empirical research [1]. In 2011, China's National Development and Reform Commission (NDRC) declared a pilot carbon emissions trading scheme, approving Beijing, Shanghai, Tianjin, Chongqing, Hubei, Guangdong, and Shenzhen to start carbon emissions trading. In June 2013, the pilot project gradually started carbon emission trading.

At the end of 2016, Fujian launched carbon emissions trading. In 2017, the national power industry issued the policy. In 2021, the national carbon emissions trading market opened. The implementation of the carbon emission trading policy in different regions in China covers different industries. The specific industries covered include power, heat, cement, chemical, metal, petrochemical, automobile, public construction, etc. [4]. It can be seen that the power, steel, and cement industries are the key regulated industries. Looking back at the policy implementation of the first six pilots, as of December 31, 2016, the seven carbon market pilots (including Fujian) had a transaction volume of 160 million tons, valued at nearly 2.5 billion yuan [2]. Undoubtedly, the implementation of the policy has had a significant impact on energy consumption in pilots [5].

China's construction industry is a national pillar industry, which not only contributes to the world economy; but also makes important contributions to energy consumption and pollution emissions [6]. Based on life cycle assessment, the energy consumption of the construction industry in China has increased rapidly. In 2016, its total energy consumption was 410 million tons of standard coal, accounting for about 9% of the whole society, and it quadrupled from 2000 to 2016 [7]. Actually, the implementation of the carbon emission trading policy provides us with an opportunity to find solutions to the energy consumption problem in China. In addition, compared with developed countries, China's energy technology and management level are relatively low and underdeveloped, and energy efficiency is not high [8]. For the construction industry, energy efficiency is a key indicator for evaluating the sustainable development of the construction industry [6]. Therefore, the study uses energy efficiency to measure and evaluate the impact of the carbon emissions trading policy on the energy efficiency of the construction industry in China.

This article takes the implementation of the carbon emission trading policy as a quasi-natural experiment. Difference-in-differences (DID) approach is used to evaluate the policy effect of the carbon emission trading policy on EEI, while Propensity Score Matching (PSM)-DID approach is used to further test the benchmark results and simulated repeated random sampling is used for the placebo test. The robustness of the benchmark results is further examined by other methods. The article explores three ways to strengthen the policy effect through mechanism analysis. At the same time, several influencing factors of EEI are presented. According to the research results, policy implications for the implementation of the carbon emission trading policy to enhance EEI are proposed.

The rest of this study is organized as follows. Section 2 is the literature review. Section 3 describes methods and data. Section 4 presents the empirical analysis. Robustness tests are provided in Section 5. Section 6 explores the mechanism analysis. In the end, Section 7 is the conclusion and policy implications.

2. Literature Review

The implementation of carbon emission trading policies mainly depends on the carbon emission trading system. The

carbon emissions trading system refers to a market trading system for the control of greenhouse gas emissions and targets greenhouse gas emission allowances or greenhouse gas emission credits [9]. The party that produces more emissions gets the right to emit coal from the other party, and the other party produces lower levels of carbon emissions. Buyers can use emissions reductions to mitigate greenhouse effects and meet emissions reduction goals [10].

The carbon emissions trading market has been effectively implemented in Europe, the USA, and other places after years of development. The EU has an earlier and more mature organization of carbon trading in the world [11]. There are many studies to evaluate the policy effect of carbon emissions trading policy. Lise et al. analyzed the impact of the EU Emissions Trading Scheme on electricity prices by studying 20 countries [12]. Martin et al. studied the EU's carbon emission system and found that carbon trading could reduce the pollutants emitted by these companies [13]. Murray and Maniloff demonstrated that a regional emissions trading program of the Regional Greenhouse Gas Initiative lead to substantial reductions in carbon dioxide emissions in the northeastern USA [14]. Simulation results of Choi et al. suggested that South Korea's emissions trading scheme had significant abatement effects [15]. As these studies have shown, carbon emissions trading policies can reduce carbon dioxide emissions.

In China, recent studies related to carbon emission trading policy are increasing and varying. Such as the impact on carbon emission reduction [16], carbon trading prices [17], carbon market maturity [18], and carbon trading efficiency [19]. The evaluation of the impact of carbon emission trading policy on the economy and the environment is one of the main research topics, which is highly relevant to this study. Dong et al. proved that the carbon emission trading policy had a significant impact on the joint benefits of total carbon reduction and air quality improvement [20]. The empirical work of Chen and Lin identified the role of carbon emission trading policy in promoting energy conservation and emission reduction as an effective policy tool to promote carbon neutrality [21]. Wu et al. confirmed that the carbon emission trading policy had a significant impact on agricultural ecological efficiency [22]. Chai et al. called carbon emission trading policy an effective market-driven environmental regulation policy and demonstrated it from the perspective of carbon emission efficiency [11]. The fact that China's coal emissions trading policy improves regional energy efficiency was demonstrated in the article of Zhang et al. [5]. More interestingly, the research results of Yu et al. show that carbon emission trading policy may significantly reduce urban-rural income inequality [3], and there are more studies on the evaluation of carbon emission trading policy.

As mentioned above, the economic and environmental impact of carbon emission trading policy involves various aspects. However, there is a gap in the assessment of carbon emission trading policies involving the construction industry. As suggested by Zhang et al. [23], future research can be carried out in sectors and industries most responsive to carbon emission trading. This article focuses on the impact

of the carbon emission trading policy on EECI, which fills this research gap. Furthermore, recent articles on the evaluation of carbon emission trading policy make extensive use of DID approach [1, 3, 4, 11, 20, 22]. These articles provide a practical research method for this article. DID removes the effects of individual heterogeneity and time-varying factors [24]. Using the DID approach, the net impact of policy implementation is estimated by comparing the intervention and control groups before and after the event [24]. PSM-DID has been also adopted by many researchers [3, 4, 11, 23], and it can select more suitable samples to reduce the deviation caused by sample selection [25]. In this article, DID is used for benchmark estimation, and PSM-DID is used to further test the estimation results.

In addition, evaluating energy efficiency is of great significance to energy conservation and improving the level of energy utilization. Research on EECI focuses on the measurement of energy efficiency and its influencing factors. EECI is measured mainly in terms of two methods, Single Factor Energy Efficiency (SFEE) and Total Factor Energy Efficiency (TFEE). SFEE measurement indicators include the thermodynamic index, physical-thermal index, economic-thermal index, and economic index [26, 27]. The most popular SFEE indicator is the economic-thermal index [27], which is the ratio of economic output to energy consumption and the reciprocal of energy intensity. Hu is the first to propose TFEE [28, 29]. TFEE considers a variety of inputs and outputs and uses stochastic frontier analysis (SFA) and data envelope analysis (DEA) methods to comprehensively evaluate energy efficiency. For example, Gao et al. [30] evaluated embodied energy efficiency and direct energy efficiency of the construction industry in China by DEA-SBM. The inputs are energy, capital, and technology, the outputs are the value added to the construction industry and the completed area of construction. Wang et al. [31] estimated the energy efficiency of the Chinese building industry based on the game cross-efficiency DEA model. Unlike the study by Gao et al., in their study, energy, capital, labor, and mechanical equipment are inputs, and gross output, completed area, and CO₂ emission are the outputs. Even if the same object is being analyzed, the input and output elements used by different scholars are different. That is to say, the research of TFEE without a unified standard is still in the exploratory stage. Compared with the TFEE method, the SFEE method is simple, straightforward, easy to understand, and has a high degree of consensus. Thus, this article adopts the economic-thermal index calculated by SFEE method to measure EECI in China.

After the measurement of EECI, influencing factors analysis is usually carried out, which is relevant to this article. Liang et al. [6] took urbanization, the per capita GRP, technical equipment ratio, energy consumption structure, innovation support, environmental supervision, industry contribution rate, and industry concentration as marketization as exogenous environmental variables, which can affect EECI in China. Zhu et al. [32] assessed the effects of technological progress on EECI. Chen et al. [27] listed a table of the factors influencing energy efficiency from previous literature, considering energy consumption structure,

industrial development level, industrial open degree, industrial scale structure, market ownership structure, market industry structure, market specialization-division structure, and technological innovation as environmental variables influencing EECI. Li et al.'s article show that labor productivity is considered as an important influencing factor for the assessment of the carbon emissions peak in China's construction industry [33]. Du et al. [34] and Zhou et al. [35] take the total power of mechanical equipment as an input variable of carbon emission efficiency similar to TFEE in the construction industry. Gao et al. adopt technical equipment rate as an input of TFEE in the construction industry [30]. According to Gong and Song [36] and Liang et al. [6], urbanization is an important factor of EECI. Chen et al. [27], Liang et al. [6], and Gong et al. [36] regarded electric consumption as a percentage of total energy consumption as the energy consumption structure. In accordance with Chen et al. [27] and Liang et al. [6], regional R&D expenditure intensity which stands for technological level is positive to EECI. Some variables are commonly considered to be related to EECI. The following research in this article draws on these studies to select variables in the model.

Compared with the existing literature, the main research innovations of this article are as follows: (1) there have been many evaluations of the impact of carbon emission trading policy on the economy and the environment in recent years, but there are few studies on the impact of carbon emission trading policy on sectors and industries, especially the impact of carbon emission trading policy on EECI. The widely accepted DID approach taken by these studies provides the research methodology used in this article. Therefore, this article adopts DID to evaluate the impact of carbon emission trading policy on EECI and tries to fill this research gap; (2) the positive policy effect of implementing carbon emission trading policy on EECI is confirmed by DID and some ways to strengthen the effect of carbon emission trading policy on EECI are explored by regression and mechanism analysis. Practical policy implications of carbon emission trading policy for improving EECI are proposed, which is a contribution that provides a reference for policymakers.

3. Methods and Data

3.1. DID Model. The difference-in-difference method is a common method for evaluating policy effects. This article uses the DID method to estimate the impact of the carbon emission trading policy on EECI in China. First, the implementation of the carbon emission trading policy is viewed as a quasi-natural experiment in which subjects are divided into an intervention group and a control group. The intervention group is defined as the group intervened by the policy, that is, the carbon emission trading policy pilot regions. The control group is defined as the group that is not intervened by the policy, that is, the non-pilot regions. By observing the changes in the intervention group and the control group before and after the implementation of the policy, the influence of the time effect can be eliminated, and the net effect of the policy is estimated. In this study, the first

batch of carbon emission trading policy pilots approved by NDRC in 2011 is selected as the intervention group. The intervention group included six pilot regions in Beijing, Tianjin, Shanghai, Chongqing, Hubei, and Guangdong (including Shenzhen). These six pilots actually launched the carbon emissions trading market at the end of 2013 and early 2014, so 2014 is considered to be the time for policy implementation [3, 16]; due to the launch of the carbon emissions trading market in Fujian at the end of December 2016 and the introduction of carbon emission trading policy into the national power sector in 2017, the data used are as of 2016 to avoid their interference with the experiment. Referring to previous researches [3, 4, 16], the DID model is constructed as follows:

$$\ln ee_{it} = \alpha_0 + \alpha_1 \text{treat}_i \text{post}_t + \sum \alpha_j X_{it} + \mu_i + \gamma_t + \varepsilon_{it}, \quad (1)$$

where $\ln ee_{it}$ denotes the natural logarithm of EECI at provincial region i in year t . α_0 denotes the constant. α_1 and α_j refer to the coefficient of the corresponding term. treat_i is the carbon emission trading policy dummy variable, if the region is the pilot of carbon emission trading, treat_i is equal to 1, otherwise it is equal to 0. post_t is the time dummy variable, which equals 1 when t is greater than or equal to 2014, otherwise it equals 0. $\text{treat}_i \text{post}_t$ is the interaction term, which indicates whether region i has implemented the carbon emission trading policy in year t . X_{it} indicates control variables and may affect $\ln ee_{it}$. μ_i denotes the individual fixed effect for provincial region. γ_t represents the time fixed effect for the year. ε_{it} means the random error term. The coefficient α_1 is the core coefficient to study whether carbon emission trading policy can promote $\ln ee$, indicating the net effect of carbon emission trading policy on $\ln ee$.

3.2. Mechanism Analysis Model. The article takes two methods to explore the mechanism. Referring to Xuan et al. [16], the first group of models is constructed as follows:

$$\begin{aligned} \ln ee_{it} &= \beta_0 + \beta_1 \text{treat}_i \text{period}_t + \sum \beta_j X_{it} + \mu_i + \gamma_t + \varepsilon_{it}, \\ M_{it} &= \beta_0 + \beta_2 \text{treat}_i \text{period}_t + \sum \beta_j X_{it} + \mu_i + \gamma_t + \varepsilon_{it}, \\ \ln ee_{it} &= \beta_0 + \beta_3 \text{treat}_i \text{period}_t + \beta_4 M_{it} + \sum \beta_j X_{it} + \mu_i + \gamma_t + \varepsilon_{it}, \end{aligned} \quad (2)$$

where M_{it} is the intermediary variable and the other symbols are consistent with those in model (1), and M_{it} should be checked as follows. In the first step, if β_1 is significant, it means that the carbon emission trading policy has a significant effect on $\ln ee_{it}$, then the second step of verification will be performed, otherwise, the procedure will terminate; the second step is to verify whether carbon emission trading policy has an effect on M_{it} according to whether β_2 is significant; if β_2 is significant, then go to the third step, otherwise terminate; the third step is to judge whether M_{it} is an intermediary variable according to whether β_4 is significant or not.

Referring to Qiu et al. [37], the second group of models is constructed as follows:

$$\begin{aligned} \ln ee_{it} &= \lambda_0 + \lambda_1 \text{treat}_i \text{period}_t N_{it} + \lambda_3 \text{treat}_i \text{period}_t \times N_{it} \\ &+ \sum \lambda_j X_{it} + \mu_i + \gamma_t + \varepsilon_{it}, \end{aligned} \quad (3)$$

where N_{it} is the moderator variable, $\text{treat}_i \text{period}_t \times N_{it}$ represents the interaction term between the moderator variable N_{it} and the implementation of carbon emission trading policy $\text{treat}_i \text{post}_t$. The other symbols are defined as the same as those in model (1). The article mainly focuses on the sign and significance of λ_1 and λ_3 . If both of them are significant, it means that N_{it} has a moderating effect on the impact of $\text{treat}_i \text{post}_t$ on $\ln ee_{it}$. These analysis results can provide valuable policy implications.

3.3. Variables and Data

3.3.1. Explained Variable. The explained variable is the natural logarithm of EECI at provincial region ($\ln ee$) [1], calculated by the natural logarithm of the ratio of the gross output value to the energy consumption in the construction industry. The gross output value of the construction industry in regions is from the China Statistics Yearbook of Construction (CSYC). The energy consumption of the construction industry in various regions is from the row for construction of Energy Balance Sheet by Region in China Energy Statistics Yearbook (CESY). Energy consumption refers to energy consumption in the construction stage and demolition stage [32, 36, 38]. The article uses the method of conversion of various energy sources in the sheet into a standard coal equivalent. Coefficients of conversion of various energy sources into standard coal are from the General Rules for Calculation of the Comprehensive Energy Consumption (GRCCEC, GB/T 2589–2020).

3.3.2. Core Explanatory Variable. The core explanatory variable is $\text{treat}_i \text{period}_t$. $\text{treat}_i \text{period}_t = 1$ means carbon emission trading policy is implemented in provincial region i in year t . $\text{treat}_i \text{period}_t = 0$ indicates that region i is not a carbon emission trading policy pilot or year t is not after the implementation of the policy, or neither. If the coefficient of $\text{treat}_i \text{period}_t$ is positive and significant, it indicates that carbon emission trading policy can promote EECI.

3.3.3. Control Variables and Others. The principle of variable selection is to consider the previous research and its correlation with dependent variables. Labor productivity, mechanical power equipment, urbanization, energy structure, and regional R&D expenditure intensity are the control variables. Labor productivity (proctivity) of construction enterprises in this article refers to the labor productivity calculated by gross output value from raw data of CSYC [33]. The mechanical power equipment rate (machinery) of construction enterprises from raw data of CSYC is designed to measure the mechanical equipment in the article [30, 34, 35]. It means mechanical resource allocation. The urban population as a percentage of total population

(urbanratio) which is raw data that comes from the China Statistical Yearbook (CSY) is the measurement of urbanization [6, 36]. The article defines the natural logarithm of electric consumption as a percentage of total energy consumption in the construction industry as an energy consumption structure (lnesratio) [6, 27, 36]. It is calculated by converting them into standard coal equivalent with data from Energy Balance Sheet by Region in CESY. Regional R&D expenditure intensity (rdratio) is derived from raw data of the China Statistical Yearbook of Science and Technology (CSYST) [6, 27]. It is the ratio of R&D expenditure to GDP in a region and represents regional technological innovation. The R&D expenditure is invested by the whole society in a region.

In addition, mechanical power equipment (machinery), regional R&D expenditure intensity (rdratio), and environmental regulation level (lneninratio) are used for mechanism analysis. Environmental regulation level of the government (lneninratio) which is the natural logarithm of the ratio of environmental protection expenditure to total government expenditure is adopted as a moderator variable for mechanism analysis, calculated by data from CSY. Per capita GDP (*pgdp*) raw data that comes from CSY is a covariate of PSM-DID estimation. Both of them are relevant to EECI [6]. Table 1 shows a description of the variables.

The research data of this article are panel data of 30 provincial regions (excluding Tibet, Taiwan, Hong Kong, and Macau, which have incomplete data) in China with a time span of 9 years from 2008 to 2016. The 30 provincial regions are divided into an intervention group with 6 regions and a control group with 24 regions. The year of carbon emission trading policy implementation is defined as 2014. Table 2 shows descriptive statistics of the variables.

4. Empirical Analysis

4.1. Benchmark Regression Results. The policy effect of carbon emission trading policy on EECI is estimated by model (1). Table 3 shows the estimation result, in which the province and year are fixed, that is, two-way fixed effect, and standard errors are clustered at the provincial level. The rest of the regressions below follow this standard. According to column (1) to column (5), the coefficient of $\text{treat}_i \cdot \text{period}_t$ is always positive and passes the significance test all the time. It demonstrates that the carbon emission trading policy pilot policy has significantly improved EECI and the result is robust. Compared with column (1) without control variables, the coefficient of column (5) with control variables increased from 0.210 of significance at 10% to 0.226 of significance at 1%. The estimated coefficient of 0.226 indicates a 22.6% increase in $\ln ee$ in the carbon emission trading policy regions relative to the non-pilot regions. Consistent with the conclusion proved by Gu et al. that the energy consumption per unit of GDP in the carbon emission trading policy pilot regions is significantly reduced [1], the conclusions of this study are highly similar to those of Zhang et al. [5]. Taking the natural logarithm of regional energy efficiency as the explanatory variable, the coefficients estimated by Zhang et al. range from 0.149 to 0.262 above 5% significance [5].

In addition to the carbon emission trading policy, we also find some other factors that may affect EECI. The coefficients of labor productivity (productivity), urbanization (urbanratio), energy consumption structure (lnesratio), and regional R&D expenditure intensity (ratio) are positive and pass the significance test. This indicates that they are positively correlated with EECI. In contrast, the mechanical power equipment rate (rdratio) of which coefficient is negative and passes the significance test is negatively correlated with EECI.

China's construction industry is shifting from extensive development to intensive development. Labor productivity under uneven technical levels of the labor force and irregular labor management are obstacles to intensive development. Labor productivity has a depressing effect on China's construction industry's carbon emissions [33]. As for EECI, this article shows that labor productivity promotes it. EECI can benefit from labor productivity, which is caused by the improvement of labor quality and the improvement of labor technology support.

The SFA regression results of Liang et al. represent that urbanization is negative to energy input in the analysis of EECI [30]. Urbanization is now shown to be positively correlated with EECI. With reference to Liang et al. [30], the increasing urbanization may promote the inflow of high-quality educational resources and talents, thus increasing the labor value, accelerating the development of energy-saving technologies, and improving energy efficiency.

The SFA regression results of Chen et al. indicate that energy consumption structure is negative to energy consumption in the construction industry [27]. The SFA regression results of Liang et al. represent that energy consumption structure is negative to energy input in the analysis of EECI [30]. The carbon emission trading policy has an impact on reducing total energy consumption and adjusting energy consumption structure, thus carbon emissions intensity is decreased [4, 16]. Similar to these results, the energy consumption structure of the construction industry in this article is positively correlated with EECI. The emergence of this situation may be caused by the gradual replacement of traditional coal energy with renewable energy, and this replacement also accelerates the development of energy technology.

Regional R&D expenditure intensity is positively related to technological innovation, and technological innovation can improve the utilization efficiency of social energy. The carbon emission trading policy can strengthen R&D investment [23]. Regional R&D expenditure intensity is positively correlated with EECI in this article, which is consistent with Chen et al. [27].

Unlike other variables, the mechanical power equipment rate is negatively correlated with EECI. It indicates that mechanical resource allocation is worth optimizing. The result is similar to Hydes et al.'s views [39]. They point out that reducing the use of equipment or facilities should be seen as one of the most effective ways to improve EECI [39].

4.2. Parallel Trend Test. One of the most important assumptions in the empirical analysis is that the intervention group and the control group obey a common trend prior to

TABLE 1: Description of the variables.

Variables	Definition	Description	Source
Lnee	Energy efficiency of the construction industry	The natural logarithm of the ratio of gross output value to energy consumption in the construction industry	CSYC CESY
Productivity	Labor productivity	The per capita labor productivity of construction enterprises from raw data	CSYC
Machinery	Mechanical power equipment	The per capita mechanical power equipment of construction enterprises from raw data	CSYC
Urbanratio	Urbanization	The urban population as a percentage of the total population from raw data	CSY
Lnesratio	Energy structure	The natural logarithm of electric consumption as a percentage of total energy consumption in the construction industry	CESY
Rdratio	Technological innovation	The ratio of R&D expenditure to GDP from raw data	CSY
Lneninratio	Environmental regulation level of the government	The natural logarithm of the ratio of environmental protection expenditure to total government expenditure	CSY
Pgdp	Per capita GDP	The per capita GDP from raw data	CSY

TABLE 2: Descriptive statistics of the variables.

Variables	Count	Mean	Std. Dev	Min	Median	Max
Lnee	270	3.169	0.724	1.280	3.114	4.884
Productivity	270	27.170	10.345	10.378	26.763	90.304
Machinery	270	6.360	3.060	2.100	5.800	27.400
Urbanratio	270	0.547	0.131	0.291	0.526	0.896
Lnesratio	270	-1.754	0.624	-3.604	-1.676	1.000
Rdratio	270	0.015	0.011	0.002	0.012	0.061
Lneninratio	270	-3.561	0.338	-4.639	-3.571	-2.821
Pgdp	270	4.270	2.259	0.882	3.731	11.820

the intervention of the carbon emission trading policy. Figure 1 shows that the average $\ln ee$ of the intervention group and the control group kept almost the same increasing trend excluding 2012 before the policy implementation in 2014, with no obvious deviations. However, after 2014, the mean $\ln ee$ of the intervention group continued to increase, and that of the control group almost stopped increasing in 2014 and began to decline since 2015, showing a significant deviation. The intervention group and the control group are preliminarily judged to satisfy the parallel trend test.

Referring to Liu [40], a regression model based on model (1) is built for further parallel trend tests. Model (1) is extended to the following:

$$\ln ee_{it} = \delta_0 + \delta_t \sum_{2008, t \neq 2013}^{2016} treat_i period_t + \sum \delta_j X_{it} + \mu_i + \gamma_t + \varepsilon_{it} \quad (4)$$

where $period_t$ is the dummy variable of time year, if the year is at t , the value is 1; otherwise, the value is 0. The series of coefficients (δ_t) for the interaction term ($treat_i period_t$) is the primary interest of this test. To satisfy the parallel trends, the coefficients of the interaction terms before 2014 are expected to be statistically insignificant and fluctuate within a certain range, indicating that the trends in the control and intervention groups are not statistically significantly biased. However, the coefficients of those after the carbon emission trading policy are expected to be significant, indicating a statistically significant deviation from the trends in the control and intervention groups. $period_{2013}$ is dropped and it is the base period. In addition, the model can examine the dynamics of policy effects.

TABLE 3: Impact of the carbon emission trading policy on energy efficiency of the construction industry.

	(1) lnee	(2) lnee	(3) lnee	(4) lnee	(5) lnee
$treat_i post_t$	0.210* (1.84)	0.334*** (2.76)	0.301** (2.70)	0.294*** (3.39)	0.226*** (2.92)
Productivity		0.008** (2.75)	0.008*** (2.79)	0.008*** (3.40)	0.007*** (3.11)
Urbanratio		5.798** (2.66)	5.892*** (2.79)	3.307** (2.13)	3.659** (2.28)
Machinery			-0.027*** (-3.03)	-0.014* (-1.87)	-0.017** (-2.31)
Lnesratio				0.472*** (6.01)	0.467*** (5.50)
Rdratio					29.223** (2.16)
_Cons	3.155*** (413.69)	-0.247 (-0.20)	-0.134 (-0.11)	2.033** (2.33)	1.455 (1.45)
Province FE	Yes	Yes	Yes	Yes	Yes
Year FE	Yes	Yes	Yes	Yes	Yes
Adj. R^2	0.891	0.901	0.906	0.938	0.941
N	270	270	270	270	270

Standard errors are clustered at the provincial level. t statistics in parentheses. * $p < 0.10$, ** $p < 0.05$, *** $p < 0.01$.

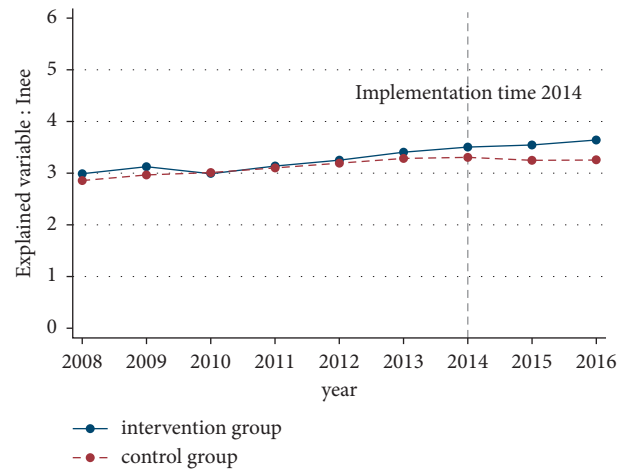


FIGURE 1: Average trend of the natural logarithm of energy efficiency of the construction industry in 2008–2016.

Figure 2 shows the evaluation results of model (6). It can be seen from Figure 2 that the coefficients from 2008 to 2012 are all statistically insignificant and fluctuate around 0, while the coefficients from 2014 to 2016 are significantly at the 10% significance level with the coefficients' significance and value increasing over time. Two important results are drawn from the regression. First, the intervention group and the control group before 2014 meet the parallel trend test; second, the significance and value of the coefficients after 2014 continue to increase, indicating that the implementation effect of the policy has become more and more prominent and carbon emission trading policy had an increasing effect on the EECI of the intervention group. This may be related to the expanding implementation scope of the carbon emission trading policy. The more industries carbon emission trading policy covers, the more relevant it is to the construction industry, and the greater the impact of the policy on EECI.

5. Robustness Tests

5.1. Placebo Test. Referring to Yu et al. [41], the placebo test is to eliminate the intervention of other unobserved missing variables on the EECI evaluated in this study. The basic idea is that 6 regions are first randomly selected from 30 regions as fake carbon emission trading policy pilots and the DID model (1) is used to estimate the coefficient of this core explanatory variable, and then the experiment is repeated 500 times. According to the distribution and significance of the coefficient values, if most of the coefficients are clustered around 0, the deviation from the estimated coefficient of the real quasi-natural experiment is large and not statistically significant, then it means that the carbon emission trading policy actually improves the EECI.

Figure 3 presents the results of the placebo test. The vertical red dashed line represents the true coefficient of 0.226, the horizontal red dashed line represents the 10% level of significance, the blue dashed line is the estimated *P* value, and the curve is the density distribution of the coefficients. Most of the coefficients deviate from the true coefficients and are not statistically significant, concentrated around 0 in Figure 3. Only a few are larger than the true coefficient and statistically significant. The policy effects of the carbon emission trading policy are not obtained by chance. Therefore, the placebo test shows that it is indeed a carbon emission trading policy that increases the EECI.

5.2. Excluding Outliers and the Counterfactual Time. According to the researches of Liu et al. [40] and Song et al. [42], the outliers are excluded or the policy implementation time is changed to test the robustness of the results. The dataset in this article may contain outliers that substantially affect the estimated results, and columns (1) and (2) in Table 4 show the regression results with the outliers excluded. The winsor2 algorithm for excluding outliers is to replace the values less than the 1% percentile and greater than the 99% percentile with the 1% and 99th percentile values, respectively. The results show that whether the

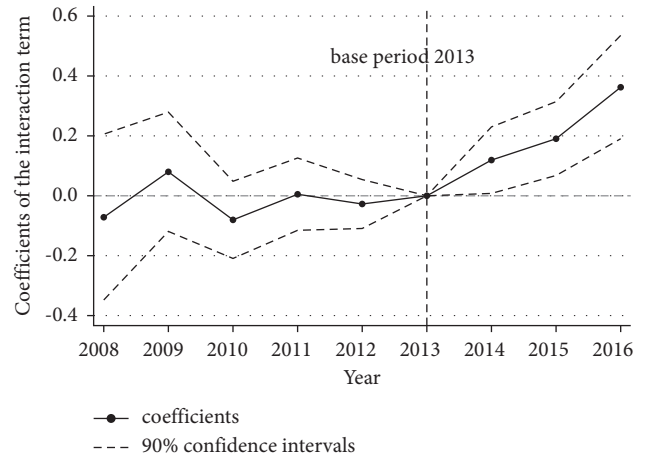


FIGURE 2: Coefficients of the interaction term and confidence intervals in the parallel trend test.

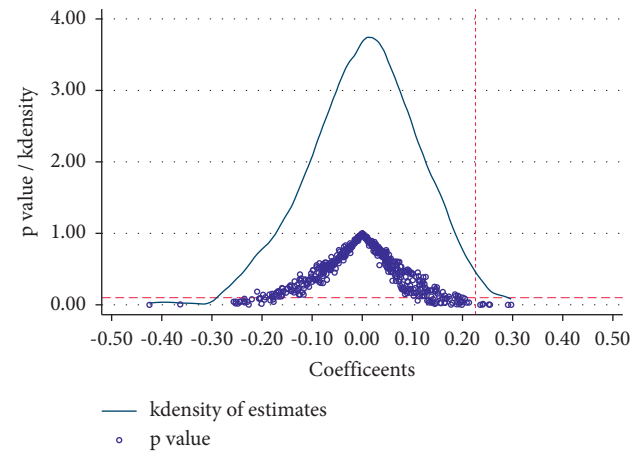


FIGURE 3: The distribution of coefficients of the core explanatory variable after random 500 simulations.

control variable is added to the regression or not, the coefficient of the core explanatory variable is around 0.2 and is statistically significant. It indicates the benchmark results are robust.

Another test is to change the “policy implementation time,” known as the counterfactual test. This test is conducted by changing the policy implementation time from 2014 to 2010, 2011, 2012, and 2013, respectively, and the other settings of the test are consistent with the benchmark regression [42]. The coefficients for the core explanatory variables from 2010 to 2012 shown in columns (3) to (8) in Table 4 are all statistically insignificant with and without the control variable, consistent with the parallel trend test. Column (9) and (10) shows that the coefficient of the core explanatory variable without the control variable in 2013 is not significant, while the coefficient of the core explanatory variable with the control variable is 0.168 at 5% significance, its value and significance are lower than the benchmark results. This result in column (10) may be due to the pre-policy effect of the carbon emission trading policy launch and the policy effect of some policy pilots

TABLE 4: Excluding outliers and changes of time.

	(1) lnee Winsor	(2) lnee Winsor	(3) lnee 2010	(4) lnee 2010	(5) lnee 2011	(6) lnee 2011	(7) lnee 2012	(8) lnee 2012	(9) lnee 2013	(10) lnee 2013
Treat _{it} pos _{it}	0.210* (1.85)	0.189** (2.69)	0.010 (0.05)	0.031 (0.24)	0.094 (0.59)	0.102 (1.11)	0.135 (0.99)	0.124 (1.45)	0.175 (1.40)	0.168** (2.14)
Productivity		0.012* (2.03)		0.007** (2.57)		0.006** (2.25)		0.005* (1.82)		0.006** (2.34)
Machinery		-0.018* (-1.97)		-0.019** (-2.49)		-0.019** (-2.45)		-0.019** (-2.45)		-0.018** (-2.39)
Urbanratio		3.582** (2.14)		2.529 (1.31)		2.730 (1.50)		2.961 (1.68)		3.294* (1.97)
lnesratio		0.525*** (6.74)		0.470*** (6.01)		0.476*** (5.83)		0.472*** (5.74)		0.470*** (5.59)
Rdratio		33.329** (2.36)		36.771** (2.52)		32.578** (2.29)		31.589** (2.26)		29.904** (2.14)
_Cons	3.155*** (415.36)	1.416 (1.44)	3.168*** (94.12)	1.998 (1.65)	3.157*** (147.88)	1.968* (1.70)	3.154*** (208.44)	1.871 (1.68)	3.154*** (284.18)	1.689 (1.60)
Province FE	Yes	Yes	Yes	Yes	Yes	Yes	Yes	Yes	Yes	Yes
Year FE	Yes	Yes	Yes	Yes	Yes	Yes	Yes	Yes	Yes	Yes
Adj. R ²	0.892	0.944	0.888	0.938	0.888	0.939	0.889	0.939	0.890	0.940
N	270	270	270	270	270	270	270	270	270	270

Standard errors are clustered at the provincial level. t statistics in parentheses. * $p < 0.10$, ** $p < 0.05$, *** $p < 0.01$.

launched at the end of 2013, but it is not robust to the result in column (9) and the benchmark result. The counterfactual time test indicates that the benchmark results are robust.

5.3. PSM-DID. Considering that the differences between samples are obvious, to further select comparable samples, this section adopts the PSM-DID for robustness testing. Referring to Liu et al. [24], the variables highly related to $\ln ee$ (such as productivity, machinery, urbanratio, lnesratio, ratio, and $pgdp$) are selected as the covariates to conduct the nearest neighbor 1:4 matching, which is statistically significant in logit regression. There should be no difference between the matched intervention (treated) group and the matched control group in terms of the selected covariates. A balance test is conducted and Table 5 lists the results of the balance test. After PSM matching, the biases of the variables in the intervention group and the control group are greatly reduced, and the biases are almost all within 10%. P -values are mostly statistically significant before matching and mostly statistically insignificant after matching which means that the PSM obtains a smaller deviation between the variables in the intervention group and the control group to obtain a better estimation.

After matching, the PSM-DID regression is performed. The estimation results in Table 6 show that the coefficients of the core explanatory variables are positive and statistically significant at 5% whether there are control variables or not, which indicates that the carbon emission trading policy does improve $\ln ee$. Additionally, the signs of control variables in column (2) are consistent with those in the benchmark results. The PSM-DID proves the robustness of the benchmark results in this article.

6. Mechanism Analysis

The benchmark regression and robustness tests aim to study the policy effect of carbon emission trading policy on EECI and the robustness of the results. Then, what is the transmission mechanism of the policy's impact on EECI? Two methods are adopted to answer this question [16, 37]. Based on model (2), model (3), and model (4), the mechanical power equipment rate (machinery) and regional R&D expenditure intensity (rdratio) are tested as mediator variables. This article examines the environmental regulation level (lnenratio) as a moderator variable by model (5).

Table 7 shows the estimation results of the mechanism analysis. The coefficient of the core explanatory variable in column (1) is negative and significant at the 1% level, indicating that the carbon emission trading policy can reduce the rate of mechanical power equipment. The coefficient of machinery in column (2) is negative and significant at the 5% level, indicating that machinery is negatively correlated with $\ln ee$. Combining columns (1) and (2), it shows that the carbon emission trading policy can improve EECI by reducing the mechanical power equipment rate. In the construction industry, construction machinery is common at the construction site. Due to extensive construction management, many mechanical equipment resources are idle and the operation efficiency is low, which leads to low EECI. Updating equipment, eliminating high-power machinery, using energy-saving and efficient machinery, and optimizing resource allocation in construction organization can reduce the rate of mechanical power equipment and improve EECI. This finding is similar to that of Qiu et al. [37] who proved that the low-carbon city pilot policy can make resource allocation more efficient, thus improving efficiency. A carbon emission trading policy can also make the allocation of mechanical equipment resources more effective, thus improving EECI.

TABLE 5: Balance test for PSM.

Variable	Unmatched Matched	Mean		%Reduct		<i>t</i> -test	
		Treated	Control	%Bias	bias	<i>t</i>	<i>p</i> > <i>t</i>
Productivity	U	36.775	24.769	105.7		8.6	0
	M	28.553	27.423	9.9	90.6	0.36	0.72
Machinery	U	6.5019	6.325	5.8		0.38	0.705
	M	5.805	5.6612	4.7	18.7	0.16	0.877
Urbanratio	U	0.72339	0.5033	188.9		14.84	0
	M	0.58937	0.59442	-4.3	97.7	-0.19	0.848
Lnesratio	U	-1.8552	-1.7292	-20.3		-1.33	0.185
	M	-1.8887	-1.8012	-14.1	30.6	-0.54	0.594
Rdratio	U	0.02823	0.01152	146.8		13.13	0
	M	0.0165	0.01601	4.3	97.1	0.3	0.762
Pgdp	U	6.6224	3.6821	128.3		10.01	0
	M	4.3698	4.3081	2.7	97.9	0.1	0.92

TABLE 6: The estimation results of PSM-DID.

	(1) lnee	(2) lnee
treat _t post _t	0.957** (2.95)	0.371** (2.58)
Productivity		0.005 (0.42)
Machinery		-0.061 (-1.37)
Urbanratio		5.814** (2.36)
Lnesratio		0.691*** (3.45)
Rdratio		35.738 (1.60)
_Cons	3.212*** (132.68)	0.889 (0.57)
Province FE	Yes	Yes
Year FE	Yes	Yes
Adj. R ²	0.843	0.945
N	45	45

Standard errors are clustered at the provincial level. *t* statistics in parentheses. **p* < 0.10, ***p* < 0.05, ****p* < 0.01.

The coefficient of the core explanatory variable in column (3) is negative and significant at the 1% level, indicating that the carbon emission trading policy is positive to regional R&D expenditure intensity (rdratio). The coefficient of rdratio in column (4) is positive and significant at the 5% level, indicating that rdratio is positively correlated with ln ee . Combining columns (3) and (4), it shows that carbon emission trading policy can improve EECI by increasing regional R&D expenditure intensity. Regional technological innovation is positively correlated with regional R&D expenditure intensity, improving technological innovation can accelerate the development of energy-saving technologies, thereby elevating EECI. This finding is consistent with that of Zhang et al. [5] who proved that green technological innovation plays a positive intermediary role in carbon emission trading policies that affect energy efficiency.

Columns (5) and (6) in Table 7 show that the coefficients for the core explanatory variable and the interaction term (treat_tperiod_t × lneninratio) are both positive and both pass the significance test. Combined with the benchmark results, this shows that the environmental regulation level has a positive moderating effect on the policy effect of the carbon emission trading policy on EECI, which indicates that strengthening environmental regulation in the carbon emission trading policy pilot can improve the promotion of carbon emission trading policy on EECI. This result is consistent with the well-known Poynter hypothesis that appropriate environmental regulation by the government can motivate firms to innovate more, while technological innovation can improve energy efficiency. Similarly, Boyd et al. [43] confirmed that environmental regulation is positive to “emission reduction” and “growth.” With the

TABLE 7: The estimation results of mechanism analysis.

Explained variable	(1) Machinery	(2).Lnee	(3).Rdratio	(4).Lnee	(5).Lnee	(6).Lnee
treat _t post _t	-1.628*** (-2.91)	0.226*** (2.92)	0.002*** (3.22)	0.226*** (2.92)	1.386*** (3.55)	1.542** (2.74)
Productivity	0.001 (0.03)	0.007*** (3.11)	0.000* (1.86)	0.007*** (3.11)		0.007*** (2.96)
Urbanratio	13.857* (1.72)	3.659** (2.28)	-0.012 (-0.72)	3.659** (2.28)		3.676** (2.45)
Lnesratio	-1.488* (-1.99)	0.467*** (5.50)	0.000 (0.21)	0.467*** (5.50)		0.469*** (5.69)
Rdratio	215.803 (1.35)	29.223** (2.16)		29.223** (2.16)		31.863** (2.48)
Machinery		-0.017** (-2.31)	0.000** (2.29)	-0.017** (-2.31)		-0.017** (-2.24)
Lneninratio					-0.065 (-0.36)	0.021 (0.17)
treat _t post _t ×Lneninratio					0.320*** (2.95)	0.366** (2.34)
_Cons	-6.950 (-1.04)	1.455 (1.45)	0.020* (1.99)	1.455 (1.45)	2.922*** (4.48)	1.493* (1.72)
Province FE	Yes	Yes	Yes	Yes	Yes	Yes
Year FE	Yes	Yes	Yes	Yes	Yes	Yes
Adj. R ²	0.571	0.941	0.984	0.941	0.892	0.943
N	270	270	270	270	270	270

Standard errors are clustered at the provincial level. *t* statistics in parentheses. * $p < 0.10$, ** $p < 0.05$, *** $p < 0.01$.

increase in environmental regulation, Qiu et al. [37] pointed out that the rising environmental costs force enterprises to innovate and reduce their dependence on energy.

7. Conclusions and Policy Implications

This article aims to evaluate the performance of China's carbon emissions trading policy in terms of EECI. DID, the parallel trend test, robust tests, and mechanism analysis are used to explore the effect of carbon emission trading policy on EECI. Based on the above research, the following conclusions are drawn: (1) carbon emission trading policy can improve the EECI in pilot regions relative to non-pilot regions, and its policy effect gets better over time. The robustness of the benchmark results is demonstrated by several methods; (2) results of mechanism analysis show that carbon emission trading policy can improve EECI by reducing the mechanical power equipment rate or increasing regional R&D expenditure intensity. Increasing the environmental protection expenditure ratio in the carbon emission trading policy pilot can improve the promotion of carbon emission trading policy on EECI; (3) labor productivity, urbanization, energy consumption structure, and regional R&D expenditure intensity are positive to EECI, while the mechanical power equipment rate is negative to EECI.

The main policy implications are as follows: (1) for EECI, as the carbon emission trading policy is implemented longer and more widely, the greater the relationship between the policy effects and EECI. More specifically, the government

should increase the time, intensity, and scope of implementing the carbon emissions trading policy; (2) the government can improve EECI by stimulating regional technological innovation and appropriately strengthening environmental regulations in the regions where the carbon emission trading policy is implemented. In terms of mechanical resource allocation, the government can use the carbon emission trading policy market effect to promote construction enterprises to strengthen resource allocation management and construction organization, eliminate high-power and inefficient equipment, and use new energy-saving equipment with the goal of increasing EECI. Construction enterprises can also take the initiative to adopt the above measures to reduce the rate of mechanical power equipment for increasing EECI; (3) the government can take measures to reduce the use of traditional energy such as coal to adjust the energy structure for improving the EECI. Construction enterprises can increase labor productivity by improving the professional ability and technical level of workers, thus increasing the EECI.

The conclusions and policy implications are summarized above, but this article has some defects. Short-term policy effects are estimated while long-term policy effects are omitted due to the selection of periods. Besides, policy effects and mechanisms analysis cannot be fully explored. Further research is expected to address these issues.

Data Availability

The data used to support the findings of this study are available from the corresponding author upon request.

Conflicts of Interest

The authors declare no conflicts of interest.

Authors' Contributions

S.X. conceptualized and supervised the study, administrated the project, and carried out funding acquisition; J.W. developed methodology, helped with software, validated the study, carried out formal analysis, and wrote and prepared the original draft. All authors have read and agreed to the published version of the manuscript.

Acknowledgments

This research was funded by the Graduate Innovative Fund of Wuhan Institute of Technology (Grant no. CX2021104), the Philosophy and social science research project of colleges and Universities in Hubei Province (Grant no. 21Q099), and the Science Research Foundation of Wuhan Institute of Technology (Grant no. K202020). Special thanks should be given to Associate Professor S.X. for her advice.

References

- [1] G. Gu, H. Zheng, L. Tong, and Y. Dai, "Does carbon financial market as an environmental regulation policy tool promote regional energy conservation and emission reduction? Empirical evidence from China," *Energy Policy*, vol. 163, Article ID 112826, 2022.
- [2] Q. Weng and H. Xu, "A review of China's carbon trading market," *Renewable and Sustainable Energy Reviews*, vol. 91, pp. 613–619, 2018.
- [3] F. Yu, D. Xiao, and M. S. Chang, "The impact of carbon emission trading schemes on urban-rural income inequality in China: a multi-period difference-in-differences method," *Energy Policy*, vol. 159, Article ID 112652, 2021.
- [4] S. Z. Qi, S. H. Cheng, and J. B. Cui, "Environmental and economic effects of China's carbon market pilots: empirical evidence based on a DID model," *Journal of Cleaner Production*, vol. 279, Article ID 123720, 2021.
- [5] X. M. Zhang, F. F. Lu, and D. Xue, "Does China's carbon emission trading policy improve regional energy efficiency?—an analysis based on quasi-experimental and policy spillover effects," *Environmental Science & Pollution Research*, vol. 29, no. 14, Article ID 21166, 2022.
- [6] X. Liang, S. Lin, X. Bi, E. Lu, and Z. Li, "Chinese construction industry energy efficiency analysis with undesirable carbon emissions and construction waste outputs," *Environmental Science and Pollution Research*, vol. 28, no. 13, Article ID 15838, 2021.
- [7] Y. Zhang, D. Yan, S. Hu, and S. Y. Guo, "Modelling of energy consumption and carbon emission from the building construction sector in China, a process-based LCA approach," *Energy Policy*, vol. 134, Article ID 110949, 2019.
- [8] L. Zhu, Y. Wang, P. P. Shang, L. Qi, G. C. Yang, and Y. Wang, "Improvement path, the improvement potential and the dynamic evolution of regional energy efficiency in China: based on an improved nonradial multidirectional efficiency analysis," *Energy Policy*, vol. 133, Article ID 110883, 2019.
- [9] K. Tang, Y. C. Liu, D. Zhou, and Y. Qiu, "Urban carbon emission intensity under emission trading system in a developing economy: evidence from 273 Chinese cities," *Environmental Science & Pollution Research*, vol. 28, no. 5, pp. 5168–5179, 2021.
- [10] X. G. Zhao, G. W. Jiang, D. Nie, and H. Chen, "How to improve the market efficiency of carbon trading: a perspective of China," *Renewable and Sustainable Energy Reviews*, vol. 59, pp. 1229–1245, 2016.
- [11] S. L. Chai, R. X. Sun, K. Zhang, Y. T. Ding, and W. Wei, "Is emissions trading scheme (ETS) an effective market-incentivized environmental regulation policy? Evidence from China's eight ETS pilots," *International Journal of Environmental Research and Public Health*, vol. 19, no. 6, p. 3177, 2022.
- [12] W. Lise, J. Sijm, and B. F. Hobbs, "The impact of the EU ETS on prices, profits and emissions in the power sector: simulation results with the COMPETES EU20 model," *Environmental and Resource Economics*, vol. 47, no. 1, pp. 23–44, 2010.
- [13] R. Martin, M. Muûls, and U. J. Wagner, "The impact of the European union emissions trading scheme on regulated firms: what is the evidence after ten years?" *Review of Environmental Economics and Policy*, vol. 10, no. 1, pp. 129–148, 2016.
- [14] B. C. Murray and P. T. Maniloff, "Why have greenhouse emissions in RGGI states declined? An econometric attribution to economic, energy market, and policy factors," *Energy Economics*, vol. 51, pp. 581–589, 2015.
- [15] Y. Choi, Y. Liu, and H. Lee, "The economy impacts of Korean ETS with an emphasis on sectoral coverage based on a CGE approach," *Energy Policy*, vol. 109, pp. 835–844, 2017.
- [16] D. Xuan, X. W. Ma, and Y. P. Shang, "Can China's policy of carbon emission trading promote carbon emission reduction?" *Journal of Cleaner Production*, vol. 270, Article ID 122383, 2020.
- [17] J. Liu, Y. Y. Huang, and C. P. Chang, "Leverage analysis of carbon market price fluctuation in China," *Journal of Cleaner Production*, vol. 245, Article ID 118557, 2020.
- [18] X. F. Liu, X. X. Zhou, B. Z. Zhu, K. J. He, and P. Wang, "Measuring the maturity of carbon market in China: an entropy-based TOPSIS approach," *Journal of Cleaner Production*, vol. 229, pp. 94–103, 2019.
- [19] S. Y. Zhang, K. Jiang, L. Wang, G. Bongers, G. P. Hu, and J. Li, "Do the performance and efficiency of China's carbon emission trading market change over time?" *Environmental Science & Pollution Research*, vol. 27, no. 26, Article ID 33140, 2020.
- [20] Z. Dong, C. Xia, K. Fang, and W. Zhang, "Effect of the carbon emissions trading policy on the co-benefits of carbon emissions reduction and air pollution control," *Energy Policy*, vol. 165, Article ID 112998, 2022.
- [21] X. Chen and B. Q. Lin, "Towards carbon neutrality by implementing carbon emissions trading scheme: policy evaluation in China," *Energy Policy*, vol. 157, Article ID 112510, 2021.
- [22] G. Y. Wu, Y. Xie, H. X. Li, and N. Riaz, "Agricultural ecological efficiency under the carbon emissions trading system in China: a spatial difference-in-difference approach," *Sustainability*, vol. 14, no. 8, p. 4707, 2022.
- [23] Y. Zhang, S. Li, T. Luo, and J. Gao, "The effect of emission trading policy on carbon emission reduction: evidence from an integrated study of pilot regions in China," *Journal of Cleaner Production*, vol. 265, Article ID 121843, 2020.
- [24] X. Liu, Y. Li, X. Chen, and J. Liu, "Evaluation of low carbon city pilot policy effect on carbon abatement in China: an empirical evidence based on time-varying DID model," *Cities*, vol. 123, Article ID 103582, 2022.

- [25] J. J. Heckman, H. Ichimura, and P. E. Todd, "Matching as an econometric evaluation estimator: evidence from evaluating a job training programme," *The Review of Economic Studies*, vol. 64, no. 4, pp. 605–654, 1997.
- [26] M. G. Patterson, "What is energy efficiency?: concepts, indicators and methodological issues," *Energy Policy*, vol. 24, no. 5, pp. 377–390, 1996.
- [27] Y. Chen, B. Liu, Y. Shen, and X. Wang, "The energy efficiency of China's regional construction industry based on the three-stage DEA model and the DEA-DA model," *KSCE Journal of Civil Engineering*, vol. 20, no. 1, pp. 34–47, 2015.
- [28] J.-L. Hu and S.-C. Wang, "Total-factor energy efficiency of regions in China," *Energy Policy*, vol. 34, no. 17, pp. 3206–3217, 2006.
- [29] T. Huo, M. Tang, W. Cai, H. Ren, B. Liu, and X. Hu, "Provincial total-factor energy efficiency considering floor space under construction: an empirical analysis of China's construction industry," *Journal of Cleaner Production*, vol. 244, Article ID 118749, 2020.
- [30] J. Gao, H. Ren, X. Ma, W. Cai, and Q. Shi, "A total energy efficiency evaluation framework based on embodied energy for the construction industry and the spatio-temporal evolution analysis," *Engineering Construction and Architectural Management*, vol. 26, no. 8, pp. 1652–1671, 2019.
- [31] L. Wang, X. Song, and X. Song, "Research on the measurement and spatial-temporal difference analysis of energy efficiency in China's construction industry based on a game cross-efficiency model," *Journal of Cleaner Production*, vol. 278, Article ID 123918, 2021.
- [32] W. Zhu, Z. Zhang, X. Li, W. Feng, and J. Li, "Assessing the effects of technological progress on energy efficiency in the construction industry: a case of China," *Journal of Cleaner Production*, vol. 238, Article ID 117908, 2019.
- [33] B. Li, S. Han, Y. Wang, Y. Wang, J. Li, and Y. Wang, "Feasibility assessment of the carbon emissions peak in China's construction industry: factor decomposition and peak forecast," *Science of the Total Environment*, vol. 706, Article ID 135716, 2020.
- [34] Q. Du, Y. Deng, J. Zhou, J. Wu, and Q. Pang, "Spatial spillover effect of carbon emission efficiency in the construction industry of China," *Environmental Science and Pollution Research*, vol. 29, no. 2, pp. 2466–2479, 2022.
- [35] W. Zhou, W. Yu, and A. Farouk, "Regional variation in the carbon dioxide emission efficiency of construction industry in China: based on the three-stage DEA model," *Discrete Dynamics in Nature and Society*, vol. 2021, Article ID 4021947, 13 pages, 2021.
- [36] Y. Gong and D. Song, "Life cycle building carbon emissions assessment and driving factors decomposition analysis based on LMDI—a case study of wuhan city in China," *Sustainability*, vol. 7, no. 12, Article ID 16670, 2015.
- [37] S. L. Qiu, Z. L. Wang, and S. Liu, "The policy outcomes of low-carbon city construction on urban green development: evidence from a quasi-natural experiment conducted in China," *Sustainable Cities and Society*, vol. 66, Article ID 102699, 2021.
- [38] T. Huo, H. Ren, X. Zhang et al., "China's energy consumption in the building sector: a Statistical Yearbook-Energy Balance Sheet based splitting method," *Journal of Cleaner Production*, vol. 185, pp. 665–679, 2018.
- [39] K. R. Hydes and L. Creech, "Reducing mechanical equipment cost: the economics of green design," *Building Research & Information*, vol. 28, no. 5-6, pp. 403–407, 2000.
- [40] F. Liu, "The impact of China's low-carbon city pilot policy on carbon emissions: based on the multi-period DID model," *Environmental Science and Pollution Research International*, 2022.
- [41] D.-J. Yu and J. Li, "Evaluating the employment effect of China's carbon emission trading policy: based on the perspective of spatial spillover," *Journal of Cleaner Production*, vol. 292, Article ID 126052, 2021.
- [42] M. Song, X. Zhao, and Y. Shang, "The impact of low-carbon city construction on ecological efficiency: empirical evidence from quasi-natural experiments," *Resources, Conservation and Recycling*, vol. 157, Article ID 104777, 2020.
- [43] G. A. Boyd and J. D. McClelland, "The Impact of Environmental Constraints on Productivity Improvement in Integrated Paper Plants," *Journal of Environmental Economics and Management*, vol. 38, 1999.